



HAL
open science

Multiscale modeling of solidification: from microstructures to castings

Miha Založnik

► **To cite this version:**

Miha Založnik. Multiscale modeling of solidification: from microstructures to castings. Materials. Université de Lorraine, 2020. tel-03095191

HAL Id: tel-03095191

<https://hal.science/tel-03095191>

Submitted on 4 Jan 2021

HAL is a multi-disciplinary open access archive for the deposit and dissemination of scientific research documents, whether they are published or not. The documents may come from teaching and research institutions in France or abroad, or from public or private research centers.

L'archive ouverte pluridisciplinaire **HAL**, est destinée au dépôt et à la diffusion de documents scientifiques de niveau recherche, publiés ou non, émanant des établissements d'enseignement et de recherche français ou étrangers, des laboratoires publics ou privés.

Copyright

UNIVERSITÉ DE LORRAINE
THÈSE D'HABILITATION À DIRIGER DES RECHERCHES
SPÉCIALITÉ : SCIENCES DES MATÉRIAUX

**Multiscale modeling
of solidification:
from microstructures to castings**

par

Miha Založnik

Soutenue le 8 décembre 2020 devant le jury :

Silvère Akamatsu	INSP, CNRS/Sorbonne Université	Rapporteur
Hervé Combeau	Université de Lorraine	Examinateur
Dmitry Eskin	Brunel University London	Rapporteur
Charles-André Gandin	Cemef, CNRS/Mines ParisTech	Examinateur
Nathalie Mangelinck-Noël	IM2NP, CNRS/Aix-Marseille Université	Examinatrice
Mathis Plapp	LPMC, CNRS/École Polytechnique	Rapporteur

...nekaj bode zmirom še ostalo, da ne bomo vedili zakaj.

JOŽEF STEFAN

Contents

1	Introduction	1
2	Macroscopic modeling	3
2.1	Introduction	3
2.2	Transport of equiaxed grains and macrosegregation	5
2.3	Transport of inoculant particles	15
2.4	Packing of equiaxed grains	23
2.5	Flexible models and algorithms for coupling micro-and macro- models	28
3	Mesoscopic modeling	31
3.1	Introduction	31
3.2	The Mesoscopic Grain Envelope Model	32
3.3	Growth of interacting equiaxed grains	36
3.4	Growth interactions in columnar growth	47
3.5	Convection effects	53
3.6	Methodological developments	60
4	Upscaling	73
4.1	Introduction	73
4.2	Methods	74
4.3	New constitutive laws for equiaxed growth	75
4.4	Outlook on upscaling	80
5	Projects	81
5.1	Mesoscopic phenomena	81
5.2	Methodological developments of the grain envelope model	84
5.3	Upscaling	86
	Bibliography	88
A	CV	109
B	List of publications	115

Chapter 1

Introduction

Solidification is a key processing step for the manufacture of most metal products. During casting or additive manufacturing the base microstructure for all subsequent processing stages is formed. Defects and nonuniformity of structure and chemical composition can be introduced at different scales, from the scale of phase interfaces to the scale of the whole product. The properties of the final product are conditioned by the structure formed during solidification.

The genesis of solidification micro- and macrostructures and defects is difficult to understand because the phenomena that need to be described span a wide range of scales and involve many aspects of physics. For example, the macrostructure (distribution of grain size and shape across a solidified piece) is the result of a complex interaction between the nucleation of solid grains, their growth and their transport. The growth of the crystal grains is controlled by diffusion and convection of solutes at the scale of the dendrite branches – the *microscopic* scale, and by collective solutal interactions between grains at the scale of a grain ensemble – the *mesoscopic* scale. The distribution across the casting is further governed by convection transport at the process scale – the *macroscopic* scale. The formation of defects such as macro- and microsegregation or microporosity, is tightly coupled with the establishment of the macrostructure.

Models of solidification need to describe the elementary phenomena at the different scales and their coupling. Because of the range of scales involved spans at least six orders of magnitude (roughly from a μm to a meter), a direct description by microscale models will not be viable in the foreseeable future. Multiscale models are therefore employed. They are based on cleverly simplified models of phenomena at smaller scales that are incorporated into models of larger scales to give a multiscale description. The assumptions introduced by simplifications of the microscale modeling are a key to the limitations of multiscale models. As I will show, the simplifications introduced at the microscopic scale can have a significant influence on the

predictions on the macroscopic scale.

The research presented in this memoir is driven by industrial applications for the production of high-performance materials. Prominent examples of major current concern include:

- Nuclear safety: macrosegregation in large steel ingots for the manufacture of nuclear reactor parts;
- Lightweighting: microstructure, microporosity and macrosegregation in aluminum alloys for aircraft structures and in TiAl-based alloys for the manufacture of aircraft engine turbine blades.

An essential driving force for my research are the collaborations with industrial partners. Starting with the collaboration with Impol Aluminium Industry (Slovenia) during my PhD, industrial partnerships thrived in the environment of the Solidification group of IJL; in chronological order: Constellium C-TEC, Sciences & Computers Consultants, Erasteel, Aubert & Duval, ArcelorMittal Industeel, Ascometal, Safran Aircraft Engines, Framatome, EDF, O2M Solutions, ArcelorMittal Maizieres Research, and ABS. Key to success are the academic collaborations. I need to point out the most important ones: Access–RWTH Aachen, Sintef Industry, Cemef–Mines ParisTech, and the Solidification Lab of the University of Iowa.

The structure of this memoir reflects the motivation and the rationale of my research. The investigation of industrial problems opens questions and problems of more fundamental nature that need to be answered to respond to the industrial issues. In a similar way, the improvement of the predictive power of multiscale models for industrial processes triggers the need for refining the description of micro- and mesoscale phenomena. Specific models at smaller scales are developed and the results are to be fed back to the macroscopic models through upscaling methods. The modeling is complemented by lab and industrial experiments. I will therefore guide you through the principal results of my research in the last 13 years following this line.

The second chapter of this memoir presents the work on industrial processes, focusing on the modeling of the coupling of process-scale transport and microstructure nucleation and growth. Through the results, the limitations of the macroscopic multiscale models in the description of small scale phenomena are also presented. In the third chapter applications and developments of a mesoscopic model are presented with one of the key objectives being to use it for upscaling to macroscopic models in order to improve the description of microstructure growth kinetics at the process scale. The first steps in upscaling are presented in the fourth chapter. The last, fifth, chapter presents research projects that will evolve in the coming years from the solid trunk grown today.

Chapter 2

Macroscopic modeling

2.1 Introduction

For the metallurgical industry, numerical simulation is a valuable tool that helps gain understanding leading to reduction of defects, enhancement of material structure, and improvement of processes. In our work on process-scale modeling of solidification the focus is on industrial applications in steel ingot casting, DC casting of aluminum alloys, and more recently on centrifugal casting of TiAl based alloys. The objective is to explain the interactions between the microstructure, the macrostructure, and the macroscopic transport in order to enable a better control of the structural and chemical homogeneity of castings.

The models of all these elementary phenomena must be formulated in a way that makes it possible to incorporate and couple them in a closed model. When formulating such models, one faces several challenges: (i) the decisive physical phenomena must be described in a simplified way that enables their solution at the process scale, (ii) all models must be coupled in a common framework, (iii) numerical algorithms to solve the strongly nonlinear models, consisting of a large number of coupled equations, must be developed. With utility as the objective, the essence of the art of modeling lies in smartly balancing the intricacy of the couplings with our ability to understand them, and the completeness of the models with the capabilities of the computing tools available to resolve them.

To couple micro-, meso-, and macroscopic phenomena, mean-field models are used in multiscale and multiphysics modeling of processes. For solidification, the volume-averaging approach is the most established. These models are based on the seminal work of Beckermann et al. [1] and Rappaz et al. [2,3] in the late 1980s and early 1990s. They were the first to couple models of dendritic microstructure growth kinetics to macroscopic heat transfer calculations in cast parts. The volume-averaging framework was applied to solidification at around the same time by Beckermann & Viskanta [4] and

Ganesan & Poirier [5]. Beckermann et al. [6–10] then extended these coupled approaches to include convection and grain motion. Later, modeling of multicomponent alloys, the consideration of the microscopic solute diffusion, and of the grain morphology were refined by Appolaire et al. [11] and Wu & Ludwig [12, 13]. Models of mixed columnar-equiaxed solidification, aimed at describing the columnar-to-equiaxed transition (CET) with grain motion were developed by Wu et al. [14, 15] and Leriche et al. [16, 17].

Despite the advance of model formulations, only little work with full-featured models has been done on industrial scale castings. The main reasons are the complexity of the model implementation, of the numerical solution schemes, and excessive computing times. A further considerable barrier to reliable simulations is the considerable lack of information on the generation of equiaxed grains by nucleation and fragmentation. Most modeling has been therefore done using simplified binary-alloy simulations with fixed-solid. Industrial applications with models of equiaxed grain motion started only around 10 years ago [18–21] and are in dynamic development today [17, 22–26].

The specificities of the models developed in our research group and through our academic collaborations are the comprehensive and detailed description of the macroscopic transport and the kinetics of microscopic growth, the strong coupling of the two scales, as well as clever numerical implementations. We developed industrial applications that are unprecedented for a model of such complexity: the numerical model allows the simulation of industrial castings and the study of the effects of operating conditions on the establishment of structures and macrosegregation.

The investigations and developments that I have been heavily involved with since 2001, first during my PhD (2001–2006, University of Nova Gorica, Slovenia) and then as a postdoc (2006–2009) and permanent researcher (from 2009) in Nancy, are motivated by industrial applications in steel ingot casting and DC casting of aluminum alloys. Model extensions were therefore developed with the objective of improving the predictive power of the models for these processes. The models were refined, extending the physics of the micro-macro couplings that they capture. For example, we were the first to explain the macroscopic picture of nucleation in DC casting, based on a model of nucleation and growth coupled with the transport of grains and nuclei [27, 28]. The general philosophy of the models developed is that they should be as computationally cheap as possible, provide a fine and physically faithful description of the phenomena, and avoid a complexity overload that could make them unmanageable even for an expert user. Furthermore, improvements of numerical algorithms for micro-macro coupling helped bring the models to full industrial maturity. Today, these models are built into *Solid*[®], an industrial simulation software. A new software generation is currently under development in collaboration with Sciences & Computers Consultants (process simulation software company), O2M Solu-

tions (startup specialized in process modeling) and a consortium of industrial partners.

In this chapter I will present the most salient developments: we explained the link between microstructure and macrosegregation in steel ingots and DC casting (Section 2.2), we proposed a multiscale theory of nucleation in grain-refined aluminum alloys that elucidates the formation of microstructure in DC casting (Section 2.3), we addressed meso-scale phenomena in equiaxed grain packing (Section 2.4), and we developed flexible algorithms for coupling of micro- and macro-models (Section 2.5).

2.2 Transport of equiaxed grains and macrosegregation

During solidification of metal alloys, solid often nucleates and grows from liquid in the form of dendritic crystal grains that freely float in the liquid melt. Because in alloys of technical interest the solid phase has a higher density than the liquid, the grains settle and eventually pack at the bottom of the solidifying zone. This happens in a wide variety of industrial solidification processes, for example, in large castings or in welding. The way the grains move and pack has important consequences on the distribution of the microstructure across the solidified piece (grain size, shape, morphology, crystallographic texture, and formation of secondary solid phases) and on several types of defects (porosity and chemical segregation) that can form during solidification.

The framework for the modeling of these phenomena was set in the 1990s by the pioneering work of Beckermann et al. [6–10, 29–32], who first extended micro-macro models of solidification with convection and grain motion. Development and application of this type of coupled micro-macro models in the Solidification Group in Nancy started around 20 years ago. The model is based on that proposed by Wang and Beckermann [10]. It has been supplemented by detailed micro-modeling of dendritic growth for multicomponent alloys and of transitions between dendritic and globular grain morphology [11], aspects that have not been investigated in detail in the earlier seminal work. In parallel, it has been pushed to sufficient maturity to allow first simulations at the full scale of industrial processes [33, 34]. This has not been attained in earlier studies, where applications of this type of models were limited to small lab-scale castings [35–37], or to partial descriptions of industrial processes [38, 39].

The modeling of grain motion was mainly motivated by the prediction of macrosegregation in steel ingots and in DC casting of aluminum alloys. A prime concern in our investigations is to recognize that the microstructure of the growing equiaxed grains has a decisive impact on their settling and packing and on the contribution of grain motion to macrosegregation.

The first decisive microstructure property is the morphology of the equiaxed grains. To illustrate this, consider on the one hand the settling of completely globular grains, and on the other hand the settling of strongly dendritic grains. As they settle, globular grains form a tightly packed sedimentation layer. This means that in this layer the volume fraction of the solute-lean solid that has displaced the solute-rich liquid is high, the effect of solute transport therefore strong. Conversely, grains with a pronounced dendritic morphology pile up into a loosely packed layer and displace less liquid. The solute mass transport induced by this settling is considerably weaker. Once packed, the grain morphology also controls the hydrodynamic permeability of the packed layer. Macrosegregation in the packed layer is largely created by the flow of liquid, which depends on the permeability. The permeability depends on the liquid fraction (higher for dendritic grains) and the characteristic length scale for microscale flow (typically, SDAS for dendritic and grain size for globular grains).

We showed and analyzed this effect, which we can intuitively understand by the foregoing illustration, in much more detail in [18], where we used a fully coupled multiscale solidification model to simulate a 3.3-ton steel ingot with either fully dendritic or fully globular grain morphology. The impact of the morphology is shown in a simple, but striking example in Fig. 2.1. Three simulations with different assumptions on grain motion and on the morphology of the moving equiaxed grains are shown and compared to experimental macrosegregation characterizations in a 3.3 ton steel ingot [18]. We can see that the intensity of macrosegregation is grossly overestimated by the simulation that assumes globular equiaxed grains (Fig 2.1(a)). A much better and actually quite accurate prediction is obtained by the simulation where the grain morphology is calculated with a model of dendritic grain growth that is coupled to the macroscopic transport and captures the influence of the local cooling rate, solute concentration, grain density, etc. on the morphology (Fig 2.1(b)). Surprisingly, in this particular case the prediction of the dendritic model is very close to the simulation with a much simpler model that assumes that the grains do not move at all (Fig 2.1(c))! The reason is that the loose packing of settled dendritic grains causes only negligible macrosegregation and most of the macrosegregation is built up by the flow of interdendritic liquid, which follows a very similar pattern as in a mushy zone with fixed solid.

In practice, the grain morphology in fairly large castings experiences transitions [40–45]; we generally find globular regions at the bottom and dendritic regions in the central part of the ingot. The reason for this is that the grains in the bottom pile up and the higher grain density favors globular morphology. Higher grain density means that we have a large number of small grains instead of having a small number of large grains. At a given solid fraction, small grains have a larger surface area of the solid-liquid interface and smaller distances between the grains. The consequence

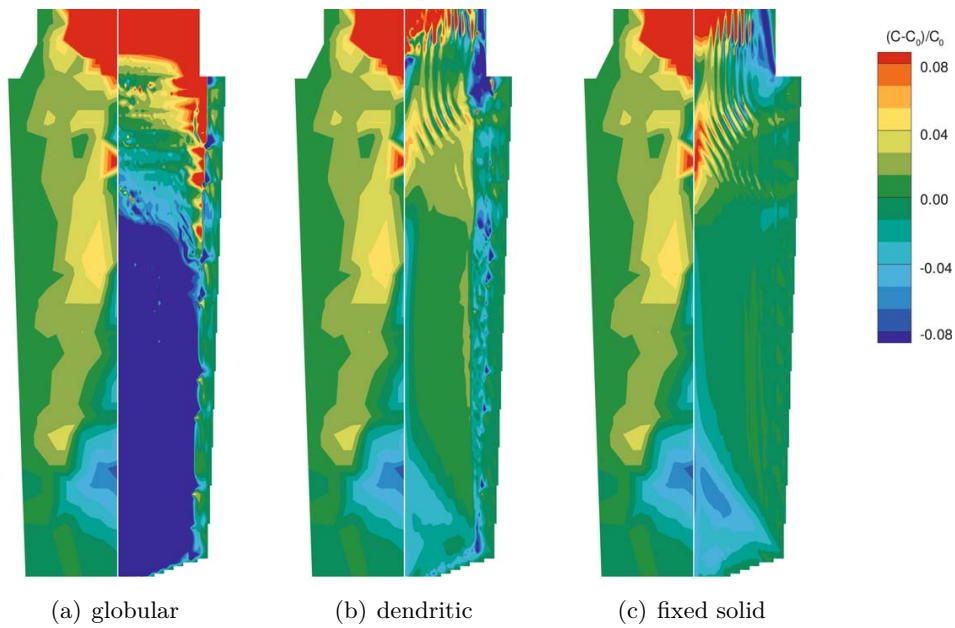


Figure 2.1: The influence of the modeled morphology of equiaxed grains on the prediction of macrosegregation in a steel ingot. The segregation ratio $(C - C_0)/C_0$ for carbon is shown, where C_0 is the nominal alloy concentration. Left: experimental results. Right: numerical simulation. (a) Globular moving grains with a predefined morphology. (b) Dendritic moving grains with morphology calculated by a grain growth model. (c) Fixed solid phase. The density of nucleation sites is 10^9 m^{-3} in all cases.

of this is that the constitutional (solutal) undercooling of the liquid between the grains is lower if grains are small. The growth of dendrite branches is stifled more by lower undercooling than the growth of the solid phase. The grains thus globularize. Conversely, if the grain density is low, growth of branches is favored and dendritic morphologies develop. This happens in the upper part of the casting that solidifies later in the process and where less nucleation sites are available.

The competition between branch growth and solid growth can be roughly illustrated by comparing scaling laws for the growth of the solid-liquid interface and for the primary tip of an equiaxed dendrite. First, consider the local solute balance at the solid-liquid interface that reads

$$(1 - k_p)C_1^*v^* = D_1 \left. \frac{\partial C_1}{\partial n} \right|_* , \quad (2.1)$$

where C_1^* is the liquid concentration at the solid-liquid interface, k_p is the equilibrium partition coefficient, v^* is the interface velocity, D_1 is the liquid diffusion coefficient, and the superscript $*$ stands for the interface. It follows that the interface velocity scales linearly with the dimensionless supersaturation, $\Omega = \frac{C_1^* - C_1}{(1 - k_p)C_1^*}$:

$$v^* = \frac{D_1}{\delta_1} \Omega , \quad (2.2)$$

where C_1 is the liquid concentration far from the solid-liquid interface and δ_1 is a characteristic diffusion length in the liquid at the interface. On the other hand, the link of the velocity of the primary tips to the undercooling can be expressed by the Ivantsov solution, $\Omega = \text{Iv}(\text{Pe}_{\text{tip}})$ and the tip selection criterion, $R_{\text{tip}}^2 v_{\text{tip}} = d_0 D_1 / \sigma^*$. If we approximate the inverse of the Ivantsov function by $\text{Pe}_{\text{tip}} = 0.61(\Omega / (1 - \Omega))^{1.32}$ and combine it with the tip selection criterion, we obtain the scaling for the tip velocity

$$v_{\text{tip}} = \frac{1.49 \sigma^* D_1}{d_0} \left(\frac{\Omega}{1 - \Omega} \right)^{2.64} . \quad (2.3)$$

For low supersaturations ($\Omega < 0.1$, applicable in all practical situations in casting) we can simplify the relation and show that the tip velocity scales with a bit more than the square of the supersaturation.

$$v_{\text{tip}} \sim \Omega^{2.64} \quad (\Omega \ll 1) \quad (2.4)$$

Very similar concepts are used in volume-averaged models of dendritic microstructure, where an ‘‘average’’ grain is conceptually represented by a dendrite envelope that contains solid and intragranular (or interdendritic) liquid, as shown in Fig. 2.2. The liquid outside the grain envelopes is called extragranular (or extadendritic). The growth of the envelope is determined

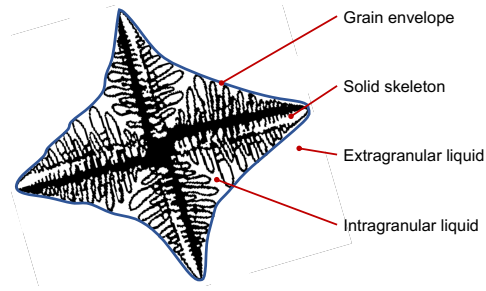


Figure 2.2: Representation of a dendritic grain by an envelope containing a solid skeleton and an interdendritic liquid.

by the speed of the primary dendrite tips, which depends on the undercooling of the extragranular liquid. The envelope has a predefined geometry and the tips correspond to the surface of a spherical or the vertices of an octahedral envelope, for example. The growth of the solid phase in the envelope is represented by diffusion-controlled growth of a shape characteristic for the internal microstructure of the grain (for example, sphere for globular grains; cylinder or plate for secondary dendrite arms) and depends on the undercooling of the liquid, as well as on the diffusion in the solid. With this representation of a dendrite, the grain morphology is quantified by the volume fraction of solid in the envelope, called the internal solid fraction:

$$g_{\text{si}} = \frac{V_{\text{s}}}{V_{\text{env}}} = \frac{g_{\text{s}}}{g_{\text{env}}}, \quad (2.5)$$

where V is the volume, g is the volume fraction and subscripts 's' and 'env' denote the solid and the envelope, respectively.

Globular-dendritic morphology transitions in the casting imply that macrosegregation is dominated by grain settling in the bottom part of the casting and by interdendritic flow in the upper equiaxed part. In such cases the morphology transition has to be accounted for in the solidification model to properly describe the macrosegregation formation. These ideas were already formulated in the past by Lesoult et al. [42, 43]. Coupled multiscale models that are able to capture the grain morphology were developed by Beckermann et al. [10], but the aspect of morphology was not investigated in detail. Detailed investigation of morphology evolution during grain motion was limited to simplified 1D models of grain settling [11]. The novelty of our studies is in the comprehensive analysis through multiscale process simulation using state-of-the-art models.

The grain density in the ingot depends on the density of nucleation sites. To explore the morphology transition we therefore varied the nucleation density in the simulations of the ingot shown before. Starting from a nucleation density of $N_0 = 10^9 \text{ m}^{-3}$, we increased it up to $N_0 = 10^{12} \text{ m}^{-3}$ along a geometrical series with a multiplier of 10. Fig. 2.3 shows the maps of the final

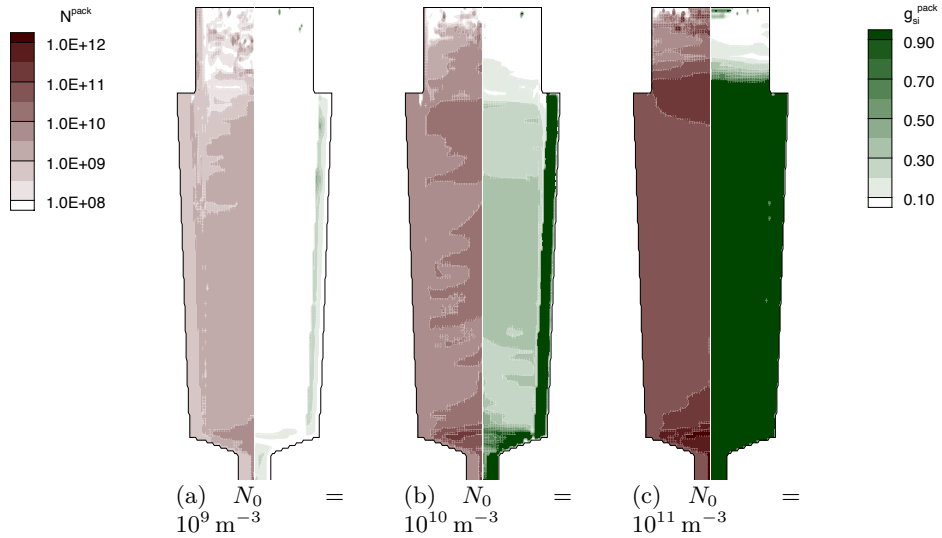


Figure 2.3: Predicted grain density (left half) and morphology (right half) in the solidified ingot for different nucleation densities, N_0 .

grain density (N^{pack}) and of a morphology parameter – the internal solid fraction at packing ($g_{\text{si}}^{\text{pack}}$) – in the solidified ingot. The internal solid fraction at the instant of packing is taken as a quantifier for the final grain morphology. If $g_{\text{si}} \ll 1$, the grains are considered dendritic, if $g_{\text{si}} \rightarrow 1$, they are globular. With a nucleation density of $N_0 = 10^9 \text{ m}^{-3}$ (Fig. 2.3(a)) the grains are strongly dendritic ($g_{\text{si}}^{\text{pack}} \sim 0.1$) throughout the ingot. They settle with a relatively small velocity and form a very permeable sedimentation layer. When the nucleation density is increased to $N_0 = 10^{10} \text{ m}^{-3}$ (Fig. 2.3(b)), the grains initially develop a globular morphology. During this initial phase a globular tightly packed sedimentation layer at the bottom of the ingot is formed. Later on, the free-floating grains in the ingot core develop to a more dendritic shape and pile up in a manner similar to the previous case. The dendritic morphology is less pronounced ($g_{\text{si}}^{\text{pack}} \sim 0.3$). With a nucleation density of $N_0 = 10^{11} \text{ m}^{-3}$ (Fig. 2.3(c)) the grains in the whole ingot are already clearly globular; an exception is only the hot top, where the grain density is reduced by the settling and the large grains develop into a more dendritic morphology.

The morphology developments observed in the simulations are summarized in a plot of the internal solid fraction versus the local grain density, shown in Fig. 2.4. We can see a clear trend and a transition that occurs at a local grain density slightly above 10^{10} m^{-3} . This transition is achieved in ingot B ($N_0 = 10^{10} \text{ m}^{-3}$), where due to grain settling the grain density is above the transition limit at the ingot bottom, and below the limit in the main part of the ingot.

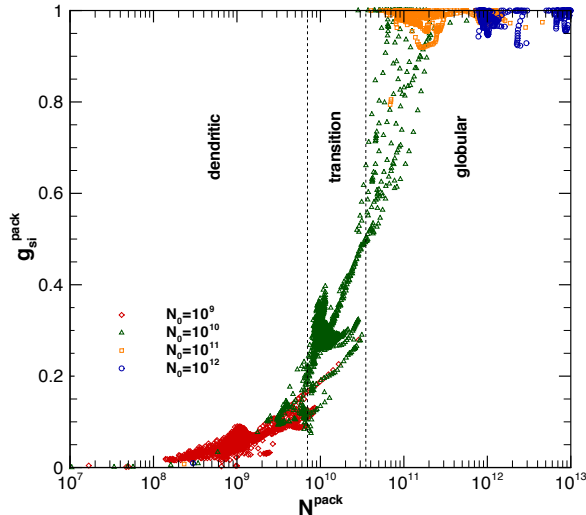


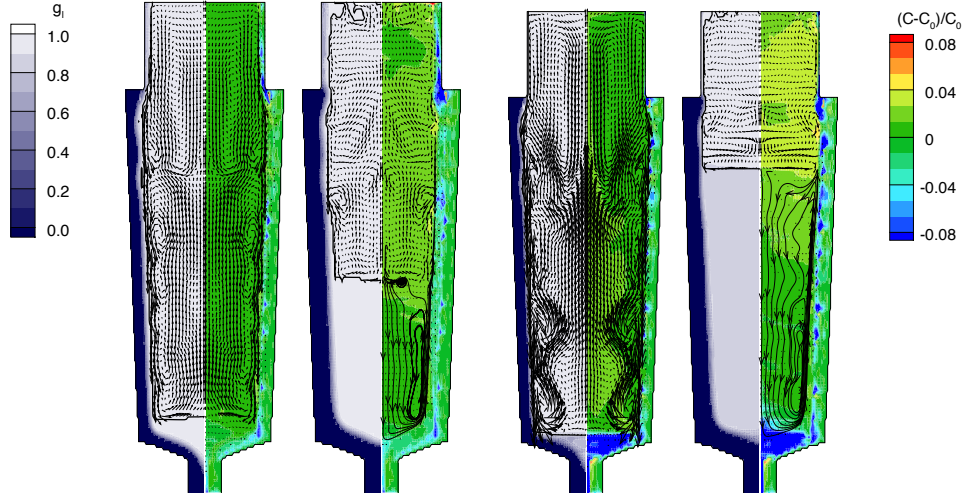
Figure 2.4: The final grain morphology in dependence of the local grain density. The trend is constructed from a compilation of results in all mesh points from four computations with different nucleation densities N_0 . The grains are dendritic for $g_{\text{si}}^{\text{pack}} \ll 1$ and globular for $g_{\text{si}}^{\text{pack}} \rightarrow 1$.

It is now interesting to take another look at the intensity of the macrosegregation induced by grain settling. We must realize that the packing front is macroscopically a discontinuity. The grain volume fraction jumps from g_{mov} in the moving grain zone just above the packed layer to g^{pack} in the packed layer. Upon packing, solid, with concentration C_s , ejects liquid, with concentration C_l . The total average concentration therefore undergoes a jump from C_{mov} above the packing front to $C^{\text{pack},*}$ below the packing front. For simplicity, we can assume that the concentration of solid and liquid (C_s and C_l , respectively), and the grain morphology (in terms of the internal solid fraction, g_i) do not change across the packing front. Furthermore, we assume that solid and liquid are in equilibrium ($C_s = kC_l$). The solute balance across the packing front then gives the concentration right after packing:

$$C^{\text{pack},*} = C_{\text{mov}} - g_i(g^{\text{pack}} - g_{\text{mov}})(1 - k)C_l \quad (2.6)$$

This shows that the settling-induced segregation, characterized by the jump ($C^{\text{pack},*} - C_{\text{mov}}$), is the more pronounced the more globular the grains (already discussed earlier in this section) and the larger the jump of grain fraction upon packing, ($g^{\text{pack}} - g_{\text{mov}}$).

We can now point to the hydrodynamic behavior of the equiaxed grains in the flow as the second key ingredient in the link between microstructure,



(a) $N_0 = 10^9 \text{ m}^{-3}$, left: 450 s, right: 900 s. (b) $N_0 = 10^{10} \text{ m}^{-3}$, left: 450 s, right: 900 s.

Figure 2.5: Evolution of the solidification of the ingot. Left half: solid fraction, solid velocity and packing front (line for $g_{\text{env}} = 0.4$). Right half: macrosegregation and liquid velocity.

macrostructure and macrosegregation. It determines the packing fraction and the grain fraction in the slurry flow prior to packing. Further, it determines the time during which the grains grow during settling and therefore determines their morphology and their final size once they are packed. Last, but not least, it determines the time the packed layer takes to build up and therefore the time during which the liquid flow through the packed layer generates macrosegregation.

Let us look at the formation of the packed layer in the 3.3 ton ingot with different grain size and morphology. With a nucleation density of $N_0 = 10^9 \text{ m}^{-3}$, i.e., an average final grain size of $\sim 1 \text{ mm}$, the whole equiaxed zone is composed of grains with a pronounced dendritic morphology. Fig. 2.5(a) shows that the dendritic grains pile up to packed layer the reaches around 1/3 of the ingot height after 15 min of solidification. With a nucleation density of $N_0 = 10^{10} \text{ m}^{-3}$ (average final grain size of $\sim 0.5 \text{ mm}$) most of the equiaxed grains are still dendritic, but with a higher internal solid fraction (Fig. 2.5(b)). Although the grain size is now smaller, their apparent weight is several times higher, due to the less pronounced dendritic morphology. The settling velocity therefore increases drastically and in 15 min the packed layer is twice as high as in the previous case.

A mass balance across the packing front gives the velocity of the packing front, $v^{\text{pack},*}$, as a function of the packing fraction, g^{pack} , the moving grain fraction, g^{mov} , and the settling velocity of the grains above the packing front,

v_s^{mov} :

$$(g^{\text{pack}} - g_{\text{mov}})v^{\text{pack},*} = g^{\text{mov}}v_s^{\text{mov}} \quad (2.7)$$

$$v^{\text{pack},*} = \frac{g^{\text{mov}}}{g^{\text{pack}} - g_{\text{mov}}}v_s^{\text{mov}} \quad (2.8)$$

The packed layer thus grows with a rate that depends on the grain settling velocity and on the jump of grain fraction. Using a weight-drag balance one can show that at low grain Reynolds numbers ($\text{Re} = \frac{d_g(1-g_{\text{env}})|\vec{v}_s - \vec{v}_l|}{\nu_l}$) the drift velocity of the grains, i.e., the difference of the solid and liquid velocity can be approximated by [46]

$$\vec{v}_s - \vec{v}_l \sim d_g^2 g_i, \quad (2.9)$$

where d_g is the diameter of the grain envelope and g_i is the internal solid fraction in the grain envelope. For globular grains $g_i = 1$ and the drift velocity increases with the square of the grain size. For dendritic grains the situation is somewhat more complex because the drift velocity also depends on the grain morphology. It turns out that for grains that are close to the transition between globular and dendritic the drift velocity *increases* with grain size. For pronounced dendritic grains (very low g_i), on the other hand, the effect of the decreasing internal solid fraction prevails and the drift velocity *decreases* with the grain size.

The determination of the packing fraction and the grain fraction in the region above the packing layer is more complex. The packing fraction for equiaxed dendrites is cannot be easily determined. A partial answer to this open question is presented in Section 2.4. The grain fraction in the moving zone depends on the packing fraction, on the rate of settling and on the growth of the moving grains.

Grain motion is a decisive phenomenon for the columnar-to-equiaxed transition (CET). The classical representation of the CET accounts for the competition of the two growth modes due to the undercooling in front of the columnar front. A key parameter is the number density of equiaxed grains, represented by a nucleation density [47]. In realistic conditions the equiaxed grain density does not depend only on nucleation, but also on grain transport and can strongly vary with time and space. Furthermore, equiaxed grains do not form exclusively on heterogeneous nuclei in the liquid zone, but often (even predominantly) on dendrite fragments spreading from the columnar zone. The source of the grains (fragments or heterogeneous nuclei) is important for their distribution across the casting and for the competition with the columnar grains. An example of the CET in the 3.3 ton ingot predicted by a CET model that accounts for grain motion (PhD of Nicolas Leriche) is shown in Fig. 2.6. We have shown that the CET observed experimentally could not be explained realistically by heterogeneous nucleation, but only by fragments as the main source of equiaxed grains. The CET depends significantly on the fragment flux, because the columnar front is blocked earlier if

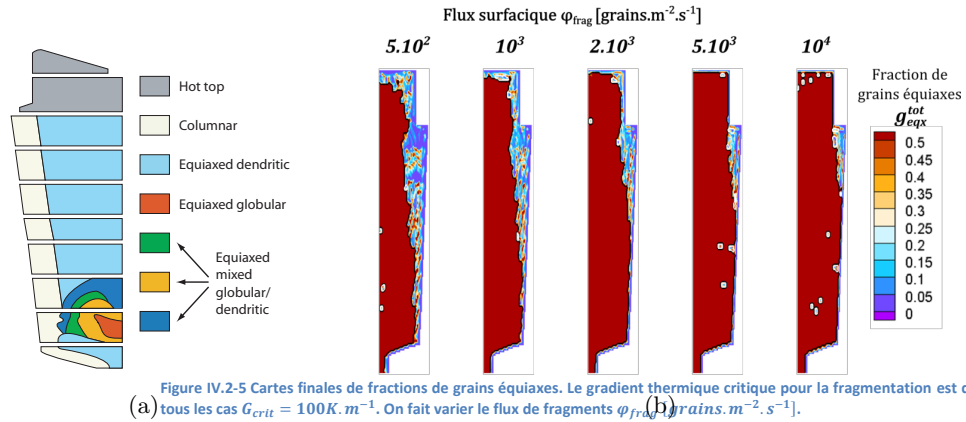


Figure 2.6: CET in the 3.3 ton ingot. (a) Experimental characterization of the macrostructure. (b) Model prediction of the CET assuming dendrite fragments from the columnar zone as the only source of equiaxed grains. The shape of the columnar zone depending on the flux of the fragments at the columnar front [fragments/(m² s)] is shown.

more equiaxed grains are generated by the fragments. Detailed analyses of CET and grain transport have been made on other ingots and can be found in Refs. [16, 17, 26, 45].

We used similar principles as for steel ingot casting in the modeling and in the analysis of the DC casting of aluminum alloys. We have been working on DC casting in collaboration with Constellium (Phillippe Jarry, Emmanuel Waz). Starting with my postdoc at LSG2M (later merged into Institut Jean Lamour), supervised by Hervé Combeau, the investigations expanded through collaboration with Arvind Kumar and the PhD theses of Marie Bedel and Laurent Heyvaert. Key to success of this work was the close collaboration with the group of Mohammed M’Hamdi of Sintef Materials and the co-supervision of the PhD theses of Knut O. Tveito and Akash Pakanati.

We performed the first comprehensive analysis of the interplay of the microstructure formation (nucleation and grain growth kinetics) and the main transport phenomena (natural convection, solidification shrinkage and grain transport) on macrosegregation in DC casting [27, 48]. This work reaches well beyond the few earlier studies on grain motion in literature, which made rather simplistic assumptions on grain growth and on nucleation [49–56] and did therefore not correctly capture the impact of grain morphology and of grain refinement. We have provided an answer, but alas, not a simple one, to the longstanding controversy on which transport phenomenon is dominant in macrosegregation formation in DC casting. We have shown that the answer depends on the alloy [25] and on the microstructure [24]. This is in line with earlier experimental studies [42, 50, 57–60] and affirms that

microstructure is a key aspect in the formation of macrosegregation.

For example, we have shown that the transition of the grain morphology between dendritic and globular is the key to the explanation of the macrosegregation profiles measured experimentally in Al alloy billets and slabs cast with and without grain refiner [24, 25, 61–65]. Figure 2.7a shows the radial profiles of Cu concentration in grain-refined and non-grain-refined Al–6%Cu billets [24]. Simulations are compared with experimental data from literature [50]. The non-grain-refined billet is simulated by using an inoculant particle density a 100 times smaller than for the grain-refined billet. Figure 2.7b shows that the progressive decrease of the inoculant density triggers a morphology transition from globular to dendritic. Further, it shows that the macrosegregation intensity, quantified by the segregation index, SI , defined as the standard deviation of the solute concentration across the billet radius, is a non-monotonous function of the microstructure that peaks for large globular grains just at the onset of the transition to dendritic morphology. We have also shown that the size of the grains and their morphology strongly depend on the transport of the inoculant particles and the grains through the mushy zone [22, 25, 27, 28, 66], which I discuss in detail in Section 2.3. Furthermore, the models enabled us to investigate the influence of process practices, such as the inlet nozzle [25, 63] and the grain-refiner addition level [24, 61]. Recently, we presented the first applications of a 3D DC casting model and comparisons to experiments on an industrial scale [63, 67, 68].

2.3 Transport of inoculant particles

Multiscale process models have brought a lot of valuable insight into the direct chill (DC) casting process for Al alloys. DC casting of aluminum alloys is remarkably different from steel ingot casting in terms of the solidification time, the size of the mushy zone, the nucleation, and the size and the morphology of the microstructures. DC casting is a semi-continuous process and the mushy zone is most of the time in a steady state. The formation of the microstructure and the macrosegregation in DC casting of aluminum alloys is also characterized by an intricate interplay of the melt flow, the motion of free-floating equiaxed grains and of inoculant particles, and the flow of extragranular liquid through the packed zone (Fig. 2.9).

A particular feature of this process is the control of the grain size by addition of Al-Ti-B or Al-Ti-C grain refiners into the molten metal. This practice introduces TiB_2 or TiC inoculant particles, which act as nucleation sites for equiaxed grains. According to the athermal nucleation theory [69], an inoculant particle becomes active and initiates the growth of a grain at the critical undercooling that is inversely proportional to the size of the particle. The size distribution of the inoculant particles (Fig. 2.10(a)) follows an

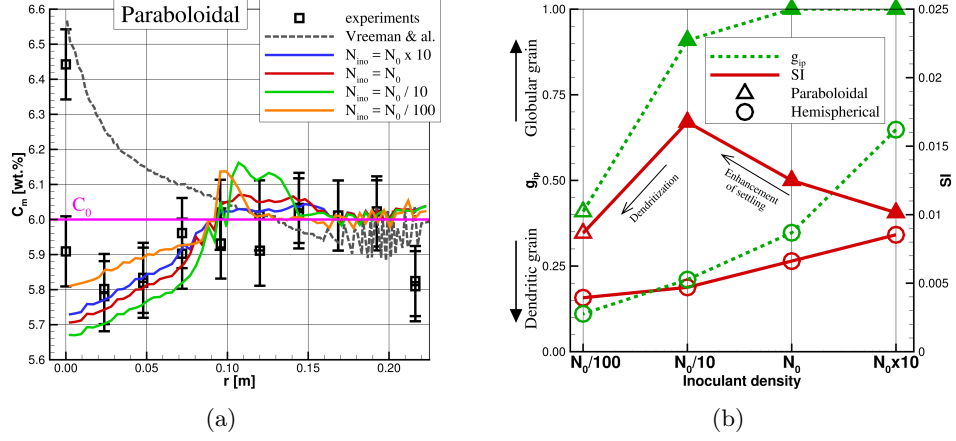


Figure 2.7: Macrosegregation and microstructure in an Al-6%Cu DC cast billet. (a) Radial macrosegregation profiles in the grain-refined and the non-grain-refined billet. Profiles of copper concentration from simulations with different nucleation densities. N_0 refers to the estimated nominal density of nuclei for the grain-refined billet. The model predictions are compared to the experimental profiles and to the simulations of Vreeman et al. [50]. (b) Mean internal solid fraction at packing (g_{si}^{pack}) and mean segregation index ($SI = [(2/R_b^2) \int_0^{R_b} (C - C_0)^2 r dr]^{1/2}$). Full symbols indicate globular and empty symbols dendritic grain morphology. Note that results for two different dendrite tip models (paraboloidal and hemispherical), which give different predictions of the grain morphology, are represented (details in Ref. [24].)

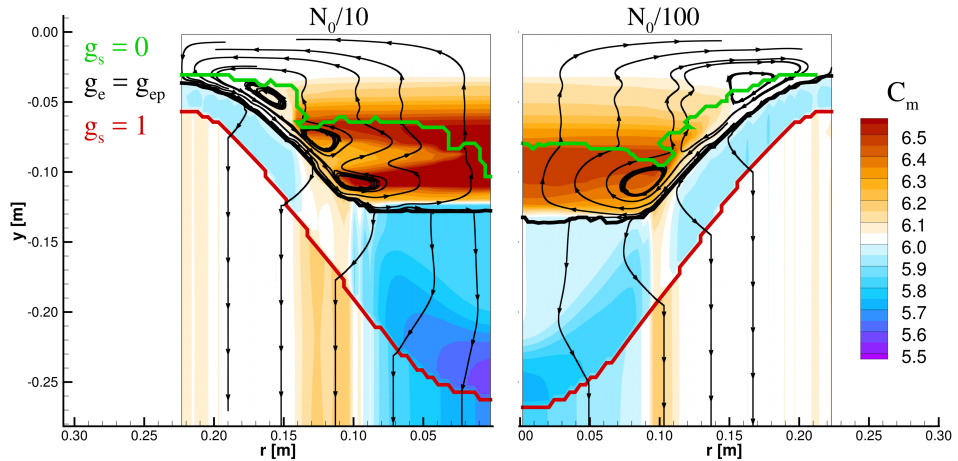


Figure 2.8: The influence of the morphology transition on the macrosegregation. Flow and fields of the average copper composition in the liquid and the solidification zone. Left: $N_{ino} = N_0/10 = 0.1$ kg/t, which gives globular grains. Right: $N_{ino} = N_0/100 = 0.01$ kg/t of grain refiner, which gives dendritic grains.

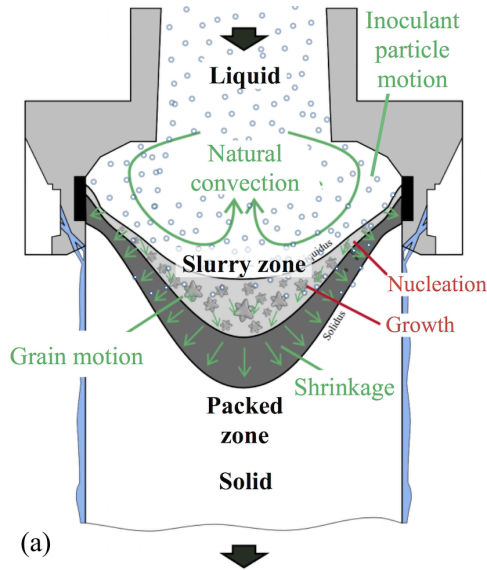


Figure 2.9: Phenomena involved in the formation of the microstructure in DC casting.

exponential distribution density function that corresponds to a distribution of activation undercooling (Fig. 2.10(b)). Due to the substantial spread of the particle sizes, nucleation occurs across a certain temperature range. A classical analysis of the ongoing nucleation events and of the concurrent growth of already nucleated grains during cooling shows that the latent heat release and the solute rejection from the growing grains at some point stifle further nucleation [69]. We call this phenomenon the nucleation-growth competition (NGC). A purely local analysis of the NGC indicates that the number of nucleated grains is then simply determined by the maximum undercooling reached during the NGC.

In casting processes the local population of both the inoculant particles and the nucleated equiaxed grains is continuously altered due to convective transport at the process scale. A local analysis of the NGC is therefore not sufficient anymore. The modeling of the grain formation requires a detailed description of the coupling of the nucleation and growth kinetics with the macroscopic transport of grain and inoculant particles. Past models were not able to capture these couplings because they used various simplifications¹. With a coupled modeling of nuclei transport and nucleation with all other solidification and transport phenomena we have succeeded for the first time to explain the mechanism of formation of the microstructure in DC casting [22, 25, 27, 28, 66]. This work also contributed to the realistic

¹Most models were based on simple equilibrium models of phase change and lacked a description of the kinetics of the microstructure nucleation and growth [49, 70–73]. Models that included grain growth kinetics did not account for grain motion [52, 74].

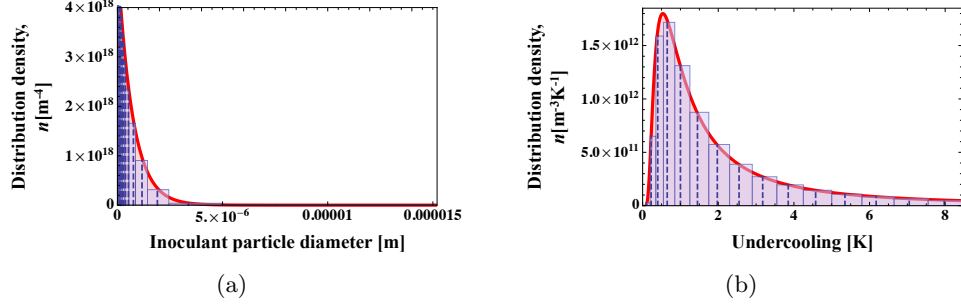


Figure 2.10: Distribution density function of the inoculant particle population with respect to the particle size (a) and activation undercooling (b), for an Al-5Ti-1B grain refiner added at 5 kg/t.

prediction of macrosegregation, as presented in Section 2.2.

To consider the transport of nuclei and the variation of the inoculant particle size distribution, the continuous distribution is discretized into classes, as shown in Fig. 2.10. Each class has its own activation undercooling, depending on the mean particle size in the class, and an initial density, calculated from the known distribution density. Moreover, the transport of nuclei is considered, assuming that they move at the velocity of the liquid. The conservation equation for nuclei of class i is

$$\frac{\partial N_{\text{nucl}}^i}{\partial t} + \nabla \cdot (\vec{v}_l N_{\text{nucl}}^i) = \Phi^i \quad (2.10)$$

$$\Phi^i = \begin{cases} -N_{\text{nucl}}^i \delta(t) & \text{if } \Delta T_{\text{uc}} > \Delta T_{\text{nucl}}^i \\ 0 & \text{else} \end{cases} \quad (2.11)$$

$$\Delta T_{\text{nucl}}^i = \frac{4\Gamma}{d_{\text{nucl}}^i} \quad (2.12)$$

where N_{nucl}^i is the volume density of nuclei of class i , \vec{v}_l is the intrinsic velocity of the liquid, Φ^i is the nucleation source term, δ is the Dirac delta function, $\Delta T_{\text{uc}} = -m_L(C_1^* - C_1)$ is the local undercooling, m_L is the liquidus slope, C_1^* is the concentration of liquid at the solid-liquid interface, C_1 is the local average concentration of the liquid, ΔT_{nucl}^i is the activation undercooling for the nuclei particles of class i , Γ is the Gibbs-Thomson coefficient, and d_{nucl}^i is the diameter of inoculant particles of class i . At the same time the conservation equation for grains is

$$\frac{\partial N}{\partial t} + \nabla \cdot (\vec{v}_s N) = - \sum_i \Phi^i, \quad (2.13)$$

where N is the local volume density of grains and \vec{v}_s is the velocity of the solid grains. The source term accounts for nucleation of grains from the

inoculant particles. The nucleation is solved coupled with the macroscopic transport and the likewise local (microscopic) phase-change.

I will use our study on the solidification of a 5182-alloy industrial scale sheet ingot [61] to illustrate the phenomena involved in microstructure formation in DC casting. We modeled the solidification of an ingot that was cast partly with 1 kg/t of Al-3Ti-1B grain refiner and partly without grain refiner. The cross-section of the ingot was 510×1897 mm and the casting speed was 1 mm/s. These experiments had been done earlier in the framework of the BRITE EURAM project EMPACT and included extensive characterizations of the microstructure and the micro- and macrosegregation in the ingots [42, 57, 58]. In the simulation, the inoculant particle size distribution introduced into the molten alloy during the casting of the grain-refined part of the ingot was approximated by the distribution of TiB_2 particles measured for an Al-5Ti-1B grain refiner [75] and corresponded to the same addition level as used in the experiments. The non-grain-refined part was modeled by the same distribution reduced by a factor of 8. This is a rough estimate that corresponds to the observed increase of the average grain size by a factor of around 2. The growth of the equiaxed grains was modeled by a three-phase volume-averaged model that calculates the grain morphology [24, 64]. The predicted grain morphologies were globular. The equiaxed grains were supposed to pack at a grain volume fraction of 0.3. In addition to the refined and non-refined case, a hypothetical case without motion of equiaxed grains and of inoculant particles was simulated. A comparison with this case shows the importance of accounting for grain and inoculant motion in the modeling of microstructure in DC casting.

Fig. 2.11(a) shows the predicted grain size across the ingot thickness. The simulations with moving grains and inoculant particles correctly predict the order of magnitude of the grain size in both the grain-refined and the non grain-refined case. All details of the grain size variations are not captured however. Note that no parameters were fitted in the grain-refined case. In the non grain-refined case the nuclei population was reduced by the same factor as the population of grains observed experimentally in the cast structure. Yet such an estimate is not enough to ensure a correct prediction. Because of the nonlinearity of the NGC, the grain density of the cast structure cannot be inferred a priori. A physically correct description of the coupled phenomena is required.

It is striking to see that the simulation without grain motion entirely fails to reproduce the grain size and its variation across the ingot thickness. In absence of grain motion, the variation of the cooling rate across the thickness is the only mechanism that controls the NGC and thus the grain size. The higher the cooling rate, the higher is the maximum undercooling attained due to the NGC and the larger is the number of activated nuclei. In a DC casting the cooling rate and thus the maximum reached undercooling are the largest at the ingot surface and decrease towards the

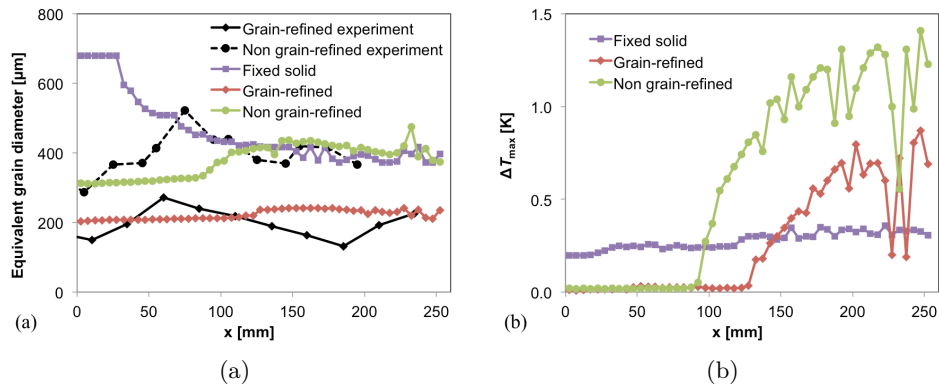


Figure 2.11: Predictions of the grain size profile across the ingot thickness. (a) Profiles of equivalent grain diameter. (b) Profiles of maximum undercooling as an indicator of the activation of inoculant particles.

centerline (Fig. 2.11(b)). If grains cannot move, the predicted grain size therefore increases from the surface to the center, as shown in Fig. 2.11(a) (“fixed solid”). This mechanism alone obviously fails to capture the essential physics.

The simulation with moving equiaxed grains and inoculant particles shows an entirely different picture. The NGC-controlled link between maximum undercooling and grain size does not hold anymore; any correlation fails. The reason is that the local population of grains is not only a result of the NGC, but also of grain and nuclei particle transport. In this way the micro-scale coupling between the nucleation and the growth of the equiaxed grains is strongly influenced by the flow at the process scale. It is therefore important to understand the flow structure, shown in Fig. 2.12. We can see a flow loop that runs as a fast current downward along the solidification front (mushy zone) to the centerline and then slowly ascends in the center. The free-floating equiaxed grains are entrained by the flow and basically follow this trajectory. They also tend to settle towards the bottom of the mushy zone because the solid grains have a higher density than the liquid.

With such a flow structure the downward current is continuously supplied with “fresh” melt carrying inoculant particles from the mold inlet. The undercooled area just below the liquidus isotherm can be imagined as a “grain factory”² in which a part of the incoming particles nucleates and forms grains. The nucleated grains are continuously drained off with the downward oriented flow current. The nucleation rate in the grain factory depends on the local undercooling (the part of the particle distribution that is activated) and on the flow rate of particles passing through the grain factory. A higher flow velocity does not only supply the inoculant particles at

²Term coined in [66] by Ph. Jarry and M. Rappaz in reference to our work.

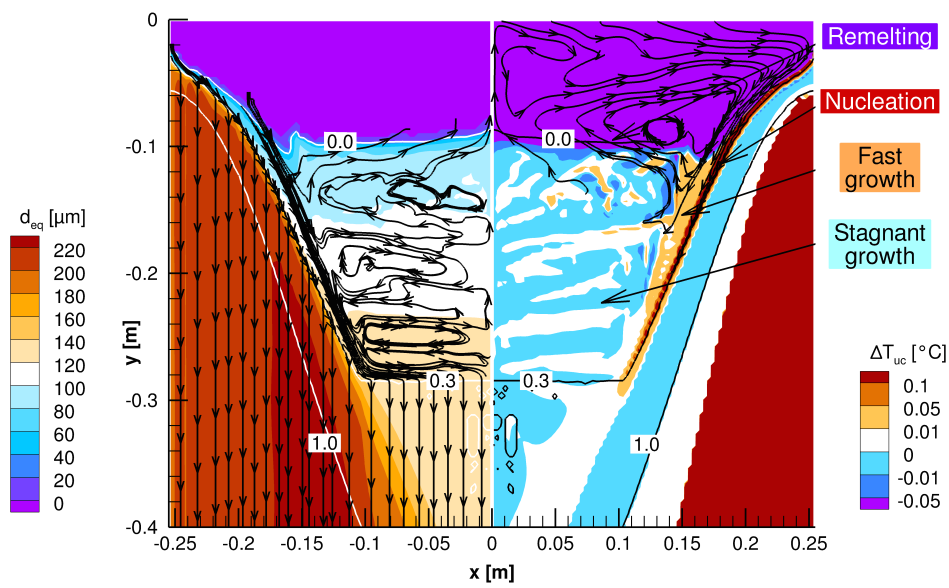


Figure 2.12: Nucleation, growth, and transport of free-floating equiaxed grains. Left: grain size and solid velocity streamlines. Note that the streamlines give a good approximation of the grain trajectories because the flow structure is in a steady state. Right: undercooling and liquid velocity streamlines in the liquid zone. Note that nucleation occurs only at undercooling of more than 0.1 K. Solid fraction contours indicate the liquidus ($g_s = 0$), the packing ($g_s = 0.3$), and the solidus ($g_s = 1$) fronts.

a higher rate, but also carries away the nucleated grains faster. Through the NGC, a faster evacuation of growing grains further increases the undercooling and promotes nucleation. Incidentally, the cooling rate in this part of the mushy zone is also rather high, ensuring efficiency of nucleation. We can also note that the undercoolings are much higher than in the simulation without grain motion, thus activating a larger portion of the nuclei particle distribution. In the non grain-refined ingot the reached maximum undercoolings are almost twice as high as in the grain-refined ingot (Fig. 2.11(b)). Due to the smaller population density of growing grains in this case, the NGC results in higher undercooling and a much larger portion of the inoculant particle size distribution is activated in the nucleation process.

The most interesting thing is that *all* the melt that enters the mushy zone first passes through the grain factory. This can be seen from the streamlines in Fig. 2.12. Furthermore, the map of undercooling in Fig. 2.12 shows that the highest undercooling in the whole mushy zone is reached in the grain-factory area. This means that all sufficiently large inoculant particles that enter the mushy zone are activated in the nucleation area. Only smaller particles that require larger undercoolings remain. They cannot be activated later on their trajectory because the undercooling in the rest of the slurry zone is much lower. This means that nucleation happens *exclusively* in the thin grain factory area running along the sloped part of the mushy zone (marked in Fig. 2.12). This area is the generator of equiaxed grains for the *whole* casting.

A part of the grains that nucleate in the grain factory is carried directly to the bottom to the packed zone. A part is first spread out throughout the slurry zone and settles later. The undercooling map of the grain-refined ingot in Fig. 2.12 shows the different areas of grain nucleation and growth. An undercooling higher than 0.1 K indicates a nucleation area. An undercooling higher than 0 K indicates an area of grain growth. Higher undercooling results in faster growth. A negative undercooling means superheat and indicates dissolution of the solid grains. The model thus reveals four regions of grain nucleation and growth in the slurry zone: (i) the “grain factory”, a very small nucleation region at the packing front close to the entry point of the melt flow, (ii) a region of fast solidification next to the inclined packing front, (iii) a stagnation region in the core of the slurry zone, and (iv) a remelting region close to the liquidus front. The model results also indicate the disparate origin and evolution of the grains found in different parts of the cast structure across the ingot thickness. The grains in the outer parts of the ingot undergo a short period of fast growth before packing at the inclined part of the packing front. The grains in the center are a mix of two types of grains with different histories. The fast-growing grains packed immediately after settling from the descending flow current, and the slow-growing grains settled to the bottom only after a prolonged trajectory through the stagnant growth region. The two types of grains form a duplex structure, observed

in many experiments [42, 57, 59, 76–84]. Such a duplex structure consists of slowly growing coarse (cellular) grains and fast growing dendrites. Apart from the grain morphology, microsegregation characterizations indicate a mark of a different thermal history for the two types of grains.

Formerly, nucleation in DC casting was thought to take place across the whole mushy zone, in a wide region just below the liquidus isotherm [66, 74]. Our analysis, assisted by modeling [22, 27, 28, 48, 85, 86] showed us that nucleation events are limited to an extremely small region. This region generates all grains that constitute the entire ingot. Together with the flow in the mushy zone, the growth and nucleation kinetics in this zone govern the final grain size across the whole ingot cross-section.

Key to the modeling of the NGC in presence of grain and nuclei motion is an accurate description of grain growth kinetics and of interactions, needed to ensure a realistic prediction of the undercooling. This aspect would warrant further investigation with the objective of refining the volume-averaged models. Both well controlled lab scale experiments and mesoscopic simulations could contribute to an accurate characterization of the growth kinetics in the nucleation zone. Upscaling to macroscopic models could then improve the predictive power of process-scale models of microstructure. I will discuss this further in Chapters 4 and 5.

2.4 Packing of equiaxed grains

We have shown that the formation of the packed layer of equiaxed grains is one of the keys to the understanding of macrosegregation and of macrostructure in various processes. We were able to distinguish between the packing of different grain morphologies by making the rudimentary assumption that grains pack at a certain envelope volume fraction. It followed that the solid fraction of packing depends on the grain morphology.

Unfortunately, little is really known about the packing of dendritic grains. Even the most elementary piece of information on the packing, the packing fraction, is poorly characterized. Because of the particular morphology of the dendrites, packing fractions of spheres or other particles of simple convex shape cannot be used. Models of casting processes, where the packing fraction is one of the key parameters, resort to values in a very wide range, from 0.20 up to 0.637 [16, 18, 24, 27, 50, 87]. The choice is mostly justified indirectly, by a good fit of the model prediction to experimental characterizations of the piece, for example, in terms of chemical segregation [18, 24]. The disparities in packing fraction are speculated to be due to differences in grain morphology and in hydrodynamic conditions during the settling of the grains; however, clear understanding is lacking.

Particle packing has historically been an important problem in physics, essential for the understanding of the properties of granular media as well

as of the atomic structure and state transitions in matter [88]. Extensive work has been done on assemblies of spherical particles. Much less knowledge exists on nonspherical particles and most studies tackle only convex particles [89–91]. Dendritic crystal grains have a nonconvex shape and the packing properties of such particles are strikingly different from convex particles. The packing fraction depends strongly on their topology and various shape parameters. Values of solid fraction as low as ~ 0.1 have been reported for random arrangements of dendrite-like spiky equiaxed particles [92]. Research on nonconvex particles is scarce and is only emerging [93, 94].

The packing fraction for random arrangements of particles does not only depend on their shape. It also depends on mechanical interactions with the fluid and contact interactions of the particles prior to packing. Imagine tapping on the side of a coffee can. For example, for monodisperse hard noncohesive spheres, the random packing fraction has theoretically been shown to be between 0.536 (random loose packing) and 0.634 (random close packing) [95]. Viscous dissipation is expected to play a dominant role in packings resulting from settling of dendritic grains during solidification. The inertia of the grains is low due to the small solid-liquid density difference (e.g., $(\rho_s \rho_l)/\rho_s = 0.06$ in an Al-Zn alloy).

In a mushy zone, the two phase flow with free-floating grains goes through the whole range of possible flow regimes, from dilute to dense. It undergoes a particularly sharp transition at the packing front, where the dynamics changes entirely across a length scale of several grains. The description of this transition in macroscopic models is certainly not satisfactory. In macroscopic models the transition is described by an abrupt change in flow regime at the packing front. Above the packing front a gradual change of grain fraction is assumed. The question is at what length scale does the transition from free-floating to packed state take place and which are the governing phenomena for the grain motion dynamics in this transition zone.

Our work on grain packing gravitated around two central questions. The first is that of the structure of the packed layer. At what volume fraction do the grains pack and how does the packing fraction depend on the grain morphology? The second question is that of the dynamics of grain motion on the transition from free-floating grains to packed immobile grains. Over what length and traveling time does the transition occur and which forces govern the dynamics of the grains during this transition?

These questions were clarified in our study of the dynamics of motion and packing of solid particles in a viscous liquid. Within the framework of the PhD thesis of Antonio Olmedilla we used an approach that combines experiments of sedimentation of model particles and the modeling of the granular medium based on the discrete element method (DEM). Following the principles of hydrodynamic similarity we were able to reproduce the conditions of the metallurgical processes in a lab experiment using a transparent liquid and model particles. The key in the design of the experiment

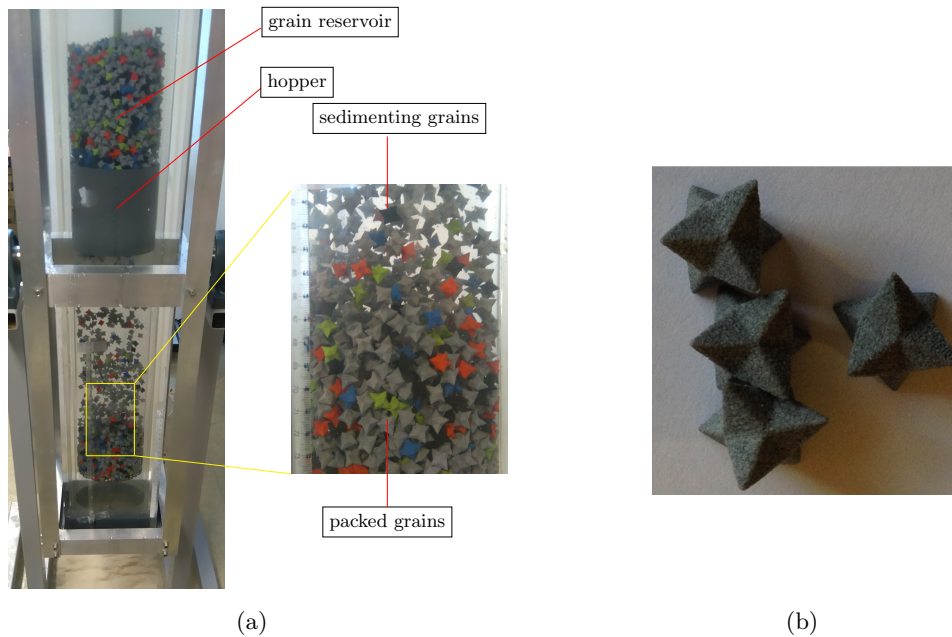


Figure 2.13: Experimental setup for the study of particle sedimentation and packing: (a) sedimentation column, (b) dendrite-like model particles used in the experiments.

was the right combination of materials and fluids. It enabled us to build a sedimentation column, shown in Fig. 2.13(a), large enough to eliminate confinement effects on the grain population and small enough for easy handling of a large number of experiments. The dendrite-like model particles, shown in Fig. 2.13(b), were built by additive manufacturing using a quasicrystal-polymer composite that ensured an accurate and stable target density – a critical parameter due to the very small density difference between solid and liquid. The DEM model was used to simulate settling configurations. Examples of settling simulations and of the particles used in the simulations are shown in Figs. 2.14 and 2.15, respectively. DEM simulations gave us access to information on the collective grain dynamics that cannot be obtained experimentally, such as the individual grain trajectories, rotations, and contacts, or the time evolution of the local solid fraction. A larger variety of grain morphologies was also studied by numerical simulation. The originality of the in-house model GGDEM [96–99], entirely developed by Antonio Olmedilla, is the simplified description of the influence of the liquid (drag, lubrication) by smartly formulated constitutive models. Thanks to this simplification, the computation time is several orders of magnitude smaller than with coupled CFD-DEM models that resolve the flow of the liquid directly.

We have shown that the most important influence on the packing fraction

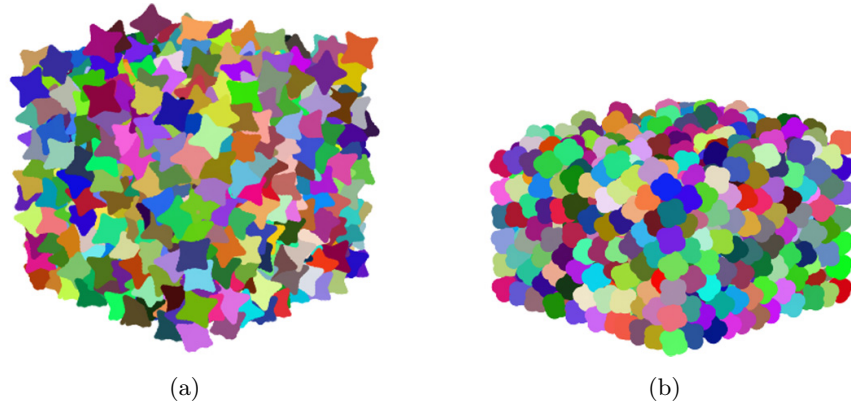


Figure 2.14: DEM simulations of packings of (a) dendritic and (b) globular grains.

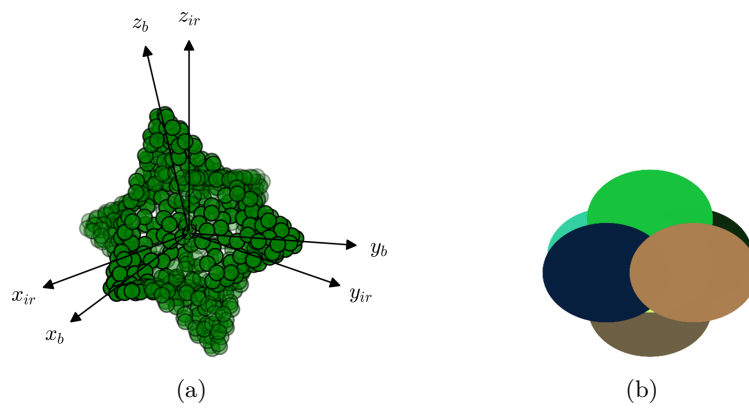


Figure 2.15: Clumped-sphere particle models used in the DEM simulations to represent: (a) dendrite envelopes, (b) globular grains.

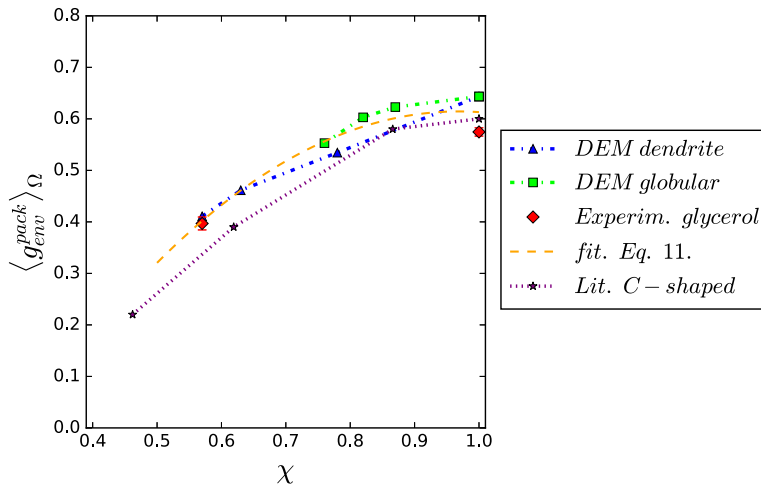


Figure 2.16: Universal relation between the shape of hexapod (dendrite-like) particles and the average packing fraction. The shape is characterized by the parameter χ , the ratio between the equivalent diameter and the widest length of the particle. Data from DEM simulations and from experimental results for sphere and dendrite packings in glycerol are shown. Simulation results for hexapod particles packed by sequential deposition under gravity (“Lit. C-shaped”) of Malinouskaya et al. [92] are also included.

of dendrite-like hexapod particles is that of the envelope shape. As the shape of the particles changes from spherical (globular) towards more nonconvex (dendritic), the packing fraction decreases. This trend is shown in Fig. 2.16 in a manner that appears to be universally valid for hexapod particles. To describe the influence of the hexapod particle shape on the packing fraction we proposed the ratio between the equivalent diameter and the widest length of the particle as a universal shape parameter [98].

The influence of the fluid in which the grains settle is defined by the particle Stokes number, St^3 . Grain settling in solidification processes is clearly in the low inertia regime, $St \approx < 10$. We have shown that in this range the packing fraction depends only weakly on St and is close to the limit of random loose packing [98]. The influence of hydrodynamic conditions on packing in solidification processes is thus much smaller than the impact of the particle morphology.

The dynamics of grain sedimentation near the packing front has also been characterized [99]. We have shown that the grains begin to decelerate at a distance from the packing front of approximately 6 times the equivalent diameter of the grain. This gives a length scale for the transition zone between bulk settling and final packing. In this zone the interactions between grains are dominated by the effects of lubrication, by collisions, as well as

³ St is the ratio of the viscous relaxation time to the characteristic time scale of particle motion, d_p/v_{ss} , where d_p is the particle diameter and v_{ss} is the steady-state settling speed.

by the effect of the liquid ejected upwards. These collective effects considerably increase the residence time of the grains in the sedimentation zone in comparison with the sedimentation of a single grain.

The impact of this work reaches beyond solidification; it also represents an important contribution in the field of granular media. Indeed, these works are among the rare ones to address packing of nonconvex particles as well as the packing in viscous fluids. Possible future work should investigate the influence of particle growth during the settling on packing. More complex hydrodynamic conditions that can be present in solidification processes, such as settling to an inclined packing front and in the presence of a shear flow, should also be investigated. Additionally, the results provided in this work can be applied to improve the current modeling tools of industrial casting processes.

2.5 Flexible models and algorithms for coupling micro-and macro-models

This section presents the highlights of our model and algorithm developments for macroscopic models.

We developed a new algorithm for the coupling of the governing equations of macroscopic solidification models [100, 101]. Most of the conservation equations in such Euler-Euler type models are convection-reaction equations. As an example, consider the volume-averaged solute conservation equation for phase k ,

$$\frac{\partial}{\partial t} \left(g_k \langle C_k^i \rangle^k \right) + \nabla \cdot \left(g_k \langle C_k^i \rangle^k \langle \vec{v}_k \rangle^k \right) = \frac{1}{\rho} \left(\underbrace{J_k^{i,j}}_{\substack{\text{Interphase} \\ \text{solute} \\ \text{diffusion}}} + \underbrace{J_k^{i,\Gamma}}_{\substack{\text{Phase} \\ \text{change}}} + \underbrace{J_k^{i,\Phi}}_{\substack{\text{Grain} \\ \text{nucleation}}} \right), \quad (2.14)$$

where g_k is the phase volume fraction, $\langle C_k^i \rangle^k$ is the volume-average solute concentration in phase k , and $\langle \vec{v}_k \rangle^k$ is the volume-average velocity of phase k . We can see that this equation involves an advection operator that operates on the macroscopic scale and reaction operators that describe the nucleation and the solid-liquid phase change and operate locally. In the full model, six equations of this type are involved (conservation of grain population, phase fractions, solute concentrations, etc.). They are all coupled with the equations of momentum and heat transport, and with each other via the reaction terms. In a general notation we can write this type of equation as

$$\frac{\partial \phi}{\partial t} = A\phi + B\phi, \quad (2.15)$$

where the operators A and B represent the advection and the reaction, respectively. There are different ways of solving the equation system. We

proposed an algorithm based on the ideas of the separation of time scales. We show that a time scale separation between the microscopic and macroscopic phenomena allows the use of a so-called *operator splitting* procedure [102, 103]. This procedure solves and integrates the macroscopic advection in a first solution step (transport – *tr*) and the contributions of the microscopic phenomena (growth – *gr*) in a second solution step that is initialized with the result of the transport step.

$$\begin{aligned} \frac{\partial \phi^{\text{tr}}}{\partial t} &= A\phi^{\text{tr}}, & \phi^{\text{tr}}(t_0) &= \phi_0 & \text{on } [t_0, t_0 + \Delta t] \\ \frac{\partial \phi^{\text{gr}}}{\partial t} &= B\phi^{\text{gr}}, & \phi^{\text{gr}}(t_0) &= \phi^{\text{tr}}(t_0 + \Delta t) & \text{on } [t_0, t_0 + \Delta t]. \end{aligned} \quad (2.16)$$

The final value of the integration is then given by $\phi^{\text{gr}}(t_0 + \Delta t)$. This scheme allows one to integrate the macroscopic advection operator separately for each equation, i.e., in a decoupled way, because it only involves the velocity field. The growth operator involves other quantities ϕ and is nonlinear. It is therefore solved in a coupled way using a custom coupling algorithm. The developed splitting algorithm is attractive for several reasons: (i) improved stability of the solution scheme due to the separation of the stiff (nucleation, growth) from the nonstiff operators, (ii) possibility of using different timesteps for different operators, (iii) better flexibility of code development.

In static ingot casting and in continuous casting of steel the columnar-to-equiaxed and the equiaxed-to-columnar structural transitions (CET and ECT) are important features of the macrostructure. They are the result of a competition between the two modes of growth. In the modeling of these transitions it is necessary to take into account the motion of equiaxed grains that can either nucleate heterogeneously in the bulk liquid or result from the fragmentation of columnar dendrites [17, 26, 104]. These phenomena are also determining for the evolution of the morphology of the grains (globular/dendritic) and for the macrosegregation [26, 45, 105]. In the framework of the PhD of Nicolas Leriche [16] we developed a novel model of the CET and ECT, where the growth of the columnar zone is described and is fully coupled with the motion of equiaxed grains and macrosegregation. An original numerical strategy has been developed, which allows application on industrial size castings. The main characteristic of the model is that it considers coupled growth of both types of structures only in the zone where they coexist, i.e., near the tips of the primary columnar dendrites. In this zone a specially designed constitutive model of concurrent columnar and equiaxed growth is used. It accounts for six hydrodynamic phases (solid, extra-granular liquid, and intra-granular liquid for each structure type). Everywhere else, the structure is considered to be either fully columnar or fully equiaxed. The columnar front is tracked with a simple grid-based method. Furthermore, we developed a clever formulation of the model [64] that reduces the number of solute transport equations (PDEs) that need to be solved, from five to

only two. These features allow for reasonable computational times even in industrial size castings, while describing the solutal and mechanical blocking phenomena responsible for the CET. The model has been successfully applied on industrial steel ingots of up to 100 tons. Comparisons with experimental characterizations of macrosegregation and macrostructure (CET and ECT, grain size, grain morphology) of ingots cast under different conditions were made. The model studies show that: (i) the structure of the ingots strongly depends on the origin of the equiaxed grains (heterogeneous nucleation or fragmentation) and (ii) that it can be predicted realistically only by taking into account the motion of the grains. Further, they show that fragmentation of the columnar dendrites is often the main source of equiaxed grains in the ingots analyzed and that the hot top part is the main source of fragments.

All model developments reported here have been implemented in the industrial version of the software SOLID[®], distributed by Sciences & Computers Consultants, and are therefore available to our industrial partners. Currently, a new generation of industrial software is being developed in a collaboration joining forces of IJL, O2M Solutions (an startup originating from IJL), Sciences & Computers Consultants, and several partners from the metallurgical industry.

Chapter 3

Mesososcopic modeling

3.1 Introduction

Dendritic (treelike) crystals or grains are the most common growth form in solidification of metal alloys. Their growth is governed by an intricate interplay between diffusions or convection of heat and chemical species (solutes) and capillary effects. Furthermore, in castings the growth of dendritic crystals is influenced by adjacent grains. The grains can “feel” each other due to the overlap of thermal and solutal fields surrounding each growing grain. Analytical solutions of dendritic growth are limited to the description of a single isolated dendrite tip that grows by diffusion in an infinite, uniformly undercooled melt [106, 107].

Complex dendritic structures can be simulated directly by phase-field methods, which directly resolve the dendritic structure in detail but are computationally expensive. These and other microscopic methods thrived and matured in the last decade [108–113]. Phase-fields methods have become the most common approach to the numerical simulation of dendrite growth. However, because phase-field methods need a very fine mesh, computing and memory requirements are large. Most simulations are limited to the scale of a few dendrites, to two dimensions and purely diffusive conditions. Only recently simulations of large ensembles of grains in 3D have been reported [114, 115]. They required complex high-performance parallel computing algorithms and massive supercomputing resources.

A number of approaches has been proposed at the scale of grains – the mesoscopic scale. The common denominator of these approaches is that the description of the grain geometry is simplified in order to lower the required mesh resolution. Several models are based on the tracking of a dendrite envelope [116–122]. Another approach for dendritic growth is a simplified description of the branched dendritic arrays by a network of thin needles [123–125]. Models for globular growth are based on tracking of polyhedral geometries defined by Voronoi tessellation [126, 127]. Some

models lower the computational cost and reach to mesoscopic scales by a simplified, less accurate description of the solid-liquid interface [128–130].

The interest of mesoscopic methods is in the simulation of phenomena at the scale of an ensemble of grains where collective interactions need to be described. These interactions can be thermal, solutal, hydrodynamic, or mechanical. Phenomena such as grain interactions in equiaxed growth, grain competition and texture in columnar growth, equiaxed growth during grain settling, CET, freckles, and hot tearing can be simulated. Furthermore, mesoscopic methods are necessary to bridge the gap between microscopic and macroscopic methods in upscaling. Simulations at the scale of an REV used in macroscopic methods is only possible with mesoscopic methods. With this objective in mind, we chose to use the mesoscopic grain envelope model (GEM) of Steinbach, Beckermann et al. as the most promising method. The GEM is particularly suitable for our applications because it gives an accurate description of solutal interactions, it naturally provides a conservative description of solute transport and of phase fractions, and can accommodate the description of convection. Another convenient aspect is that it is built on the same volume-averaging formalism as the macroscopic methods we use for process-scale modeling, and thus on very similar equations. This means that similar numerical methods and coupling algorithms can be used as for macroscopic models.

3.2 The Mesoscopic Grain Envelope Model

The mesoscopic Grain Envelope Model (GEM) was originally developed for diffusion-controlled dendritic growth in pure substances by Steinbach et al. [118, 131]. It was later extended to binary alloys [132] and to convection [133, 134]. In the envelope model the complex branched shape of a dendritic grain is described in a simplified way by an envelope, a smooth surface that links the tips of the actively growing dendrite branches and by a continuous solid fraction field inside the envelope. The growth of the envelope is calculated from the growth velocities of the tips, using a constitutive model. In an alloy, the growth of the dendrite tips is governed by the solute flux that the tips eject into the liquid and is therefore determined by the local supersaturation of the liquid in the vicinity of the envelope. The details of the branched dendritic structure inside the envelope are not resolved; the interior of the envelope is instead described in a volume-averaged sense by a phase-fraction field, as shown in Fig. 3.1. The phase change that determines the evolution of the structure, i.e., of the phase fraction field, inside the growing envelope is controlled by the exchange of solute with the surroundings of the grain. The transport of solute at the mesoscopic scale is described by volume-averaged transport equations.

Two key assumptions of the mesoscopic model are: (i) the phenomena

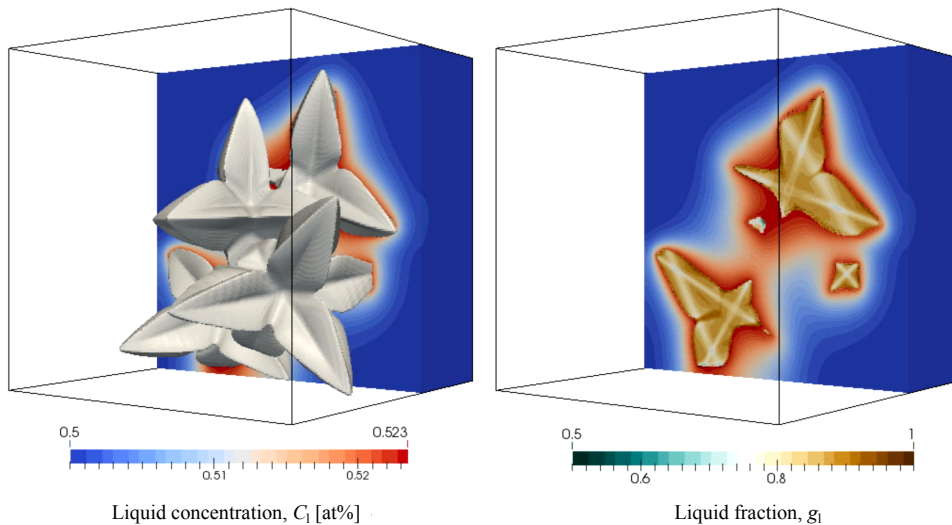


Figure 3.1: Example of results of a simulation with the mesoscopic model. Left: four interacting equiaxed grain envelopes. Right: a slice across showing the liquid fraction field in the interior of the envelopes and the concentration field in the liquid outside the envelopes.

controlling the growth of a dendrite tip are universal and are therefore valid for tips of any order (primary, secondary, tertiary, ...) and (ii) the characteristic time of the solute transport at the small (tip) scale is much smaller than at the large (grain) scale. These assumptions enable us to use the Ivantsov analytical solution [135] in the stagnant-film formulation of Cantor & Vogel [136] to describe the growth of all dendrite tips.

The Cantor & Vogel solution of steady-state diffusion around a growing parabolic tip relates the tip growth Péclet number, Pe_{tip} , to the supersaturation, Ω_δ , in the liquid at a finite distance, δ , from the tip. For a 3D tip,

$$\Omega_\delta = Pe_{\text{tip}} \exp(Pe_{\text{tip}}) \left\{ E_1(Pe_{\text{tip}}) - E_1 \left[Pe_{\text{tip}} \left(1 + \frac{2\delta}{R_{\text{tip}}} \right) \right] \right\} \quad (3.1)$$

The Péclet number is defined by $Pe_{\text{tip}} = R_{\text{tip}} V_{\text{tip}} / (2D_1)$, where R_{tip} is the tip radius, V_{tip} is tip growth velocity, and D_1 is the solute diffusion coefficient in the melt. The supersaturation is defined by $\Omega_\delta = (C_1^* - C_1^\delta) / ((1 - k_p) C_1^*)$ where C_1^* is the liquid equilibrium solute concentration (concentration at the interface), C_1^δ is the solute concentration in the liquid at the distance δ from the tip, and k_p is the alloy partition coefficient. The tip velocity is obtained from Pe_{tip} by a tip selection criterion that reads $R_{\text{tip}}^2 V_{\text{tip}} = d_0 D_1 / \sigma^*$, where $d_0 = \Gamma / (m_L C_1^* (k_p - 1))$ is the capillary length, m_L is the liquidus slope, Γ is the Gibbs-Thomson coefficient, and σ^* is the tip selection parameter. It

follows that the tip speed is given by

$$V_{\text{tip}} = \frac{4\sigma^* D_l \text{Pe}_{\text{tip}}^2}{d_0}. \quad (3.2)$$

The tips are assumed to grow in prescribed preferential growth directions. For example, a typical cubic crystal dendrite is given six possible growth directions perpendicular to each other ($\langle 100 \rangle$ directions). The normal envelope growth velocity, \vec{v}_n , is then calculated from the local tip speed, V_{tip} , by the relation

$$\vec{v}_n = V_{\text{tip}} \vec{n} \cos \theta, \quad (3.3)$$

where θ is the angle between the outward drawn normal to the envelope, \vec{n} , and the preferential growth direction that forms the smallest angle with the local envelope normal. To propagate the envelope on a numerical mesh an interface-capturing method [137] is used, combined with a surface reconstruction method for improved accuracy [119].

The fluid flow and the solute transport by diffusion and by convection at the mesoscopic scale are described by volume averaged equations that are valid in the whole domain, i.e., both inside and outside the envelopes. Solidification inside the envelope is modeled using the Scheil assumptions: thermodynamic equilibrium at the solid-liquid interface, negligible diffusion in the solid and instantaneous diffusion in the liquid. This implies that the concentration of the binary liquid inside the envelope is linked to the temperature field by $C_1^* = (T - T_f)/m_L$, where C_1^* is the liquid equilibrium concentration, T is the temperature, and T_f is the melting temperature of the pure solvent. These assumptions lead to the conservation equation for the solute in the liquid phase:

$$g_l \frac{\partial C_1}{\partial t} + \nabla \cdot (g_l \vec{v}_l C_1) = D_l \nabla \cdot (g_l \nabla C_1) + C_1 (k_p - 1) \frac{\partial g_l}{\partial t}, \quad (3.4)$$

where \vec{v}_l is the volume averaged liquid velocity. This solute transport equation is identical to the one in the diffusive model [138], but has an additional convection term.

The solution of Eq. (3.4) gives C_1 outside the envelope and g_l inside the envelope. Outside the envelope, the material is fully liquid ($g_l = 1$) and Eq. (3.4) reduces to a single phase convection-diffusion equation. Inside the envelope, the liquid is in thermodynamic equilibrium, such that $C_1 = (T - T_f)/m_L$, where the temperature is assumed to be known. With C_1 known, Eq. (3.4) gives the evolution of the liquid fraction inside the envelope. The concentration of the solid, C_s , inside the envelope is given by

$$\frac{\partial (g_s C_s)}{\partial t} = -k_p C_1 \frac{\partial g_l}{\partial t}, \quad (3.5)$$

where $g_s = 1 - g_l$ is the solid fraction.

In the modeling of the liquid flow the interior of the envelopes is considered as a porous medium. The drag on the liquid flowing through the envelopes depends on the permeability of the porous medium. The flow is described by the volume averaged mass and momentum conservation equations:

$$\nabla \cdot (g_1 \vec{v}_1) = 0 \quad (3.6)$$

$$\begin{aligned} \frac{\partial (g_1 \vec{v}_1)}{\partial t} + \nabla \cdot (g_1 \vec{v}_1 \otimes \vec{v}_1) = & -\frac{g_1}{\rho_0} \nabla p + \nabla \cdot (g_1 \nu_1 \nabla \vec{v}_1) \\ & - \frac{\nu_1 g_1^2}{K} \vec{v}_1 + g_1 [1 - \beta_C (C_1 - C_0) - \beta_T (T - T_0)] \vec{g} \end{aligned} \quad (3.7)$$

where ρ_0 is the reference density, p the pressure, ν_1 the kinematic viscosity, K the hydrodynamic permeability, β_C and β_T the solutal and thermal volume expansion coefficients, respectively, C_0 and T_0 the reference solute concentration and reference temperature, respectively, and \vec{g} the gravity acceleration. Note that the Boussinesq approximation for buoyancy-driven flow is used and that the thermal expansion of the liquid is neglected in this work, but can easily be incorporated in the model. The permeability of the intra-granular dendritic structure is modeled by the isotropic Blake-Kozeny relation and depends on the liquid fraction and on a characteristic length of the porous structure, ℓ_c :

$$K = \frac{\ell_c^2 g_1^3}{180 (1 - g_1)^2}. \quad (3.8)$$

This relation is certainly an oversimplification, but it provides the basic physical ingredients of permeability. An accurate determination of ℓ_c is not trivial, however it is expected to be of a similar order of magnitude as the secondary dendrite arm spacing. Note that permeability models for dendrites at this scale do not exist. We may speculate however, that they would need to account for anisotropy due to the branch directions and for more than one characteristic length scale.

To propagate the envelope on a numerical mesh the phase-field sharp-interface capturing method [137] is used. In this method the tracked front is given by the level set of a continuous indicator field ϕ . The transition of ϕ from 1 to 0 in the vicinity of the front follows a hyperbolic tangent profile given by the so-called kernel function [139]

$$\phi(n) = \frac{1}{2} \left[1 - \tanh \left(\frac{n}{2W} \right) \right], \quad (3.9)$$

where n is the distance from the center of the profile. The phase-field equation that is used to propagate the field ensures that the profile is self-preserving and retains its shape and its characteristic width W . The phase-field

equation for the propagation of the indicator function ϕ is [139]:

$$\frac{\partial \phi}{\partial t} + v_n \vec{n} \cdot \nabla \phi = - b \underbrace{\left[\nabla^2 \phi - \frac{\phi(1-\phi)(1-2\phi)}{W^2} - |\nabla \phi| \nabla \cdot \left(-\frac{\nabla \phi}{|\nabla \phi|} \right) \right]}_{\text{stabilization term}} \quad (3.10)$$

The term on the right hand side of the equation is a stabilization term that ensures that the phase-field ϕ retains the hyperbolic tangent profile. The coefficient b is a relaxation factor. The parameters W , b , the mesh spacing, and the timestep have to be chosen appropriately to ensure good accuracy and stability of the method. Guidelines are given by Sun & Beckermann [137] and by Souhar et al. [119].

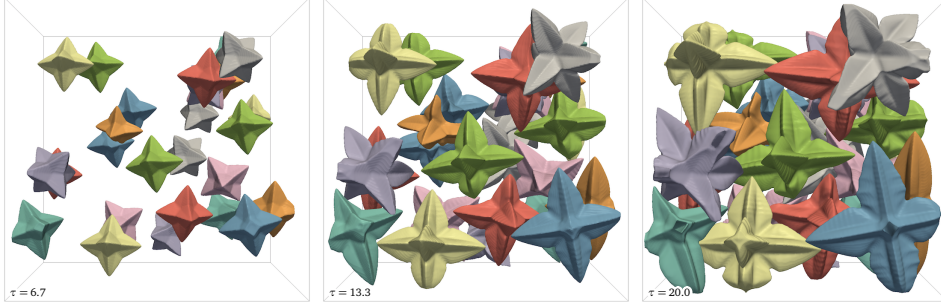
3.3 Growth of interacting equiaxed grains

Solutal grain interactions are a crucial aspect for the description of the grain growth kinetics in an ensemble. They determine

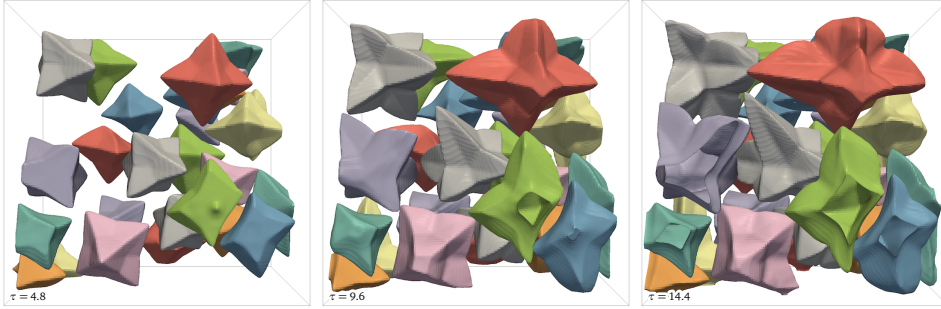
- microstructural characteristics: the distribution of grain size, morphology, elongation [140], hydrodynamic permeability of the mushy zone [127, 141];
- the solidification path of the grain ensemble: the evolution of solid fraction, the grain (envelope) fraction, the solute concentration of the different phases;
- the formation of defects: intergranular segregation, microporosity [142], hot tearing [143].

The mesoscopic grain envelope model (GEM) can simulate the solutal interactions leading to these phenomena. It can provide some of the resulting microstructural characteristics and, combined with a suitable scale-bridging method, it can give detailed information on the behavior of the ensemble. Consider, for example, the shapes of randomly arranged equiaxed grains, growing at different grain densities (mean distances between grains), shown in Fig. 3.2. The dependence of the grain shape on the interaction level can be quantified by a mean shape parameter, the mean sphericity of all grains, shown in Fig. 3.3.

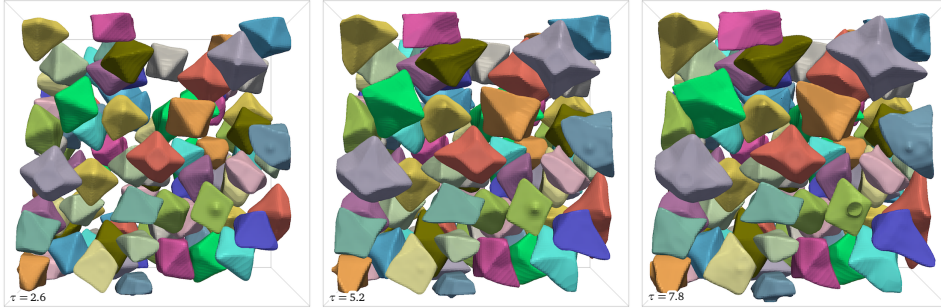
The objective of our work on solutal interactions during equiaxed growth, presented in this section, is twofold. We use modeling to gain insight into the 3D structure and interactions that goes beyond readily measurable experimental data. Further, we need to assess the capacity and the limitations of the GEM to accurately simulate the interactions. This is important because



(a) 27 grains with a mean distance of $\bar{d}_{cc} = 22 l_{\text{diff}}$ ($N_V^{\text{diff}} = 1.25 \cdot 10^{-4}$).



(b) 27 grains with a mean distance of $\bar{d}_{cc} = 11 l_{\text{diff}}$ ($N_V^{\text{diff}} = 10^{-3}$).



(c) 108 grains with a mean distance of $\bar{d}_{cc} = 7 l_{\text{diff}}$ ($N_V^{\text{diff}} = 4 \cdot 10^{-3}$).

Figure 3.2: Snapshots from simulations of randomly distributed and oriented grains growing isothermally in a cubic enclosure at an initial supersaturation of $\Omega_0 = 0.05$ and at three different mean distances between the grain centers, \bar{d}_{cc} , where $l_{\text{diff}} = D_1/V_{\text{LGK}}$ is the diffusion length for a freely growing dendrite tip that grows at the steady-state speed V_{LGK} . The grain arrangement can also be expressed as a grain population density, N_V^{diff} , where N_V^{diff} is the number of grains in a volume of l_{diff}^3 .

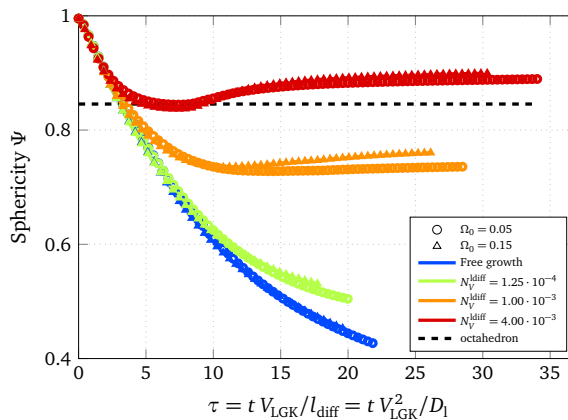


Figure 3.3: Evolution of the average sphericity of the envelope over the dimensionless time for four grain densities: from a free, non-confined grain (blue) to strongly confined grains (red).

we want to be able to perform reliable mesoscopic simulations of grain structure and defects, and to obtain quantitative results on the growth kinetics of grain ensembles, to be used in upscaling to macroscopic models.

The assessment of the capacity of a model to give accurate predictions is called validation. Validation can be done by comparing simulations of carefully chosen representative configurations to experiments or to quantitative models that provide a more detailed and accurate description of the physics. Apart from telling us how accurate a model is, validation helps to determine in which range of conditions (physical parameters) it can be reliably used. The process of validation can also help to form a guideline for the choice of model parameters, i.e., of parameters that stem from the model formulation and do not have a simple link to measurable quantities or material properties. Beckermann, Steinbach et al. [118, 131–133] have performed validation of the GEM on some aspects, such as the quantitative simulation of the grain envelope shape [118], of the velocity transients during interaction of two dendrite tips [131], and of the solid fraction distribution within a grain [131, 132]. These applications have clearly shown the potential of the model. We found that a more systematic approach was needed to clearly define the accuracy and the limitations of the model. The first efforts of our group to provide general validation and guidelines for the simulation of equiaxed growth were made by Souhar et al. [119]. Further investigations followed and consisted of validations and comparisons to phase-field simulations and to careful and well-controlled experiments. This work is presented in this section. Recent advances made in the framework of an ongoing benchmark study are presented in Section 3.6.

In experiments certain quantities can be difficult to measure. The lack of information can limit the interpretation of the observations and of the

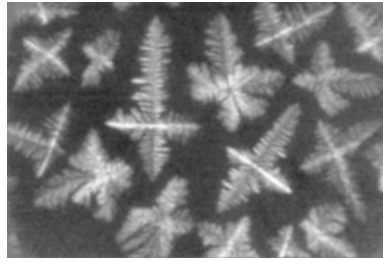
measurable data. In situ observations of solidification by X-ray transmission imaging are an example. These formidable experiments provide the possibility to observe and to measure various phenomena during solidification of opaque alloys. To ensure sufficient transmission the samples need to be thin, typically of the order of 100–300 μm . Such a confinement is much larger than the smallest radius of curvature of the solid-liquid interface – that of the dendrite tip, typically $\sim 10 \mu\text{m}$ – but much smaller than the size of a dendritic grain, typically $\sim 1 \text{ mm}$. The structure of the samples is therefore essentially three-dimensional, but the growth is strongly confined in the direction of the sample thickness. Like in a shadow theater play, transmission imaging can only provide a two-dimensional projection image. The lacking information on the 3D structure of the samples can limit the usefulness of the quantitative information from these experiments. 3D numerical simulations can provide further insight into the 3D structure and can thus help in the quantitative analysis of the observations.

To study grain interactions we chose a recent, rather well documented experiment of Murphy et al. [144, 145]. In this experiment the growth of equiaxed dendrites under the influence of solutal interactions was observed in situ by X-ray transmission projection imaging. Growth rates of individual grain envelopes and of dendrite tips were measured from the projected images. Murphy et al. have clearly shown that models of a freely growing dendrite tip cannot explain the observed growth rates and attributed this to the strong solutal interactions and to the confinement due to the thin dimension of the sample.

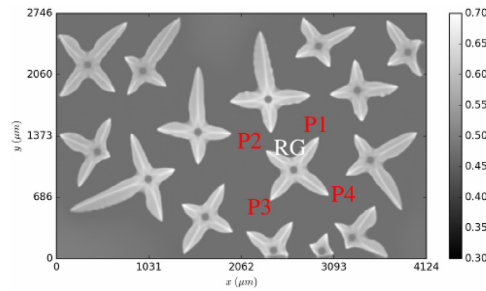
In the experiment of Murphy et al., an Al-20 wt%Cu alloy sample, grain refined with 0.1 wt% Al-5Ti-1B master alloy, of 200 μm thickness was solidified at a constant cooling rate of 0.05 K/s in a furnace that ensures a virtually homogeneous temperature in the sample [144]. The furnace was oriented horizontally, i.e., with the thickness direction parallel to the terrestrial gravity, in order to minimize natural convection in the melt. During the cooling stage 15 equiaxed dendritic grains progressively nucleated in the observation window, shown in Fig. 3.4. Their irregular shapes indicate that they are strongly affected by solutal interactions.

The results of our 3D simulations, shown in Fig. 3.5, are presented in form of transmission images, which were obtained by calculating light transmission through the thickness of the simulation domain using the Beer-Lambert law¹. Although only approximate in terms of intensity, the simulated transmission images can be used to measure the area and the shape of the grain projections, as well as the growth velocity of the primary tips. We made several interesting observations on the 3D structure of the samples

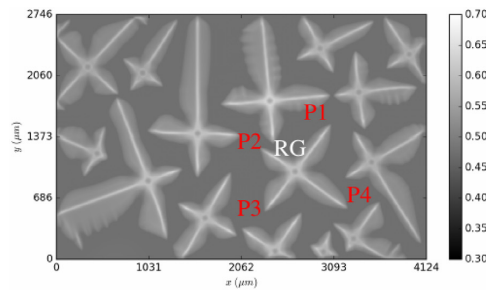
¹The transmitted intensity across the domain thickness, z , is thus $T_I = \exp\left(-\int_0^{L_z} \mu dz\right)$, where the transmission coefficient, μ , depends on the solute concentration.



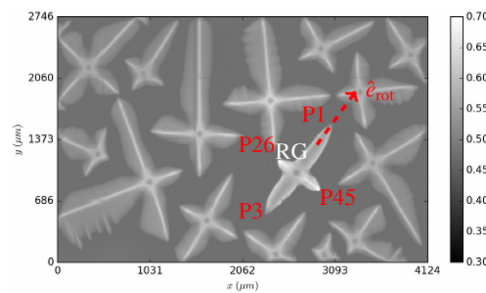
(a) XRMON-SOL experiment.



(b) 2D simulation



(c) 3D simulation – Reference Case (RC)



(d) 3D simulation with rotation and displacement

Figure 3.4: X-ray transmission projection images of growing grains. (a) XRMON-SOL experiment [144]. Image courtesy of D.J. Browne. Numerical Beer-Lambert transmission for (a) 2D mesoscopic simulation, (c) 3D mesoscopic simulation reference case (RC), and (d) 3D mesoscopic simulation with rotated and displaced grain RG. The reference grain (RG) and its tips are indicated. The gray scale bar refers to the transmitted light intensity, T_I .

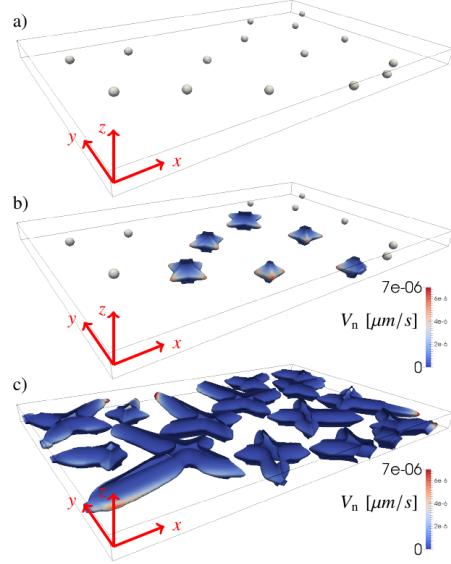


Figure 3.5: 3D simulation of the XRMON-SOL experiment. a) initial configuration with the seeds, $t_{\text{sim}} = 0$, b) $t_{\text{sim}} = 50$ s, and c) $t_{\text{sim}} = 130$ s. The color map indicates the normal growth velocity of the envelopes, V_n .

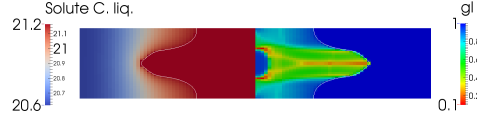


Figure 3.6: 3D solute diffusion around a grain in the thin sample. A slice across the 3D domain by a (100) plane containing the grain center is shown. The liquid concentration, C_1 , is shown in the left and the liquid fraction, g_1 , in the right half; the thin white line is the grain envelope.

through the analyses of these results [146].

First, we could clearly show that the three-dimensional diffusion around the grains must be accounted for to explain the grain growth rates observed in the experiment. Fig. 3.4(b) shows that grains obtained by simulating a 2D domain are much smaller than observed in the experiment. Note that only the diffusion field around the grains was assumed to be two-dimensional in these simulations. A 3D dendrite tip kinetics law was used to calculate the envelope growth in this simulations. With a 2D growth law the growth would be even slower. The three-dimensional diffusion is further illustrated in Fig. 3.6, which shows the concentration field around the primary tip of an envelope in a plane perpendicular to the tip growth direction and to the sample thickness.

While the 3D simulations give grain sizes similar to the experiment,

we can clearly see that shapes of some grain projections are considerably different. We shall closely examine the grain labeled RG (reference grain) in Fig. 3.4. Its direct neighbors are all visible in the field of view, the solutal interactions can thus be correctly simulated. The length of branches P1 and P3 of the RG are similar as in the experiment, but branches P2 and P4 are much longer in the simulation. Interactions with neighboring grains do not seem to be the cause; the lengths of the neighbors' branches in the direction towards RG are all predicted rather well. We have shown that the most important effects on the arm length are the position of the grain in the sample thickness and the rotation of the grain.

The position of the grain in the sample thickness can influence the confinement that the solute diffusion around the grain “feels” and may affect its growth speed. The primary solid phase growing from an Al-20 wt%Cu melt has a lower density than the liquid and in the experiments the grains can be expected to float towards the top wall [144, 147, 148]. Figs. 3.7(c)–3.7(d) shows the influence of the grain position on the primary arm growth. We can see that small shifts of position out of the central plane do not affect the growth speed significantly. Only a shift by $100\ \mu\text{m}$, i.e., onto the top sample wall causes a significant acceleration of the tip. The effect is thus not as simple as it might seem. When the tip is only partly shifted from the central position towards one of the walls, the confinement on one side increases, but decreases on the other side. It appears that the resulting effective confinement effect is very close to the symmetric situation. Only when the tip is shifted to the wall, the non-symmetry is removed and the “half” branch grows in a confinement with an effectively twice larger spacing. The growth speed thus increases significantly.

Because of the small thickness of the sample, the interaction of a dendrite branch with the confining walls is very sensitive to the orientation of its growth direction. In the experiment, the spatial orientation of the preferential growth directions $\langle 100 \rangle$ of the dendrites with respect to the sample is arbitrary. Figs. 3.7(a)–3.7(b) show the length of the four primary arms seen in the projection images as a function of the rotation angle around the axis \hat{e}_{rot} (Fig. 3.4(d)). We can see that the rotation slows down the growth of the tips P26 and P45, which grow perpendicular to the rotation axis. When rotated out of the central plane, these tips interact with the top and bottom walls of the furnace and slow down early. The rotation does not affect the growth speed of the arms aligned with the rotation axis (P1 and P3), which is easy to understand.

The study on the interacting confined growth was extended to investigate the influence of solute convection. Even in the horizontal experimental configuration solutal buoyancy drives a flow that can be strong enough to enhance the solute flux ejected by the dendrite tips. The flow speed and the solute flux enhancement depend a lot on the geometry of the flow and on the position of the tip in the flow. Our simulations indicate a flow with

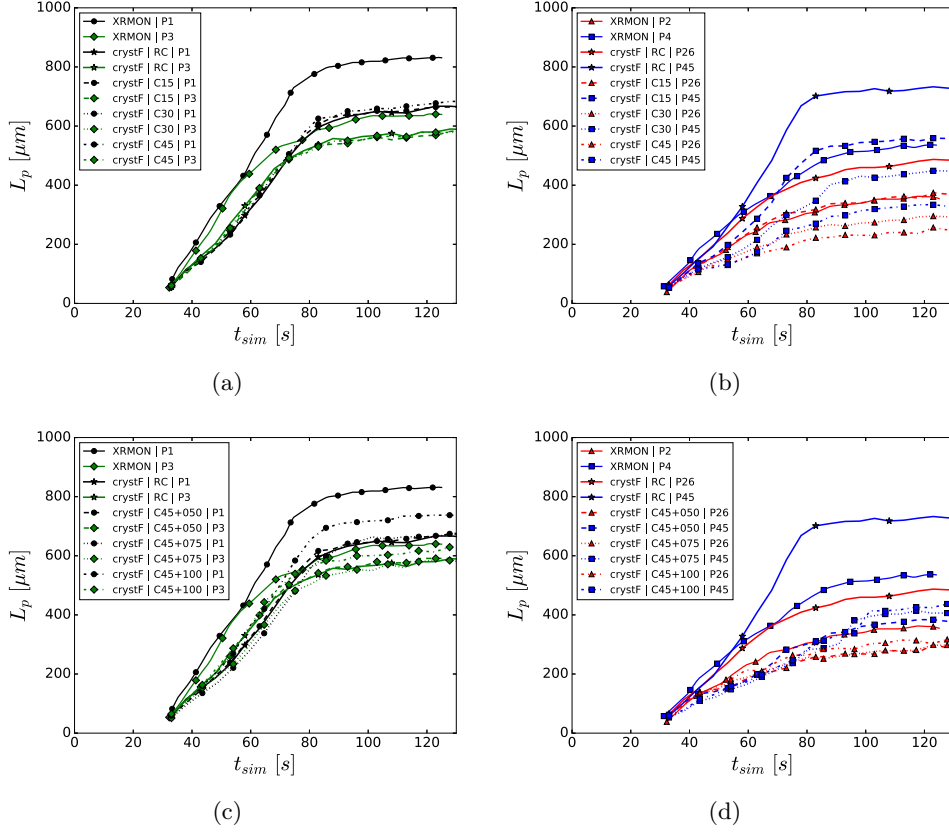


Figure 3.7: Evolution of the length of the primary arms, L_p , for the reference grain, RG. See Fig. 3.4 for the tip labeling (P1, P2, P3, P4, P26, P45). (a–b) Three cases with RG rotated by an angle θ (crystF | $C\theta$). (c–d) Three cases with the grain nucleus of GR located at distance Δz from the sample mid-plane, in all cases with RG rotated by $\theta = 45^\circ$ (crystF | C45 + Δz [μm]). Additionally, the reference case (crystF | RC) and the experimental results of Murphy et al. [144] (XRMON) are also shown.

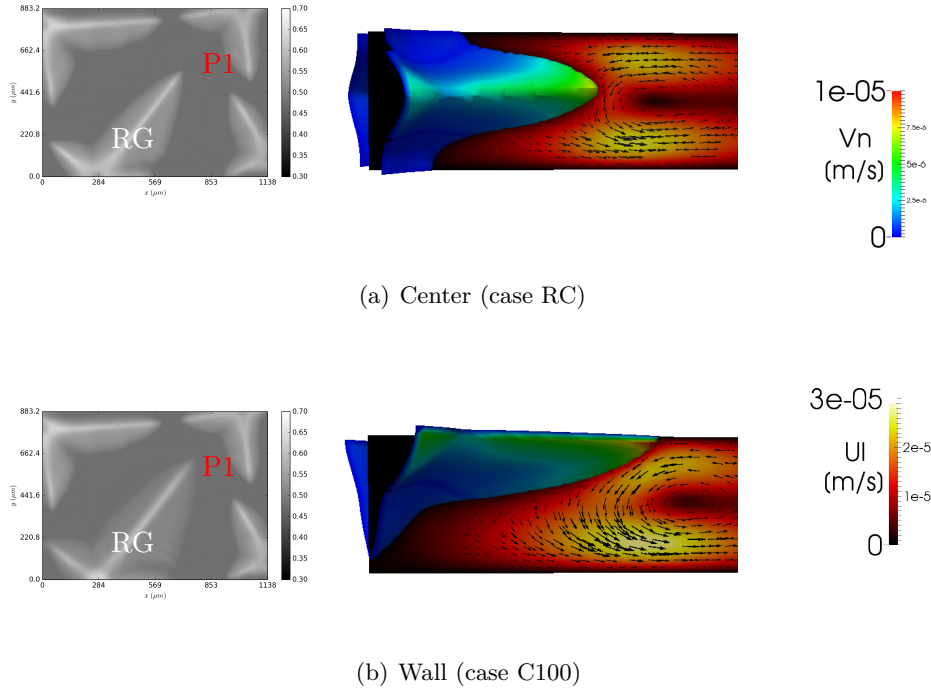


Figure 3.8: The influence of natural convection on the primary arm growth in a thin sample depends on the grain position: (a) grain in the center of the sample thickness; (b) grain at the top wall. Left: simulated X-ray radiographs. Right: envelope growth velocity, V_n , and liquid velocity, U_l , in a plane perpendicular to the x - y plane and containing the grain center and the tip P1.

two horizontal boundary layers, the top stream carrying solute-lean liquid towards the grain and the bottom stream carrying solute-rich away from the grain². A tip growing in the middle between the furnace walls thus experiences a cross flow, shown in Fig. 3.8(a), and is only weakly affected by the convection. A tip growing along the top wall, on the other hand, grows in the counterflow direction – a configuration that maximizes the convection effect on the growth, shown in Fig. 3.8(b). In this case the convection effect alone is as important as the effect of the grain position. We can see this in Fig. 3.9, where the influence of convection on the evolution of the primary tip is shown for a centered and a wall-adjacent tip.

We can see that the GEM gives quantitatively sound predictions on grain interactions in rather complex conditions. How far can these simulations reach? When do the limitations due to simplifying assumptions inherent in the model or due to numerical approximations of the solution methods

²This flow structure corresponds to the shallow enclosure regime of natural convection in an enclosure subject to an imposed *horizontal* concentration difference [149]

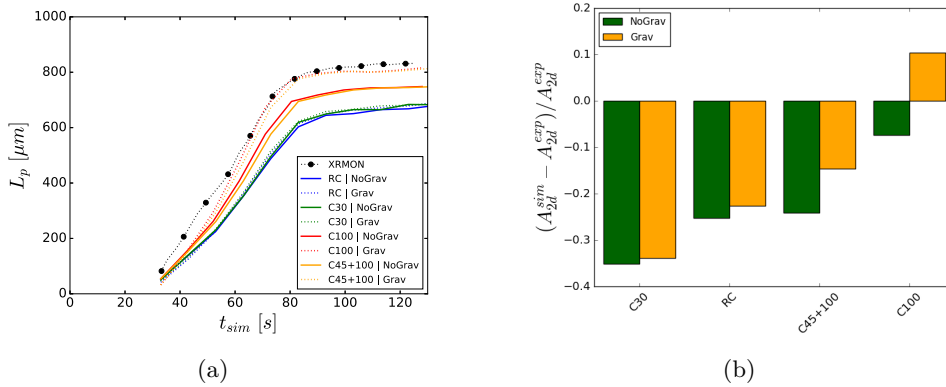


Figure 3.9: (a) Length evolution of the primary arm P1 over time for the simulation cases RC (reference case: grain center at mid sample thickness, no rotation), C30 (rotation by 30°), C100 (grain center at the top wall), C45+100 (rotation by 45° and grain center at the top wall). Cases with gravity (dotted line) and without gravity (solid line) are shown and compared to the experiment (XRMON) of Murphy et al. (with gravity). (b) Relative difference between the projected final area of P1 in the simulation cases and the experiment of Murphy et al. [144].

weaken the predictions and make them inaccurate or unphysical? A way to find this out is to compare the model to a phase-field model that provides a more detailed description of the physics and reaches to smaller space and time scales. The phenomena of interest: growth transients, grain morphology, interactions at small distances, departure from the assumption of a paraboloidal tip are inherently predicted with accuracy and the simulations can be used as a reference for models at higher scale. Efforts on comparing to phase-field model have been made on several frontlines. The close collaboration with Access (Alexandre Viardin and Markus Apel) provides the opportunity to make detailed comparisons to phase-field simulations. An example is shown in Fig. 3.10, where 2D simulations of equiaxed growth in a Ti-45 at.%Al alloy are compared for purely diffusive growth and for growth in a forced flow. These comparisons, detailed in [150], have shown a high fidelity of the mesoscopic predictions for transient growth in both diffusive and convective regimes.

Another set of comparisons was made for diffusive growth in 3D in collaboration with Damien Turret (IMDEA Materials, Madrid). It addresses specifically the transient growth from nucleation until the final interactions between grains [151]. It also provides a comprehensive investigation into the influence of model and numerical parameters with the objective of providing generally valid guidelines for the selection of parameters for quantitative simulation with the GEM. An illustration of grains in interaction is shown in Fig. 3.11. These comparisons have shown that quantitatively reliable growth velocities and grain shapes are obtained even well into the interact-

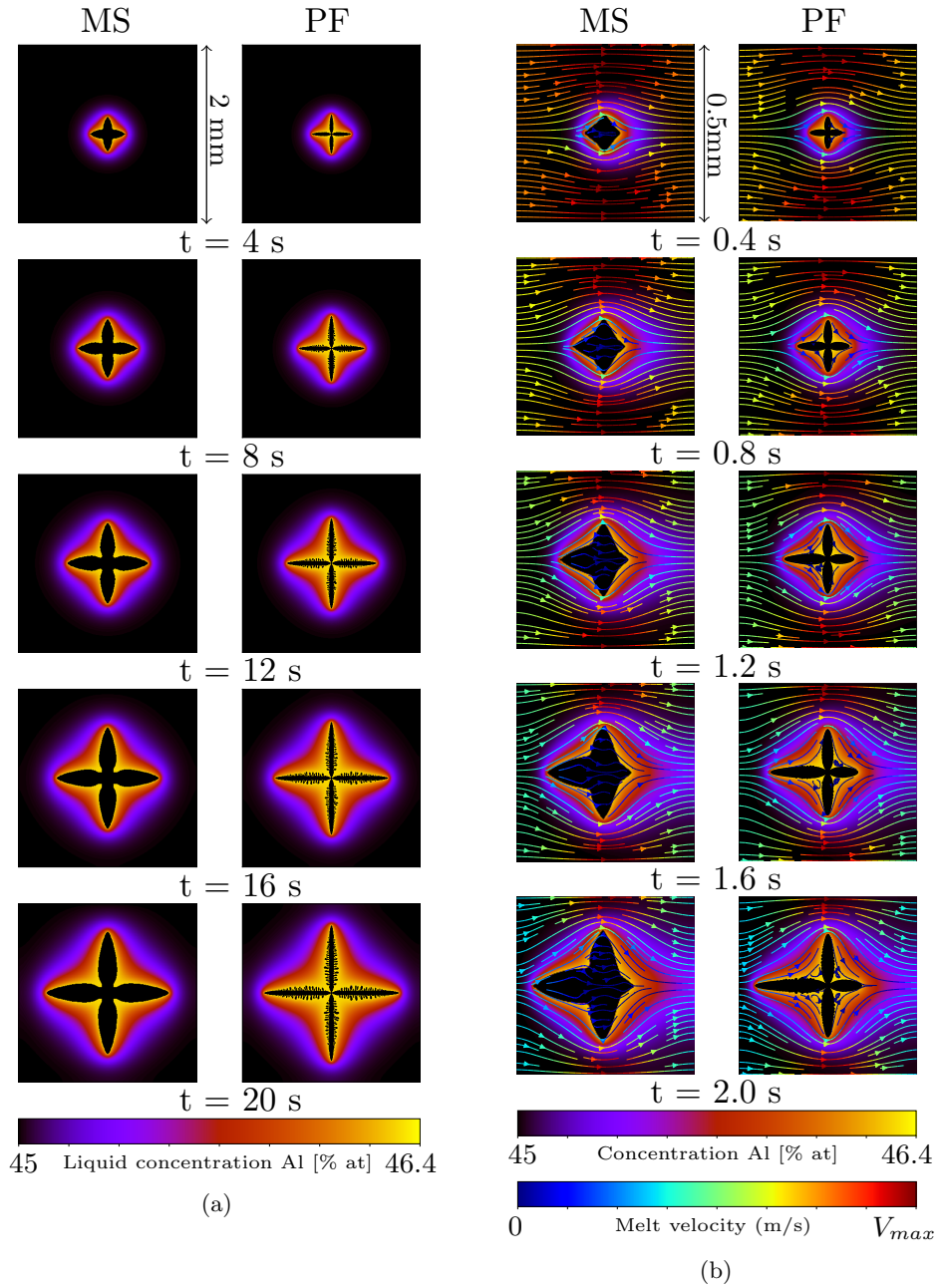


Figure 3.10: Evolution of the equiaxed grain during (a) purely diffusive growth and (b) growth in a forced flow. Simulations by the mesoscopic envelope model (MS) and by the phase field model (PF). Fields of liquid concentration, streamlines, dendrite envelope (MS), and solid-liquid interface (PF) are shown.

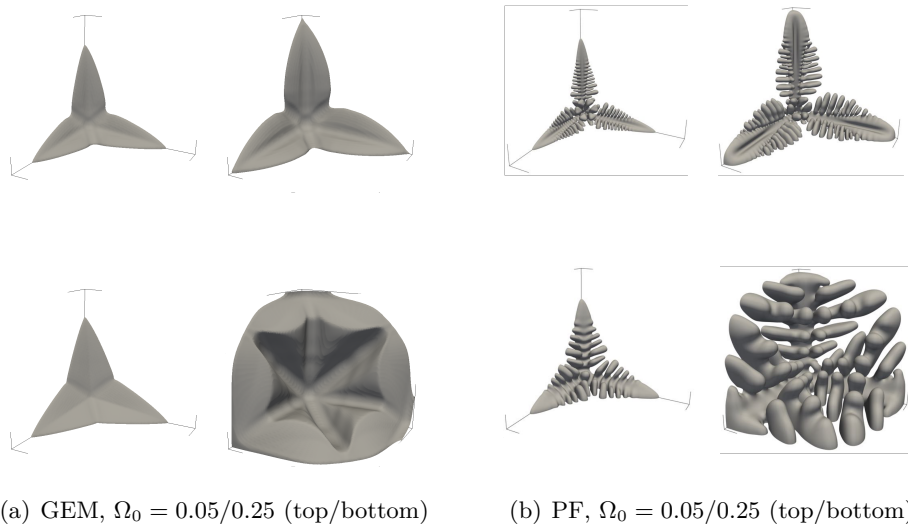


Figure 3.11: Evolution of the grain shape (1/8 of an equiaxed dendrite) during isothermal equiaxed growth with interaction (in a cubic confinement). Comparison of the grain envelope model (GEM) and the phase-field model (PF) for two different supersaturations, $\Omega = 0.05$ and 0.25 . (phase-field images courtesy of Damien Tournet, IMDEA Materials).

ing regime. We have shown that the growth can be simulated down to a distance of only a small fraction of the diffusion length (D_l/V_{tip}). This is an important message, because it tells us that the assumptions on which the method is based (paraboloidal tip, Ivantsov diffusion field around the tip, steady state at the tip scale) are not as restrictive as one might expect. This is particularly important for simulations that reproduce conditions found in casting processes – low supersaturation and small distances between grains. Such simulations are required for upscaling to macroscopic models (Chapter 4), where most of the growth is in a transient interacting regime.

3.4 Growth interactions in columnar growth

So far we have seen how the mesoscopic envelope model can describe the growth of a smooth envelope. In the examples covered in the previous section, the primary branches of an equiaxed grain envelope develop due to the imposed growth anisotropy. The envelope of the resulting hexapod or cross-shaped grain remains smooth and does not develop any higher-level branches. However, for a realistic representation of dendritic microstructure a model must be able to describe branching events from secondary or higher-order branches in certain conditions.

Such conditions are encountered in growth of polycrystalline columnar structures. The interactions between columnar grains are essentially governed by the creation of new branches and by elimination of branches at grain boundaries [152]. The sequence of rebranching and elimination events governs the evolution of the grain boundary and thus the survival or the extinction of a given grain. The grain size and crystalline texture resulting from this growth competition affect various properties of the solidified structure. It is important to understand that the competition occurs at the scale of a primary dendrite branch and can only be described if the model represents the individual branches, their creation, and their extinction.

Similar mechanisms occur in primary spacing adjustments within a single columnar grain. Let us take the ideal example of a grain growing at a steady growth speed in a constant temperature gradient with the $\langle 100 \rangle$ crystallographic direction parallel to the temperature gradient. Such a grain develops a stable structure of primary arms. If the growth velocity or the temperature gradient increase, the conditions are favorable for the development of tertiary dendrite arms. These tertiary arms can now develop into new primary arms and the PDAS decreases. Since they act as a generator of new primary branches, these branching events are determinant for the development of the PDAS. In conditions that favor an increase of the PDAS, another spacing adjustment mechanism appears. Certain primary arms are eliminated to favor the growth of the remaining arms with a larger spacing. The elimination happens due to solutal interactions. A branch that has a slight advance ahead of its neighbor can stifle the neighbor's growth due to the solute field it emits. Such events are the more likely the smaller the spacing between the branches.

It does not appear obvious that the mesoscopic envelope model can describe these phenomena crucial for spacing adjustments. Several elementary phenomena that play a role are not directly described in the GEM: capillary forces that figure in the destabilization of the solid-liquid interface leading to the development of new branches, the solute field at the scale of the primary tip, transient effects in the solute diffusion at the dendrite tip scale. Through a detailed study of GEM simulations for various cases of columnar growth [138, 153, 154] we have shown that the mesoscopic envelope model does correctly describe most of these phenomena and can thus be a powerful tool for studying columnar dendritic solidification. We looked into many aspects of the columnar structure predicted by the model and we quantitatively compared them to two-dimensional phase-field simulations that were used as a reference. These comparisons showed that the mesoscopic model accurately reproduces the primary branch structure, the undercooling of the dendrite tips, and the solidification path in the columnar mushy zone. We further showed that it can correctly describe transient adjustments of primary spacing and the growth competition in polycrystalline columnar structures.

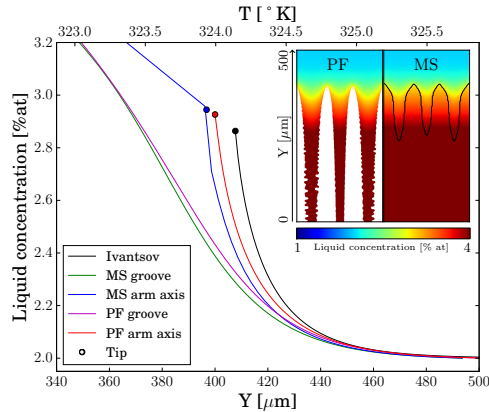


Figure 3.12: Liquid concentration profiles along the axis of a primary arm and along a groove between two arms. Comparison of a phase-field and a mesoscopic simulation in steady-state growth. The Ivantsov solution for a free tip growing at the pulling speed is also shown for comparison. The inset shows the full concentration fields from the phase-field (PF) and mesoscopic (MS) simulations, the envelope of the mesoscopic model is shown as a black line.

To demonstrate the detail of the mesoscopic representation we first examine a steady-state microstructure and the solute diffusion field surrounding the primary branches in directional solidification. Fig. 3.12 shows the branches and the solute concentration field in the liquid (inset) and compares the concentration profiles ahead of the tip and in the center of the groove between the two central branches. We can see that the profiles and the tip concentrations match very well. We can also see that the solute concentration of the interacting tips of the columnar front is higher than that of a single free dendrite tip growing at the same speed in an infinite melt (Ivantsov). This indicates solutal interaction between the tips. The mesoscopic model captures such interactions with good accuracy. The remaining difference of tip undercooling between phase field and the mesoscopic model is mostly due to the capillary undercooling, which is not accounted for in the mesoscopic model. Note that the mesh spacing used in the GEM simulations is around one steady-state tip radius, five times larger than in phase-field. The computation time was two orders of magnitude smaller.

Spacing adjustments were investigated for two configurations: an initial spacing larger and smaller than the stable spacing range, which is of the order of $\lambda_{\text{stab}} \sim 80 \mu\text{m}$. The results are illustrated in Fig. 3.13. In both cases the initial spacing, λ_0 , is imposed onto undercooled semicircular nuclei and the microstructure goes through a rather complex initial transient that first establishes an unstable branch structure. The spacing of this initial structure is then adjusted and finally a stable spacing is obtained. It is interesting that in both cases the phase-field simulation predicts an initially dense spacing. For $\lambda_0 = 1000 \mu\text{m} \gg \lambda_{\text{stab}}$, the initial branch structure is made up of

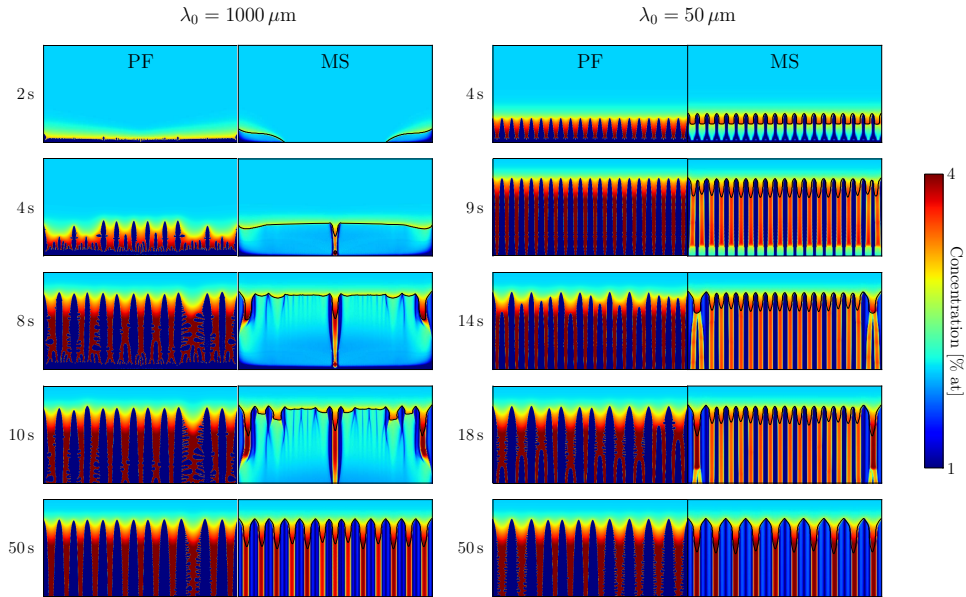


Figure 3.13: The evolution of the columnar grains from an initial spacing larger than the stable PDAS range, $\lambda_0 = 1000 \mu\text{m}$ (left column) and smaller than the stable range, $\lambda_0 = 50 \mu\text{m}$ (right column). Stable PDAS were obtained in the range of $70\text{--}115 \mu\text{m}$. The concentration field is shown for phase field (PF) and the average concentration field and the envelope (black line) are shown for the mesoscopic model (MS). The domain size shown is $500 \times 1000 \text{ mm}$.

secondary branches. For $\lambda_0 = 50 \mu\text{m} < \lambda_{\text{stab}}$, it is simply made up of primary branches growing from the initial nuclei. A competition between these new branches then takes place, eliminating most of them. In the mesoscopic simulation for $\lambda_0 \gg \lambda_{\text{stab}}$ the appearance of the vertical secondary branches is mimicked by a vertical spread of the envelope that corresponds to the lateral secondary dendrite arms. The vertically expanding envelope is initially smooth (4s). Later on it is gradually destabilized by protuberances (8–10s) that finally evolve into a steady pattern of well pronounced primary branches (50s). When $\lambda_0 \ll \lambda_{\text{stab}}$ the phase-field model (PF) predicts a fast spacing adjustment that proceeds by a sudden elimination of vertical branches (14s). The mesoscopic model (MS) gives an entirely different adjustment process. The elimination of branches proceeds symmetrically from the left and right edges of the domain by elimination of vertical branches in a cascade (14–18s). Both models give almost the same final spacing.

Interactions of dendrite branches, elimination and rebranching at grain boundaries are decisive in competition of misoriented columnar grains. A general macroscopic theory of grain competition (that would go beyond empirical rules [140]) has not yet been established. Well-controlled experiments with a systematic control of grain orientation are difficult [155]. Recently, high-performance phase-field codes [152, 156] and mesoscopic methods [157]

became promising tools that can provide “virtual experiments”, mapping the parameter space of crystal angles through a large number of accurate simulations. We assessed the capability of the GEM to simulate grain competition, first in 2D simulations. We have shown that the main phenomena that determine the competition at the grain boundaries, i.e., tertiary branching at the diverging grain boundary and tip overgrowth at the converging grain boundary, are both reproduced by the GEM. This is illustrated in Fig. 3.14(b). In the long run, repeated branching and elimination events result in a migration of the grain boundary. The prediction of such grain boundaries is shown in Fig. 3.15. The main conclusion of the study is that in many circumstances the GEM can correctly reproduce the phenomena at the grain boundaries that lead to GB migration and thus grain competition. These phenomena include tertiary branching on both the well-oriented and the misoriented grain at the diverging GB (Fig. 3.15, $\alpha_0 = 5^\circ$ and 20°) and overgrowth of the misoriented grain (Fig. 3.15, all angles) or the well oriented grain (Fig. 3.15, $\alpha_0 = 5^\circ$) at the converging GB. The latter is present only at small convergent misorientation angles α_0 and is known as “anomalous overgrowth” [114, 152, 158–160]. In the example shown here, the GEM fails at angles higher than 30° . The most likely reason is that the dendritic growth becomes degenerate and that such structures are not correctly described by the GEM. An example is the grain competition at $\alpha_0 = 45^\circ$, shown in Fig. 3.15. In this case the degenerate misoriented grain in the PF simulation grows at a substantially lower undercooling and is eliminated very rapidly, whereas it persists as a periodically branching structure in the GEM simulation. The grain competition as a function of the misorientation angle α_0 is reported in Fig. 3.16, through the grain elimination angle, the difference of the grain boundary angles, $\theta_C - \theta_D$, as a function of α_0 . The grain elimination angle characterizes the growth length needed to eliminate the misoriented grain. Note that the prediction with the GEM depends on the stagnant-film thickness, a key model parameter, which has to be chosen appropriately. A discussion on the parameter choice can be found in Ref. [138].

In summary, we can see that the mesoscopic model gives excellent predictions of steady state growth patterns of columnar growth. Furthermore, spacing adjustments both by tertiary rebranching and by elimination of primary branches are reproduced. The sequence of events adjusting a spacing outside the stability range to a stable spacing is however clearly different and takes about twice as much time as predicted by the phase-field model. Branching and elimination are also critical phenomena at the origin of growth competition between differently oriented grains. We have demonstrated that the mesoscopic model can reproduce these phenomena and thus the macroscale growth competition for small and moderate misorientation angles, i.e., up to 30° . The results also depend to some extent on the stagnant film thickness used in the mesoscopic simulations. This will be

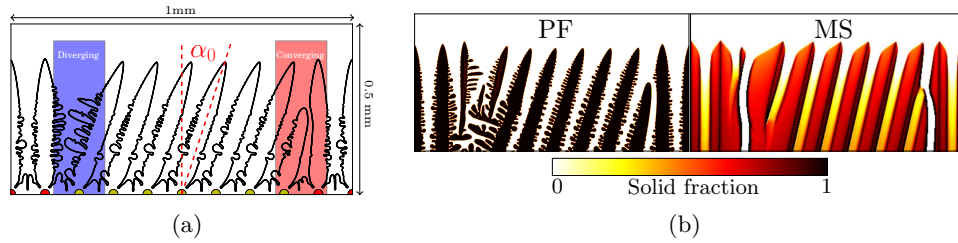


Figure 3.14: (a) Schematics of the prototype configuration for grain competition, the grain inclination angle, α_0 , and the calculation domain. (b) Snapshot of the growing dendrite structure given by the phase-field (PF) and by the mesoscopic model (MS) for $\alpha_0 = 20^\circ$ for the same physical time.

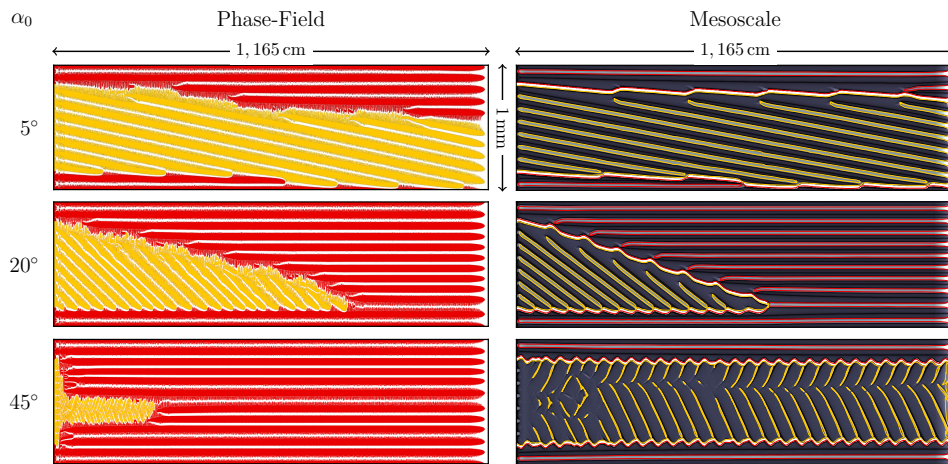


Figure 3.15: Spatiotemporal plots of growth competition predicted by the phase-field (left) and the mesoscopic model (right). The well-oriented grains are shown in red and the grain misoriented by the angle α_0 is shown in yellow (full for phase field, contour for mesoscale where solid fraction is superimposed). Note that the horizontal length is displayed compressed by a factor of 0.3.

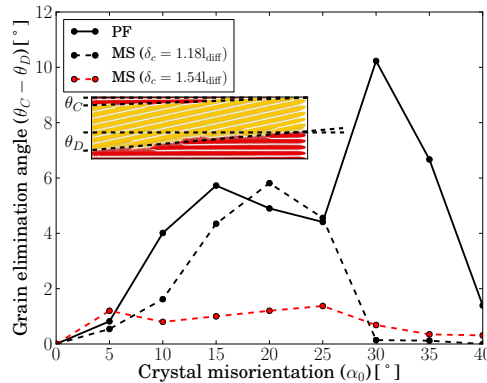


Figure 3.16: Grain elimination angles as function of the crystal misorientation angle α_0 of the misoriented grain. Comparison between mesoscopic (MS) simulations for two stagnant-film thicknesses and the phase-field (PF) simulations. Note that the stagnant-film thickness is specified in terms of the steady-state diffusion length, $l_{diff} = D_1/V_{pull}$, where V_{pull} is the pulling speed of the directional solidification.

discussed further in Section 3.6.

Recently, we used the GEM to model dendritic columnar grain growth in selective laser melting. The main challenge are the solidification conditions in additive manufacturing processes, which operate at high temperature gradients and cooling rates. They are characterized by a less pronounced disparity of the length scales involved in the microstructure formation (capillary length, tip radii, diffusion length and PDAS) and of those represented by the GEM (diffusion length and PDAS). For example, the ratio of PDAS to the diffusion length increases by almost an order of magnitude, while the ratio of diffusion length to tip radius decreases by an order of magnitude and becomes close to one. Encouraging results were obtained [161]. PDAS observed in experiments were reproduced and GB trajectories are similar as observed in our SLM experiments.

3.5 Convection effects

Convection has a significant influence on microstructure growth during solidification. This is of interest in many situations. Convection affects the growth speed of dendrite tips in equiaxed growth. In columnar growth, where the growth speed is controlled by the heat transfer, it modifies the tip undercooling and the extent of the undercooled zone in the liquid ahead of the columnar front. This can have an influence on nucleation and growth of equiaxed grains and on the columnar-to-equiaxed transition (CET). In case of strong flow, as in case of forced flow or buoyancy-driven flow in hypergravity, convection can modify the microstructure in terms of the primary dendrite arm spacing [162] and growth morphology [163].

The motion of equiaxed grains is another convection phenomenon. It enhances the relative velocity of the liquid and thus direct convection effects on an equiaxed grain. Beyond that, grain motion causes rearrangement of grains in terms of the number density and of the spatial distribution. Such rearrangement alters the interaction between equiaxed grains and thus the grain size, morphology, as well as the growth kinetics of the ensemble. Furthermore, macroscopic grain transport affects the competition with the columnar front and is thus a key phenomenon for the CET.

I will discuss two different cases where convection is a key element for the growth of grains. In columnar growth under the influence of amplified buoyancy-driven flow (natural convection) in hypergravity we investigated the adjustment of the dendrite arm spacing and of the microstructure morphology. In the case of equiaxed growth I will briefly look into growth during settling, particularly during the transition from free-floating to packed grains. While detailed results are not available yet, this reflection gives a starting point and motivation for the model developments presented in Section 3.6.

Centrifugation is employed in many metal casting processes, for example for cast iron pipes, aluminum tubes, continuous casting of steel billets, investment casting, etc. Our interest was motivated by centrifugal casting for manufacturing Ti–Al low-pressure turbine blades for aircraft engines [164–166]. Effective gravity in this process reaches up to tens of terrestrial gravity levels and buoyancy-driven convection of liquid is therefore strongly intensified. The influence of the strong convection on the growth of the solidification microstructure (including columnar morphology, CET, equiaxed grain size, and the role of the peritectic transformation) was investigated in the framework of the *Gradecet* project. One of the key elements is the columnar structure. Its growth morphology affects microsegregation, the creation of fragments, the undercooling ahead of the columnar zone, and the CET.

Recently, Viardin et al. [163] investigated the influence of hypergravity on the columnar dendritic microstructure during directional solidification of a Ti–48 at.%Al using phase-field simulations. They have shown that the direction and the level of hypergravity triggers changes of the primary dendrite arm spacing (PDAS) and of the grain morphology. These changes are particularly striking in conditions representative of industrial centrifugal processes: gravity direction opposite to the temperature gradient and gravity levels of $\sim 20 g$. Under the influence of strong convection, the microstructure is refined and the grain morphology changes from clearly structured dendrites to branched structures with less clearly defined growth directions. Viardin et al. have shown that this is linked to the transition of the growth and of the mesoscale flow from a steady-state regime at moderate hypergravity to oscillatory regimes at high hypergravity levels. These findings are consistent with experimental post mortem characterizations of Ti–Al microstructures

produced in hypergravity [166, 167].

Significant influence of the flow on the PDAS was also reported in prior investigations on gravity effects on columnar growth, based on experiments [168] and on phase-field simulations [162, 169, 170]. Notably, these studies showed that the primary dendrite arm spacing decreases for specific fluid flow configurations that promote growth of tertiary dendrite arms, while inhibiting growth of primary dendrite tips through advection of solute. These spacing adjustments are a result of interactions of diffusion of heat and solute, capillarity, and fluid flow across a range of scales: from the microscale (dendrite tip) to the mesoscale (flow structures at the scale of several PDAS). A comprehensive explanation of these interactions is yet to be developed.

Quantitative numerical simulations are indispensable as a complementary tool for the analysis of post mortem characterizations available from hypergravity experiments [166, 167]. The remarkable power of phase-field models for the detailed description of the interaction between solidification microstructures and flow [162, 163, 169–173] is impaired by their high computational cost. Mesoscopic models are particularly interesting in problems involving flow, because a larger range of scales needs to be tackled than in diffusive growth. We used the mesoscopic envelope model to simulate columnar solidification of a technical β -solidifying Ti–Al alloy under the influence of buoyancy-driven convection in hypergravity of up to $20g$. Through detailed comparisons to a phase-field model we showed that the mesoscopic model correctly predicts the main microstructure features due to convection: adjustments of primary dendrite arm spacing and the transition between dendrites and branched structures. Prior to the application to the rather complex case of columnar solidification, we thoroughly validated the model by comparisons to phase field for a case of equiaxed solidification with forced convection (see Fig. 3.10(b)).

We simulated columnar dendritic growth of Ti–45 at.%Al for different gravity levels ranging from micro- to hyper-gravity. In Fig. 3.17 the spatiotemporal plots of the microstructure obtained with the envelope model are shown. They can be directly compared to the phase-field simulations in Fig. 3.18. The same observations can be made as in the phase-field predictions. From $-3g$ to $+15g$ a single primary branch is stable. With decreasing gravity the primary tip undercooling increases and the dendrite envelope widens, representing an increasing length of the secondary branches. At $-4g$ the microstructure starts to destabilize and tertiary branching events occur. At $-15g$ the PDAS finally decreases and two stable primary branches are observed. While the destabilization of the microstructure is predicted at the same gravity level as by phase field and results in a similar reduction of PDAS, the mechanism leading to the spacing adjustment is not the same. The tip splitting events predicted by phase field cannot be correctly reproduced by the envelope model because they are governed by interface kinetics that is out of the scope of the parabolic tip model that is used to describe the

envelope propagation. Nevertheless, in the mesoscopic simulations the morphological instabilities are triggered but they appear as tertiary branching events.

These microstructure evolutions are closely correlated with the fluid flow patterns. Gravity drives the solutal natural convection in the liquid around the growing dendrites. Depending on the gravity direction with respect to the growth direction, very different flow regimes form and result in a stable or unstable dendritic growth [163]. In Fig. 3.19 flow streamlines and solute concentration fields for different gravity levels are shown. Note that the solutal expansion coefficient for Al in Ti is such that the density decreases with increasing Al concentration. When gravity and the growth direction are aligned ($g > 0$), the macroscopic density gradient in the mushy zone is parallel to gravity and is therefore hydrodynamically stable. Convection is induced by a lateral density gradient in the space between the primary dendrites. The size of the convection rolls is controlled by the PDAS. The dendrite tips experience a downward flow that stabilizes growth and the PDAS and decreases the tip undercooling. When gravity and growth are in opposite directions, the situation is more complex. In addition to the lateral gradient in the interprimary space, which is now in the opposite direction, an unstable (antiparallel to gravity) macroscopic density gradient is present in the mushy zone. An upward flow at the dendrite tips is created that destabilizes growth, leading to a drastic decrease of the PDAS and to a so-called “branched” microstructure [163] at higher gravity levels.

Our objective was to check if the mesoscopic model can predict the microstructure evolution and the fluid flow pattern during directional growth coupled with natural convection in hypergravity. The flow patterns are very similar for phase field and mesoscopic model from $-3g$ to $15g$, and differ only for high negative gravity levels, where a branched microstructure appears. For all positive gravity levels the convection rolls are symmetric with respect to the primary dendrite and the dendrite tip grows opposite to a downward flow that advects solute-lean liquid to the tip. In this case, the dendrite tip has “favorable” growth conditions [162]. The convection in this sense increases the concentration gradient that drives the solute rejection from the tip into the surrounding liquid. As a consequence, the solutal undercooling required for the tip to grow at the externally imposed pulling speed is reduced. The microstructure remains dendritic with a single dendrite predicted by both the phase field and the mesoscopic simulations. For moderate negative gravity levels ($-1g$ to $-3g$) the central dendrite remains dominant, with symmetric convection rolls but with an upward flow at the dendrite tip. Upward flow advects solute-enriched liquid from the interdendritic region to the dendrite tip. Compared to the purely diffusive case the solute gradient at the tip is reduced and the tip undercooling increases as a result.

At high negative g (upward flow at the dendrite tip at early stage of

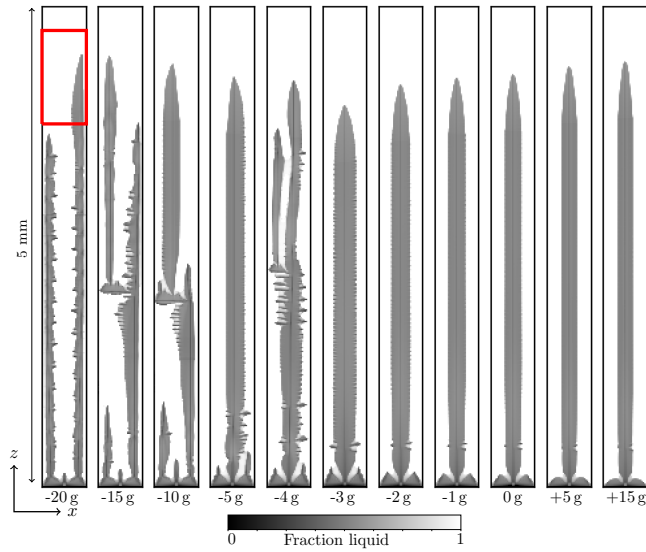


Figure 3.17: Columnar microstructure at different gravity levels predicted by the mesoscopic model. Spatiotemporal plots of the solid-fraction field after 200 s are shown. At positive gravity, the gravity vector is oriented in the growth direction, at negative gravity it is opposite to the growth direction. The red rectangle represents the moving calculation domain.

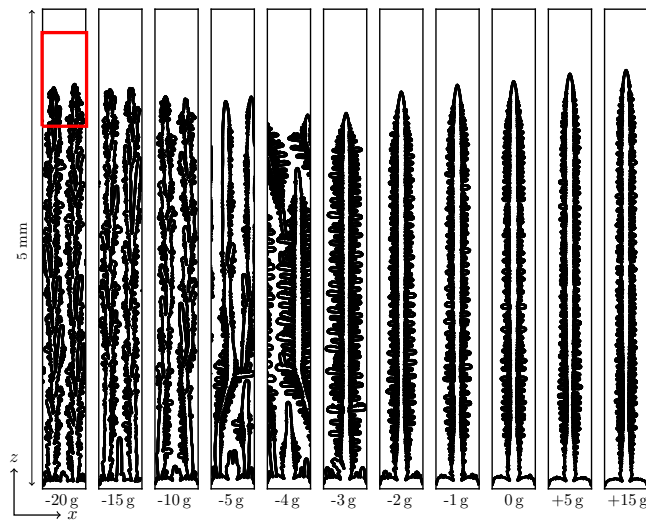


Figure 3.18: Columnar microstructure at different gravity levels predicted by the phase-field model. Spatiotemporal plots of the solid-liquid interface after 200 s are shown. At positive gravity, the gravity vector is oriented in the growth direction, at negative gravity it is opposite to the growth direction. The red rectangle represents the moving calculation domain.

growth) the flow destabilizes the dendritic growth pattern. For $-20g$ to $-5g$, a change of the PDAS is observed in the phase-field results. This

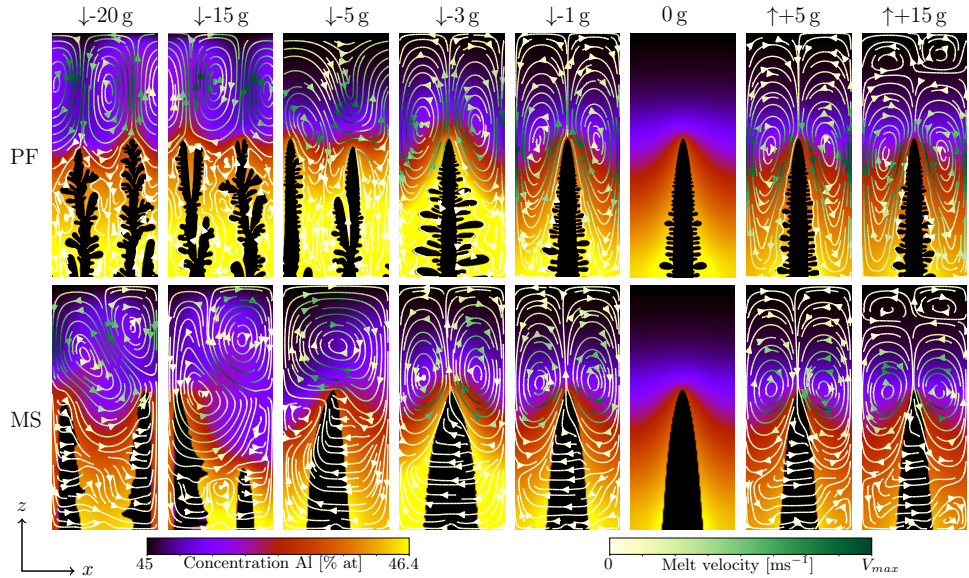


Figure 3.19: Columnar dendrite growth in Ti-45 at.%Al as function of gravity level for the phase field (PF) and the mesoscopic model (MS). Flow streamlines are superimposed onto concentration maps. Note that the maximum velocity magnitude V_{\max} is different for each frame.

change occurs at $-10g$ for the envelope model. The mechanism of spacing adjustment predicted by the two models is quite different. In the phase-field simulations it proceeds through a splitting of the primary tip with the two resulting branches initially growing tilted to the temperature gradient. One of the branches then gets eliminated and the surviving branch continues to grow roughly in the direction of the temperature gradient. In the mesoscopic simulation such events of branch splitting do not occur. Even if they did, the physical meaning could not be the same since the tips of the branches are not directly represented in the envelope model. The spacing adjustment rather occurs through tertiary branching. Although the mesoscopic envelope model cannot reproduce branched microstructures, it does predict the PDAS reduction at the correct gravity level. Instead of tip splitting, the spacing reduction is achieved by tertiary branching.

Naturally, a perspective of this work is to extend the mesoscopic simulations of columnar growth in hypergravity to larger domains and to 3D. The geometry and the dimension of the problem play a critical role on the flow characteristics [163, 174] especially on its velocity. The smaller computational cost than for phase field allows 3D simulations coupled with flow to be done at the scale of the experiments without using a massive supercomputer. Grain motion can also be included to investigate the effect of moving equiaxed dendrite on columnar growth during CET. Further, the effect of evolving solidification conditions (temperature gradient and growth speed),

such as in realistic process conditions, on the columnar microstructure is of interest.

The most obvious effect of convection on equiaxed growth is due to the relative motion of liquid. In Section 3.3 I discussed the influence of mesoscale natural convection on growth of stationary grains. We can see that it affects the growth of individual dendrite tips and slightly also the grain shape. It is interesting to quantify only for a detailed analysis of growth and grain interactions, such as in in situ experiments. For packed dendrites we can expect the natural convection in the intergranular liquid to be of no significance because the solutal gradients in the liquid pockets quickly vanish when the grains pack.

Convection can be of importance for the growth of settling grains. Several studies [31, 175–177] show that settling grains grow much faster than under diffusive conditions. Badillo & Beckermann [178], on the other hand, argue that the average of the growth speed over all branches of a settling dendrite is very close to the rate in diffusive growth.

Transport of equiaxed grains is important because it causes rearrangement of grains in terms of their number density and of their spatial distribution. Such rearrangements alter the solutal interactions between grains and thus have an influence on the growth kinetics of the ensemble.

We can imagine two limiting cases of concurrent grain settling and growth. In both cases the undercooling of the liquid through which they settle is identical, the only difference is the initial distance between the grains. In the first case the distance between grains is very *large*, such that the time needed for the grains to impinge by growth is much larger than the time needed to settle to the bottom of the container. In this case the size of a grain at packing depends only on the settling time. In the second case the distance between the grains is very *small*, such that the time needed for the grains to impinge is much smaller than the time needed to settle to the bottom of the container. In this case the grains impinge and pack due to growth and the final grain size depends only on the initial distance between the grains.

Our estimations from process simulations [179] show that realistic conditions fall between these two limiting cases. Rearrangements due to grain motion happen at time scales that are not much smaller than the solidification time. The most important rearrangement is the packing of equiaxed grains. We have shown that prior to packing, a densification of the grain population occurs above the packing front in a layer with a thickness of only about six times the grain size (see Section 2.4). The time spent in this layer is governed by the progressive deceleration due to lubrication effects and collective mechanical interactions with the average velocity around 5 times smaller than the settling velocity [99].

These ideas on concurrent grain growth and motion led us to the development of a mesoscopic model with grain motion. First model studies were

able to show the interactions of the settling grains with the packed layer and are presented in Section 3.6.

3.6 Methodological developments

This section regroups various methodological developments, which include major model developments, smaller improvements, and benchmarking.

The first improvements were made in the work of Souhar et al. [119]. We improved the calculation of the envelope velocity that is used in the interface capturing method for the description of the motion of the envelope front. All versions of the mesoscopic solidification model [118, 119, 131, 132] use the interface capturing method of Sun & Beckermann [137], which is a general method for the tracking of any moving interface. This method is very robust in many situations. Excellent accuracy is obtained, for example, when the calculation of the interface velocity does not depend on the phase indicator function itself, or in case of interface curvature driven motion [137].

In the phase-field like interface capturing method the whole indicator field, ϕ , must evolve in order to describe interface motion. This implies that the interface velocity must be defined everywhere and the field must be advected everywhere in the domain. In practice it is sufficient to define the interface velocity in a relatively narrow band around the interface ($\phi \in [0.02, 0.98]$ in practice), where the gradients of the indicator field are significant. In order to preserve the hyperbolic tangent shape in ϕ , the propagation velocity should be constant across a cross-section perpendicular to the envelope, i.e., in the direction of the envelope normal. Since the elements of the computational grid are generally not aligned along this direction, it is not possible to obtain the propagation velocity across the whole width of the transition at once. The propagation velocity has to be actually calculated for every grid cell within the transition region. The propagation velocity depends on the supersaturation of the liquid at a given *distance from the envelope* in the normal direction. The calculation of the velocity is very sensitive to the distance provided. Therefore, at each point within the interface band, the distance to the envelope and the distance to the stagnant film need to be determined with high accuracy. With the kernel function being known (Eq. (3.9)), the calculation of these distances can be based on the values of the function ϕ via the inverse of the kernel function. The problem of this method is that it gives erroneous calculation of the distances if the function ϕ is slightly deformed in the normal direction. We have shown that this error is self-reinforcing, i.e. the error that results from the deformation of the ϕ profile, produces a further deformation of the ϕ profile. The deformation is limited by the stabilization term, however the coefficients b that can be used, are not sufficient to avoid significant errors. We introduced a new, more accurate method for the determination of the

distance from a grid cell to the dendrite envelope and to the stagnant film. This improves the accuracy of the calculation of the envelope growth velocity and thus increases the application range of the mesoscopic model. The improved accuracy is achieved with the help of markers, points distributed on the level set of the ϕ field that defines the envelope. The average distance between the markers is much smaller than the grid spacing, they thus give an accurate reconstruction of the envelope surface. The distance between a point in space and the envelope surface is then approximated by the distance between the point and the closest marker. This method requires a certain additional computational cost for the surface reconstruction (the distribution of markers) and for the search of the closest markers. The clear advantage is a much better control over the interface capturing method and an improved accuracy of the velocity computation.

While the *raison d'être* of a model is to reach beyond known configurations, measurable quantities, and established solutions, it seems reasonable to expect that its soundness needs to be tested in some way. We expect to know to what degree a model is capable of representing material reality and to delineate its limits. I will not discuss the somewhat controversial (and often unclear) concepts of verification, validation, and confirmation of models [180, 181] here. It shall suffice to state that a model should demonstrate to what accuracy and fidelity it can describe the elementary physical phenomena that constitute the processes it needs to simulate. Of course, this is not a proof, nor quantification of accuracy for the simulation of the more complex processes for which the mode is used. It is rather an element of reassurance and of course if the elementary phenomena are accurately represented, this increases the likelihood that the more complex processes in which these phenomena are essential, are also accurately described.

With this rationale, several validation, comparison, and benchmarking actions were taken. In the work by Souhar et al. [119, 182] we compared the simulations of steady-state growth of equiaxed grains in a binary alloy at constant supersaturation to reference data. For the steady-state primary tip speed the analytical solution of an LGK-type dendrite tip model³ was used as a reference. For the steady-state dendrite shape the scaling laws from the experiments of Melendez & Beckermann [183] were used as a reference. The comparison to such careful experiments seems to be an ultimate validation exercise. Of course, the measurable quantities are limited even in such experiments. For example, the solute concentration field around the grain cannot be measured. Apart from this, simplifying assumptions taken in the model neglect certain effects inevitably present in the experiments: (i) in experimental conditions the dendrites are not only solutally undercooled but also have some thermal undercooling and (ii) the conditions are not purely

³consisting of the Ivantsov solution and a tip selection criterion of the form $R_{\text{tip}}^2 V_{\text{tip}} = D_1 d_0 / \sigma^*$

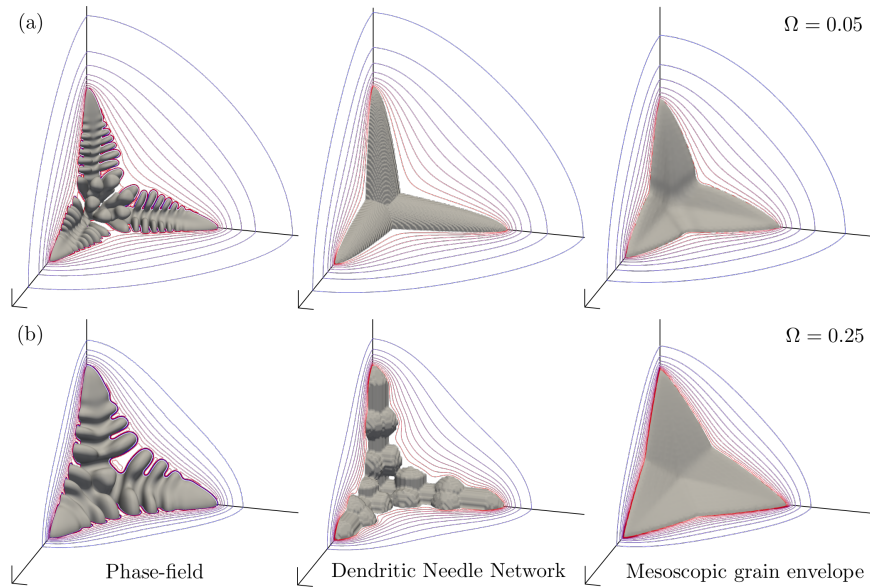


Figure 3.20: Benchmark comparisons of mesoscopic methods for isothermal equiaxed growth at two different supersaturations, Ω_0 .

diffusive – some (although weak) natural convection is present in the liquid. Although this did not preclude the use of the experimental scaling laws (see [119, 183] for discussion), more detailed and easily comparable results would be valuable.

Phase-field simulations of dendrites can give all the information for simulations of physically identical configurations. The difficulty of phase-field simulations is the relatively high computational cost in terms of CPU time and memory requirements. Until recently, the cost of well-resolved simulations of non-confined equiaxed growth in 3D made such simulations impracticable. Only recently, we were able to obtain such simulations in collaboration with Damien Tournet (IMDEA Materials) who employs a high-performance GPU phase-field code [184]. We made first benchmark comparisons of the GEM and the dendrite-needle-network model (DNN) [185] to these results for equiaxed growth [151]. An illustration of the comparison is shown in Fig. 3.20. The comparisons investigated the dependence of the model predictions on the stagnant-film thickness, δ , and on numerical parameters, grid spacing, Δx , and timestep, Δt . Additional comparisons including more detailed parameter studies and configurations of columnar growth are under way.

The stagnant-film thickness is a key parameter of the mesoscopic envelope model. It is the distance at which the locally valid analytical solution of diffusion around the dendrite tip is matched to the numerical solution of the concentration field in the vicinity of the envelope. In this way it is a parameter that controls the way the growth speed of the envelope is cou-

pled to the concentration field around the envelope. This is illustrated in Fig. 3.22. We can see that if $\delta \rightarrow \infty$, the envelope speed tends to the speed of an isolated Ivantsov tip growing at the solutal undercooling of the liquid at distance δ . For a single, essentially isolated dendrite this means that the theoretical primary tip velocity (the ‘‘Ivantsov velocity’’) is recovered by construction of the model if δ is much larger than the diffusion length D/V_{tip} . This might lead one to believe that a large stagnant film thickness should be used in order to ensure good accuracy of the model. Clearly, however, if $\delta \gg D/V_{\text{tip}}$, the dendrite tips are not affected by the concentration field in the vicinity of the envelope anymore, but only by the far field. This carries several disadvantages. First, the variations of concentration limited to the vicinity of the envelope, for example to a boundary layer in presence of convection, might not be captured. Second, any transients due to variation in undercooling (say, due to cooling) are damped due to the time necessary for the diffusion to reach the stagnant film. Third, because interactions with other grains are limited distances larger than δ , short distance interactions cannot be described. And finally, the grain shape becomes incorrect because the relations of growth speed between the primary and secondary tips are not properly reproduced. As an example we can look at an isolated equiaxed dendrite growing in an undercooled liquid. An example of the dependence of the grain shape on δ is shown in Fig. 3.21. If the stagnant film thickness is much larger than the diffusion length, $\delta \gg D/V_{\text{tip}}$, the confocal envelope lies beyond the diffusion layer that surrounds the grain and the concentration at the stagnant film is uniform for the whole grain. The tip speeds are then also identical along the whole envelope and the grain then takes an octahedral shape. The detail in the description of the envelope shape is thus lost.

It is thus clear that δ must be of the order of the diffusion length or smaller. Detailed investigations in this range have shown a dependence of the primary tip speed on δ that is not general and depends on the supersaturation, Ω_0 , of the grain. As δ decreases, the primary tip speed is underestimated for low Ω_0 and overestimated for high Ω_0 . This is shown in Fig. 3.22 [119]. These trends result from the matching of the Ivantsov solution for the tip-scale diffusion field to the numerical solution of the mesoscopic diffusion field at distance δ . Comparisons of the predicted envelope shape to an experimental reference [183] done in parallel have shown that more accurate envelopes are obtained with a small stagnant-film thickness, i.e., $\delta < D/V_{\text{tip}}$. In summary, both the primary tip speed and the envelope shape depend on the stagnant-film thickness: $\delta > D/V_{\text{tip}}$ is favorable to obtain an accurate tip velocity and $\delta < D/V_{\text{tip}}$ is favorable to obtain an accurate envelope shape.

As a compromise of these opposing tendencies, a general calibration guideline was proposed as $\delta = D/V_{\text{tip}}$ [119]. It was shown to give accurate results for the steady-state primary tip speed and envelope shape. This

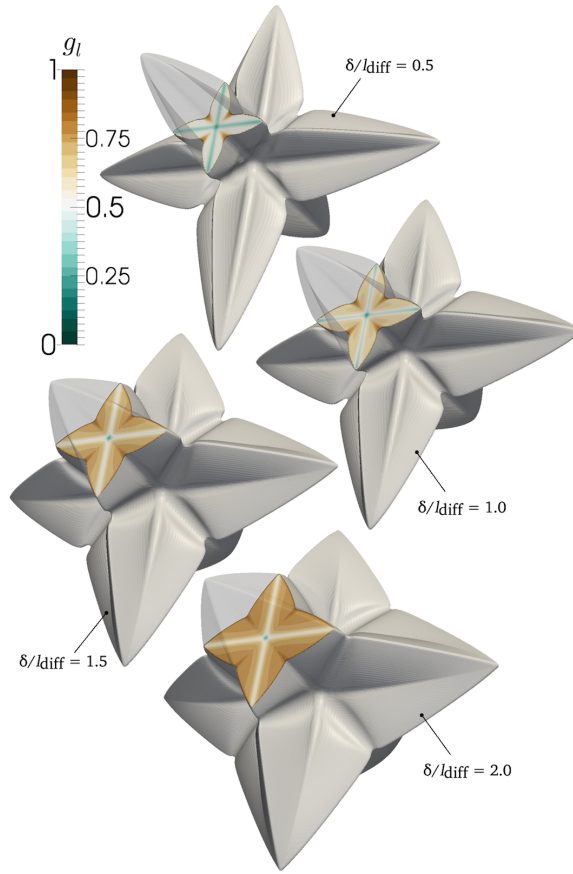


Figure 3.21: Equiaxed grain envelopes obtained with different values of the normalized stagnant film thickness, δ/l_{diff} .

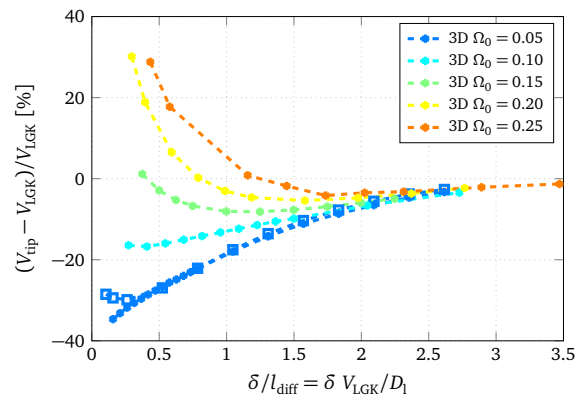


Figure 3.22: Dependence of the relative error of the predicted primary tip speed on the normalized stagnant film thickness, δ/l_{diff} .

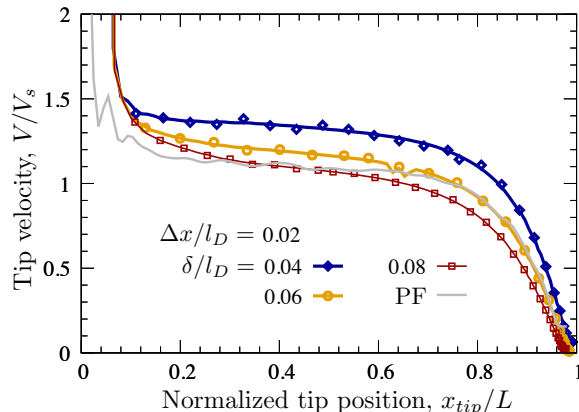


Figure 3.23: Evolution of the primary dendrite tip velocity for $\Omega_0 = 0.05$ from GEM simulations compared to phase-field. The influence of the stagnant-film thickness, δ , on the velocity transient is shown. The final length of the primary arm, L , is two times the diffusion length, $l_D = D_1/V_{\text{tip}}$, where V_{tip} is the steady-state tip speed.

is relevant for configurations where the grains are relatively far away. In this case most of the growth is in the steady-state regime and the initial growth transient is of minor importance. Also, we have to keep in mind that the interactions of grains at distance $< \delta$ cannot be described because the stagnant film overlaps with the interior of the adjacent grain envelope. A large δ is therefore limiting for the description of close interactions.

More recently, a detailed investigation for transient growth regimes was made. Comparisons were made to phase-field simulations. This investigation suggests a different scaling for the stagnant-film thickness: $\delta \approx 8\Omega^{1.6}D/V_{\text{tip}}$ [151]. This recommendation is slightly less accurate in steady state (with a difference of $< 10\%$) but is more accurate during transients, especially during the initial transient after nucleation. The main disadvantage compared to the rough general calibration (D/V_{tip}) is that it needs to be adapted to the expected tip supersaturation, which is not known in advance in general situations. Another disadvantage is that finer meshes must be used at low Ω , where smaller $\delta/(D/V_{\text{tip}})$ must be used. The constraint on the grid spacing is $\Delta x < 0.5\delta$. The advantages and disadvantages of the calibration methods for δ are summarized in Table 3.1. An example of the dependence of the tip speed transient on δ in the range close to the optimal calibration and a comparison to the phase-field simulation is shown in Fig. 3.23.

A particular configuration is encountered in case of narrow confinements, smaller than the characteristic diffusion length, D/V_{tip} . To simulate growth in such confinements the stagnant film thickness must naturally be considerably smaller than the confinement. Examples of such confinements are thin crucibles in in situ X-ray imaging experiments (see Section 3.3) and growth

Table 3.1: Advantages (+) and disadvantages (-) of calibration methods for the stagnant-film thickness, δ .

	General steady-state calibration $\delta = D/V$	Transient calibration $\delta = f(\Omega)$
steady-state tip speed accuracy	++	+
initial transient accuracy	--	+
interaction transient accuracy	+	++
grain shape accuracy	-	+
generality (independence of conditions)	++	-
required Δx	+	-

of grains at a distance smaller than D/V_{tip} . The latter case is encountered with large grain population densities and with low undercoolings (i.e., large diffusion lengths).

The concurrent motion and growth of equiaxed grains is a key phenomenon in the formation of the solidification microstructure. A description of collective interactions of moving grains is lacking, especially in regimes with steep transitions of grain size, population density, cooling rate, or other macroscopic quantities (see Sections 2.2 and 3.3). A model that could describe the concurrent motion and growth of equiaxed grains at the mesoscopic scale could make a considerable contribution to the understanding of these collective interactions. Today, no model exists, capable of describing grain motion at this scale. The principal reason is the complexity of devising a robust numerical algorithm for this type of problems. I need to mention that several efforts of developing phase field models of solidification with grain motion were undertaken in the past [186] and more recently [187–189]. These formulations were limited to 2D, some of them suffered from excessive numerical errors or were limited to unrealistic physical parameters, far from those encountered in solidification in metal alloys. Of course phase-field models are also computationally very expensive.

We recently extended the mesoscopic envelope model to describe grain motion. This is a major model extension and consists of several elements. In addition to the existing framework, the model needs to describe and resolve:

- the advection of all fields associated to grain envelopes and to the solid phase;
- the dynamics of motion of every grain following from the balance of all forces acting on it;

- the interactions of the grains with the liquid (drag, lubrication, and pressure forces);
- the forces due to contacts between grains.

We can already notice that the “single domain” description of solute transport and of momentum transport in the liquid needs to be combined with a description of grain dynamics that accounts for the identity of each grain. This is the main shift in the concepts used in the model.

The advection of mass and solute due to solid motion was included in the model quite naturally. It consists of adding advection terms to all fields linked to the solid phase: solid fraction, solid concentration and grain indicator field. For example, for the solid concentration field the equation reads

$$\frac{\partial(g_s C_s)}{\partial t} + \nabla \cdot (g_s C_s \vec{v}_s) = k_p C_1^* \frac{\Gamma_s}{\rho}, \quad (3.11)$$

where \vec{v}_s is the velocity field of the solid phase that is defined in the whole simulation domain. This field is such that it gives the translation and rotation velocity of all grains and is thus composed of the velocities of the individual grains. The main difficulty here is not the mathematical formulation, but the numerical solution of the advection operators (such as the second term on the LHS of Eq. (3.11)). In most discretization methods advection operators are prone to discretization errors that result in a non-physical diffusive effect (“numerical diffusion”) or in instabilities in form of oscillations. These errors are indeed the main obstacle for a robust model with grain motion. Sophisticated techniques have been proposed in the past [186, 188] and they have allowed to simulate the transport of a grain over long distances (more than 10 times the grain size) with good numerical accuracy. Our ambition was a little more modest. The objective was to be able to simulate the motion of grains over distances that correspond to the extent of the packing region (see Section 2.4), i.e., maximum of 10 times the grain size, with reasonable accuracy. However, it was absolutely essential that the model can be used in 3D with acceptable computation times. The most viable solution is to use sufficiently fine numerical grids and high-precision discretization schemes. Many such schemes are already available in OpenFOAM, the finite-volume numerical library used by CrystalFoam, our GEM code implementation. The SuperBee scheme was identified as the best compromise.

The dynamics of grain motion is that of rigid bodies. The dynamics of each grain is described individually by the motion of its center of mass and by the rotation around the center of mass. The linear velocity, \vec{v}_{gr}^i , and the angular velocity, $\vec{\omega}_{\text{gr}}^i$, of grain i are described by balances of forces and moments:

$$m_{\text{gr}}^i \frac{d\vec{v}_{\text{gr}}^i}{dt} = \vec{F}_{\text{bw}}^i + \vec{F}_{\text{dr}}^i + \vec{F}_{\text{col}}^i \quad (3.12)$$

$$\mathbf{I}_{\text{gr}}^i \frac{d\vec{\omega}_{\text{gr}}^i}{dt} = \vec{M}_{\text{dr}}^i + \vec{M}_{\text{col}}^i, \quad (3.13)$$

where \vec{F}_{dr}^i and \vec{M}_{dr}^i are the drag force and moment, respectively, \vec{F}_{col}^i and \vec{M}_{col}^i are the force and moment due to collisions with other grains, and \vec{F}_{bw}^i is the force of buoyancy-weight.

To describe the interactions of a grain with the liquid it is necessary to calculate the forces and moments of drag and lubrication. Because the solid-liquid interface, where these forces act, is not described in the mesoscopic model, some sort of constitutive model must be used. We should recall that every dendritic grain is defined by its envelope that contains a dendritic skeleton and intragranular liquid and is thus permeable. An idea that comes naturally is to calculate the drag on the grain from the integral of the drag force, given by the “porous medium” formulation and characterized by a hydrodynamic permeability (see Eq. (3.8)), over the envelope. Such modeling would certainly require careful calibration of the permeability law used for the envelope, but it is possible in principle. Our attempts of such modeling have however shown that the coupled calculation of force and motion is numerically very unstable. We therefore resorted to a modeling of drag at the scale of the grain. This means that the total drag force on the grain is calculated from the difference between the velocity of the center of mass of the grain and the mean velocity of the liquid in the domain. Drag coefficients formulated for low-Reynolds-number flow that account for the shape and the permeability of the grain envelope [32] are used.

Lubrication forces between two nearby grains are calculated from the distance between the facing envelope surfaces and the relative velocity of the two grains. The calculation is based on a rather sophisticated algorithm that detects facing surfaces that are closer than a given threshold distance and on that calculates the average distance and relative velocity of these two facing surfaces. This model has been validated and calibrated by comparison to experiments and simulations of settling particles [99] and has shown good accuracy. Its disadvantage is the sensitivity to numerical parameters. Because of lacking robustness when coupled to the full model, this lubrication model remains at a prototype stage.

Moving grains can collide and transfer forces. To describe these phenomena, the discrete element method (DEM) is most commonly used. The non-convex shape of the dendrite envelopes adds complexity to the modeling. One reason is that the detection of contacts between non-convex objects is much more difficult than for convex objects [190]. A second reason is that multiple contacts between two objects are possible. An advantage of the formulation of grains by indicator functions is that it can strongly facilitate contact detection. The key idea is that contacts between objects are detected and calculated from the overlap of the indicator functions (Fig. 3.24). Just like in DEM models, the contact force is then calculated from the overlap.

Instead of using the overlap distance, the overlap (intersection) volume is used. The force is expressed by a model equivalent to the Kelvin-Voigt (spring-dashpot) model.

$$\vec{F}_{\text{col}}^i = E\sqrt{V_{\cap}} + \eta \cdot \dot{\ell}, \quad (3.14)$$

where V_{\cap} is the intersection volume, ℓ is the overlap length, E is the rigidity and η is the viscous constant. A linear equation of motion is thus obtained:

$$m\ddot{\ell} + \eta\dot{\ell} + E\sqrt{R_c}\ell = 0 \quad (3.15)$$

where R_c is the curvature of the envelope at the contact point. Realistic rigidity and viscous constant would be difficult to obtain for dendrites during solidification. In the framework of the present model we do not need a quantitative description of the contact itself, since it occurs over a very short timescale. We merely seek to represent the stop of the grain on contact and to do this in a numerically robust manner. The rigidity E is thus calibrated to give a maximum allowed overlap. It therefore depends on the mass of the grain, its maximum expected speed, and on the minimum expected curvature. The critical damping of a mass-spring-dashpot system is used. Effectively, most of the kinetic energy of the grain is dissipated by lubrication forces directly prior to the contact.

We used the model to simulate the settling of growing equiaxed grains in an undercooled liquid. An illustration of such a simulation is shown in Fig. 3.25. It represents the settling of an equiaxed grain towards a group of fixed (packed) grains. The parameters of the simulations were extracted from process simulations of direct-chill casting of aluminum alloys: alloy composition, undercooling, cooling rate, temperature gradient, grain density, initial solid fraction in the settling region, and thermophysical properties. Such a configuration is the focus of our interest for future work on upscaling from mesoscopic simulations to macroscopic models. This is of interest because the description of solidification kinetics in the packing zone is one of the weakest links in macroscopic models.

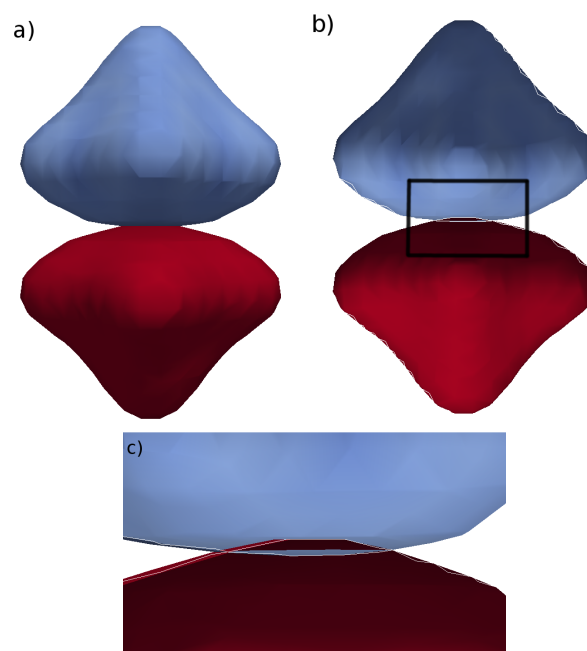


Figure 3.24: Collision between two moving 3D dendritic envelopes: a) External view; b) Internal view of the intersected volume; c) Internal view of the intersected volume (zoomed).

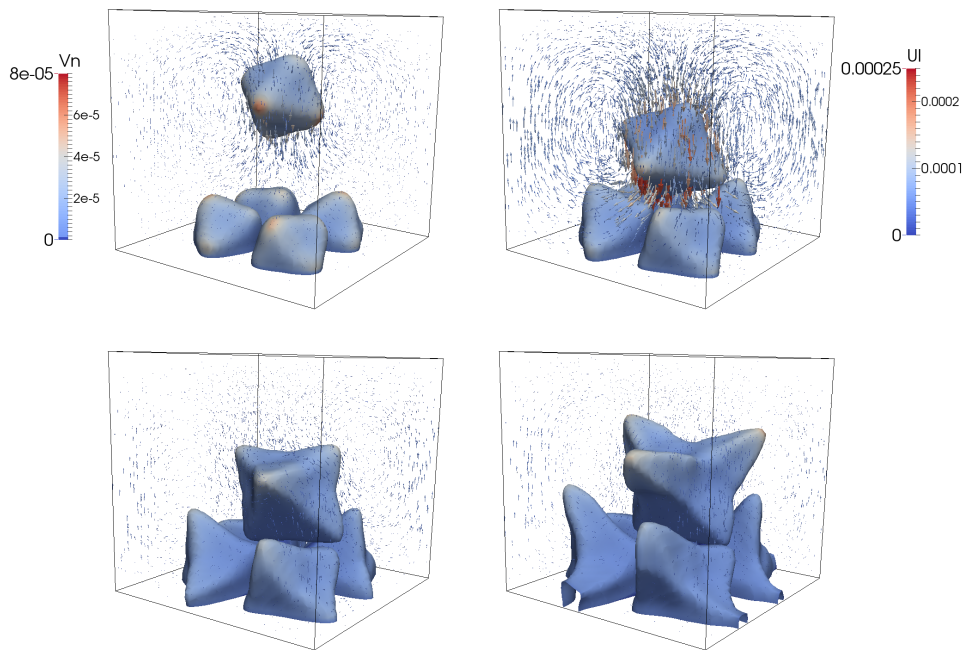


Figure 3.25: Simulation of settling and growth of an equiaxed Al-4%Cu grain and packing on a layer of packed grains. The color of the envelope surface shows the envelope growth velocity [m/s]. Arrows show liquid velocity vectors colored by speed, U_l [m/s].

Chapter 4

Upscaling

4.1 Introduction

Because of strong interscale coupling between the phenomena occurring at the different length scales, a model that simulates the macroscale behavior of a solidifying system needs to incorporate the microscale and mesoscale phenomena. Incorporating these phenomena by simulating them directly would require computing power that will clearly be out of reach in the foreseeable future [191]. My ambition is to develop a method of micro \rightarrow meso \rightarrow macroscopic upscaling for modeling of solidification of metal alloys that will be able to use simulations at the small scales to define constitutive laws used at the larger scales. This is a so-called hierarchical multiscale modeling approach. Currently, efforts for the development of different multiscale methodologies for materials modeling (ICME – integrated computational materials engineering) are under way all over the world. Their objective are modeling-assisted platforms for concurrent development of materials, processes and products.

Micro- and mesoscale phenomena can be incorporated in macroscopic solidification models using volume-averaging methods [4, 192]. Volume-averaged models are derived by formally averaging the local equations (valid at the microscopic scale) for each phase over a Representative Elementary Volume (REV). Such models are used to simulate solidification in large castings, as discussed in Chapter 2. Apart from terms that account for macroscopic transport, the resulting volume-averaged equations contain source terms, which account for the micro- and mesoscale phenomena occurring at the interfaces between the different phases. They depend on lower-scale variables that are not predicted by the macroscopic model because the information that they represent has been lost in the averaging process. The crux of the art of modeling now lies in formulating constitutive relations that accurately express the source terms as a function of the averaged macroscopic variables. Currently, even the most sophisticated available constitutive re-

lations [11, 14] are based on rather simplistic assumptions. These simplifications are one of the principal barriers on the way to quantitative modeling of microstructure in state-of-the-art process-scale models. Following the developments in the last 30 years, macroscopic models have reached a degree of maturity that allows them to finely describe the couplings between the microstructure and the convective macroscopic transport and to thus explain the link between the chemical segregation and the microstructure in casting processes. More precisely, the capability of macroscopic simulations to give predictive and quantitative results is mostly limited by an insufficient description of:

- microstructure growth kinetics in presence of convection and of collective effects;
- steep transitions of phase fraction, composition, microstructure, etc. at the mesoscopic scale: packing front formed during settling of equiaxed grains, columnar front, channels (freckles) in the mushy zone.

In first place, it is necessary to formulate more accurate representations of the solute fluxes at the solid-liquid interface, which control the phase change, of grain morphology (dendritic/globular) transitions, and of structural transitions between columnar and equiaxed structures.

Formulation of accurate constitutive relations can be done by directly simulating the REV scale and then upscaling the results to a larger scale by formal averaging. Such upscaling has never been done before in the field of solidification, mainly because of the large remaining gap between the involved micro and REV length scales. Only the recent development of quantitative mesoscopic models [118, 119, 123, 134, 138, 146, 151, 157, 185, 193] bridged this gap and opened the way to such simulations. Mesoscopic models directly resolve the transport phenomena on the REV scale and use constitutive models to incorporate microscale phenomena (such as tip growth and microsegregation). The computational power requirement of these models is much lower than the models that resolve the microscale phenomena directly, such as phase field models. This allows one to perform 3D simulations of a REV at realistic process conditions.

4.2 Methods

Substantial progress in process-scale (or macroscopic) modeling of solidification started in the mid-1980s with the advent of so-called single-domain models [194]. Prior models used a multidomain approach where distinct equations were considered in the mushy and the fully liquid zones, and boundary conditions were explicitly imposed on the liquid-mush boundary [195]. Single-domain models are based on equations valid in all regions (solid, liquid and mushy). This reduces the need to track the region

boundaries and enforce internal boundary conditions and thus facilitates implementation.

Different scale-bridging approaches were used to couple micro- and macroscopic phenomena. Models based on multiphase mixture theory were pioneered by Bennon & Incropera [196–198] and were later extended to more complex physics: ternary alloys [199, 200], equiaxed grain motion [201], and diffusion-controlled growth kinetics [202].

Today, most state-of-the-art process-scale models of solidification are based on the volume-averaging approach [7]. They have reached a good degree of maturity and can provide a detailed description of the complex couplings and interactions between the microstructure development and the macroscopic transport (heat transfer, flow, chemical segregation) in casting processes. In this way they can, for example, provide the links between the microstructures and defects of chemical segregation [44], porosity [203] or hot tearing. For example, they have contributed to improved understanding of the role of the equiaxed grain morphology [11, 14, 18, 46, 204] and of the columnar-to-equiaxed transition [16, 19] in macrosegregation in steel ingots [44]. Another example is the recent work on the influence of multiphase flow on the grain size distribution and the macrosegregation in DC cast Al alloys [27, 28, 61, 205]. An accurate description of the the grain growth kinetics is of prime importance in all these examples.

Ensemble averaging [206] is a more general theoretical framework and was used by Furmański [207, 208] and Ciobanas & Fautrelle [209, 210].

Whichever the scale bridging approach, the complexity of the macroscopic models lies in the required closure relations [211–215] and constitutive relations [11, 30, 177, 216, 217]. These relations provide a way of describing the microscopic phenomena that depend on microscopic quantities that have been lost in the scale-bridging process, through macroscopic quantities.

4.3 New constitutive laws for equiaxed growth

Recently, we performed upscaling by volume averaging to develop new constitutive relations for macroscopic modeling of equiaxed dendritic solidification [218]. We used the mesoscopic envelope model to perform three-dimensional simulations of equiaxed growth on a spatial scale that corresponds to a REV. We then upscaled the results by averaging them over the volume of the REV. The mesoscopic simulations were done for the simplest prototypal problem of interacting equiaxed growth, that is isothermal growth of periodically arranged grains at constant undercooling. We performed simulations for several initial undercoolings and distances between grains (final grain sizes). The upscaled results were then examined in detail (using expert intuition) and used to develop new, more accurate constitutive relations for macroscale solidification models. Unlike formerly available

relations, these new relations do not rely on highly simplified assumptions about the grain envelope shape or the solute diffusion conditions around it. The new constitutive relations were finally verified by comparing the predictions of the volume-averaged macroscopic model with mesoscopic results at different realistic solidification conditions that involve heat extraction.

In a volume-averaged model of equiaxed solidification the dendritic grains are described by envelopes and by the solid phase contained in the envelopes. This description reflects the fact that the kinetics that govern the growth of the envelopes and of the solid are different. The growth of the envelopes depends on the solute rejection from the dendrite tips. The growth of the solid phase depends on the solute rejection all across the complex shaped solid-liquid interface. Furthermore, the liquid contained in the envelopes (intragranular) and the liquid between the envelopes (extragranular) are considered as distinct “hydrodynamic” phases. Two liquid phases are introduced in the model because the solute diffusion is governed by length scales of different orders of magnitude: the secondary arm spacing in the inter-dendritic liquid and the distance between grains in the extra-dendritic liquid. The system thus consists of three “hydrodynamic” phases: the solid, the intragranular liquid and the extragranular liquid.

The volume-averaged equation for conservation of the mass contained in the envelope in the absence of melt convection and solid motion, and assuming equal densities of all phases, reads

$$\frac{\partial g_{\text{env}}}{\partial t} = \frac{1}{V_0} \int_{A_{\text{env}}} \vec{v}_{\text{env}} \cdot \vec{n}_{\text{env}} dA = S_{\text{env}} \bar{v}_{\text{env}}, \quad (4.1)$$

where g_{env} is the envelope volume fraction (i.e., grain fraction), A_{env} is the envelope surface area, \vec{v}_{env} is the local envelope growth velocity vector, \vec{n}_{env} is the outward pointing normal to the envelope surface, $S_{\text{env}} = A_{\text{env}}/V_0$ is the envelope surface area per unit volume of the REV, and \bar{v}_{env} is the average envelope growth velocity. This equation indicates how the envelope volume fraction increases as a function of an envelope surface area and average growth velocity.

The volume-averaged solute conservation equation for the extragranular liquid reads

$$\begin{aligned} \frac{\partial(g_{\text{lex}} \langle C_{\text{lex}} \rangle^e)}{\partial t} &= -\frac{1}{V_0} \int_{A_{\text{env}}} C_1^* \vec{v}_{\text{env}} \cdot \vec{n}_{\text{env}} dA + \frac{1}{V_0} \int_{A_{\text{env}}} D_1 \nabla C_{\text{lex}} \cdot \vec{n}_{\text{env}} dA \\ &= S_{\text{env}} \bar{v}_{\text{env}} \bar{C}_1^* + \frac{S_{\text{env}} D_1}{\ell_{\text{lex}}} \left(\bar{C}_1^* - \langle C_{\text{lex}} \rangle^e \right), \end{aligned} \quad (4.2)$$

where $g_{\text{lex}} = 1 - g_{\text{env}}$ is the extragranular liquid fraction, $\langle C_{\text{lex}} \rangle^e$ is the average solute concentration in the extragranular liquid, C_1^* is the equilibrium solute concentration in the liquid, D_1 is the liquid diffusion coefficient, and ℓ_{lex} is the average diffusion length in the liquid around the envelopes.

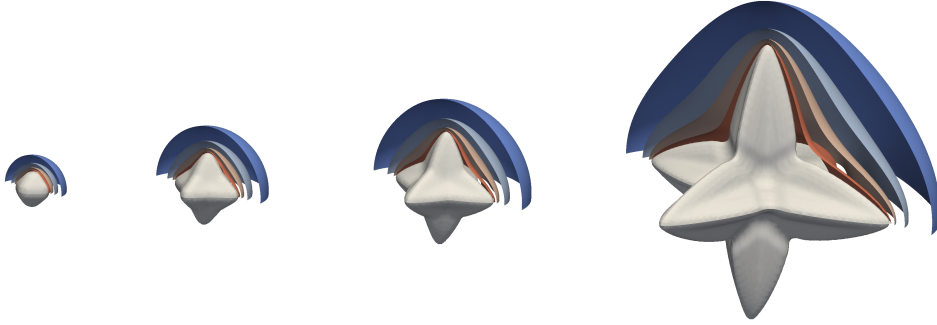


Figure 4.1: Evolution of the shape of an equiaxed grain envelope and of the concentration field around the envelope. Iso-surfaces of concentration are shown.

The two terms on the right hand side of the equation describe the exchange of solute between the envelope and the extragranular liquid due to envelope growth and the diffusion of solute from the envelope into the extragranular liquid.

In Eqs. (4.1) and (4.2), the quantities S_{env} , \bar{v}_{env} , and ℓ_{lex} all depend on local, microscale information that has been lost in the averaging process: the shape of the envelope of the dendrites, the distribution of the growth velocity on the envelope surface, and the solute concentration field in the liquid surrounding the dendrites. They therefore need to be obtained from constitutive relations.

To date, macroscopic models use highly simplified constitutive relations for these three quantities. S_{env} is determined assuming a predefined envelope shape: spherical [219, 220], octahedral [11, 12], or hexapodal [14]. This does not account for the evolution of the grain shape, such as shown in Fig. 4.1, from a compact (close to spherical) initial shape to a branched shape with elongated primary branches in later stages, and finally to a shape with widening envelope branches due to growth of secondary and slowdown of primary branches.

\bar{v}_{env} is calculated from the velocity of the primary tips, v_{tip} , assuming homothetic growth of the envelope. The primary tip velocity is determined from the Ivantsov relation and a tip selection criterion. The principal simplifying assumption of the tip model is the effective far-field undercooling, Ω_{eff} , that is used in the Ivantsov relation

$$\Omega_{\text{eff}} = \text{Pe}_{\text{tip}} \exp(\text{Pe}_{\text{tip}}) E_1(\text{Pe}_{\text{tip}}) \quad (4.3)$$

All models so far use the volume-average extragranular concentration, $\langle C_{\text{lex}} \rangle^e$ to determine the effective far-field undercooling, i.e. $\Omega_{\text{eff}} = (C_1^* - \langle C_{\text{lex}} \rangle^e) / [(1 - k)C_1^*]$. It is easy to illustrate that such an approximation systematically gives underestimated dendrite tip velocities. Let us consider the growth of peri-

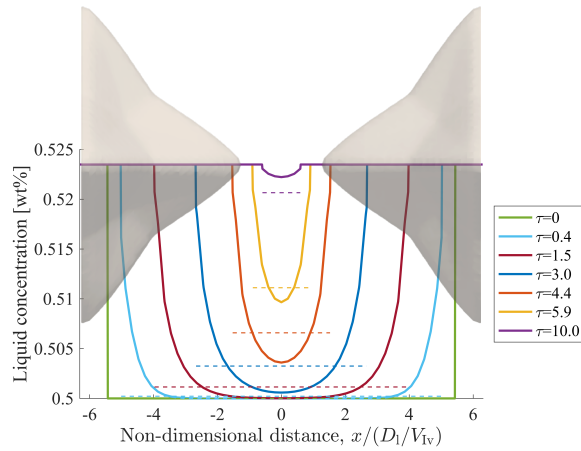


Figure 4.2: Profiles of liquid solute concentration between the primary tips of two dendrites growing towards each other (solid lines) and average concentration in the whole extragranular liquid volume (dashed lines). Different curves show the profiles at different times. The grains are arranged periodically in a BCC arrangement.

odically arranged equiaxed grains. Fig. 4.2 shows the concentration profile between two facing primary dendrite tips. We can see that the hypothetical far-field concentration, which is a prolongation of the profile to infinity, is always *lower* than the average concentration in the liquid. This is true already in the early growth stage when the solutal fields of the grains do not interact and the primary tips grow as free tips. It becomes even more pronounced in the later, interacting growth stages.

ℓ_{lex} , the volume-averaged diffusion length is simply modeled as a diffusion length around a sphere in macroscopic models. This means that it is determined from the concentration gradient on the surface of a volume-equivalent sphere growing at the same volume growth rate as the envelope [1, 10, 11, 28, 220–222]. Effects of solutal interactions, of convection, and of cross-diffusion [217] have been incorporated in these relations. However, none of the developed relations accounts for the fact that the envelope diffusion length is determined by the diffusion field around the envelope. It is therefore, in general, a complicated function of the envelope shape, size and growth velocity. This assumption might have reasonable accuracy during the initial stages of growth, when the envelope is spherical; however, as the envelope becomes dendritic with growth, the assumption can be expected to become increasingly inaccurate.

These simplistic relations have done a fairly good job, but they are one of the principal limiting factors for macroscopic models today. Their limitations have been shown, for example, already by Rappaz and Thevoz [219], who compared the cooling curves measured in the experiments with the ones predicted by their solute diffusion model and noticed that their model does not predict the recalescence very well. They attributed this partly to

the fact that in their model, the envelopes were assumed to be spherical during the entire growth. As another example, Wu et al. [14, 15] simulated the columnar to equiaxed transition (CET) with different relations for the envelope shapes and found that the CET position is highly sensitive to the envelope shape.

The new constitutive relations that we proposed [218] are based on several postulates that were formulated from the analysis of the results of the averaged mesoscopic simulations. The key ideas are the following.

- While the grains are interacting only weakly, the relation between the average envelope velocity and the primary tip velocity depends only on the geometry of the envelope.
- In later stages, when the grains interact strongly and the grain geometry does not evolve any more, the relation between the average envelope velocity and the primary tip velocity depends on a normalized average supersaturation of the extragranular liquid.
- The relation between the average diffusion length at the envelope and that at a sphere of equivalent volume growing at the same volume growth rate depends only on the geometry of the envelope.
- The geometry of the envelope can be fully described by the ratio of the primary tip length to the radius of the equivalent sphere.
- The primary tip velocity depends on the average supersaturation that is corrected by a function that depends on the ratio of the remaining distance between the primary tips and the instantaneous tip diffusion length. The idea is that the Ivantsov function can mimic the growth of an interacting dendrite tip if fed by a correctly formulated *effective* supersaturation.

These postulates were then used to fit constitutive functions onto the data from the averaged mesoscopic simulations. Relations for the average envelope velocity, the specific surface area, the effective supersaturation driving the primary tip and the volume averaged diffusion length were obtained. For details the reader is referred to the article of Torabi Rad et al. [218].

The constitutive relations were verified by comparing the predictions of the macroscopic model using the new relations with upscaled (volume-averaged) mesoscopic simulations. An example is shown in Fig. 4.3. Figure 4.3(a) compares the primary tip velocities obtained from a mesoscopic simulation of interacting grains and Ivantsov primary tip velocities that correspond to the average supersaturation in the extragranular liquid (standard constitutive law). We can see that the model based on the approximation of the far-field concentration by the average concentration grossly underestimates the tip velocity. Figure 4.3(b) makes the same comparison with the

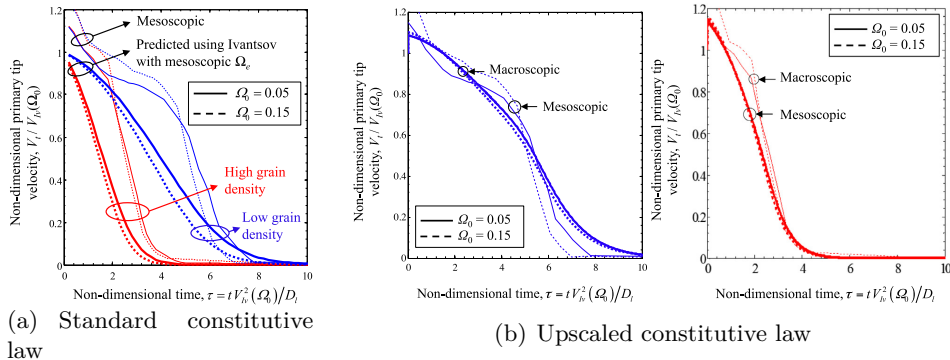


Figure 4.3: Comparison between mesoscopic primary tip velocities and primary tip velocities obtained with macroscopic constitutive laws. (a) Standard constitutive law that gives the Ivantsov primary tip velocities corresponding to the *average* supersaturation in the extragranular liquid. (b) New upscaled constitutive law that uses an effective supersaturation.

new upscaled constitutive law, which clearly gives a much more accurate approximation. Comparisons were also done for cases that are more complex than the prototype isothermal cases and are representative of realistic solidification processes. These cases involve cooling through an external heat extraction and a recalescence in the cooling curves. For all the tested cases, the predicted macroscopic quantities were found to be in good agreement with the corresponding upscaled mesoscopic results. The principal difference between the two was a minor difference in the macroscopic and mesoscopic values of the primary tip velocity, and that was attributed to the presence of an initial transient stage in the mesoscopic simulations.

4.4 Outlook on upscaling

Necessary work in the near future is the testing of the new constitutive relations coupled to the macroscopic transport equations in casting process simulations. Only such test cases can assess the impact of the new relations in process modeling. Further future work on upscaling will first focus on configurations of grains with random arrangements and orientations. Preliminary results have shown that the relations obtained for periodic arrangements might not be accurate in describing the growth kinetics of randomly arranged grain ensembles. Some other topics for future work on upscaling are discussed in Chapter 5.

Chapter 5

Projects

My research project grows from the trunk formed by the principal quest of my research in recent years: the understanding of microstructure growth under the influence of collective interactions. From this trunk the project will develop in the form of three main branches:

- Mesoscopic phenomena.
- Methodological developments of the grain envelope model.
- Upscaling.

5.1 Mesoscopic phenomena

Collective interactions at the mesoscopic scale play a determinant role in the formation of microstructure on several levels. For example, during the initial stages of equiaxed growth, the heterogeneous nucleation of new grains depends on the local undercooling of nucleation sites present in the liquid. The undercooling, in turn, depends on the diffusion and convection of solutes rejected by the already growing grains into the liquid that surrounds them. As the grain growth progresses, the liquid is gradually enriched in solute, the undercooling decreases, which progressively stifles further nucleation. This interaction between nucleation and growth, sometimes called the *nucleation-growth competition*, determines the number of grains that nucleate per unit volume and thus the mean grain size in the solidified structure. During later stages of growth, solutal interactions (among other effects) govern the growth kinetics of the dendrite branches and determine the grain morphology. The solutal interactions of course strongly depend on the spatial arrangement of the grains and of their growth directions. The fact that the arrangement of the grains continuously evolves and can strongly change because of their motion, adds to the complexity of the problem. This example shows a few of the principal ingredients that have to be accounted for in a mesoscale theory.

Interactions in random grain arrangements

In terms of the fundamental phenomena, it is first necessary to characterize the growth kinetics of an ensemble of equiaxed grains growing under the influence of solutal interactions. This has partly been done for a simplified configuration (periodic grain arrangement, isothermal growth, paraboloidal tip growth) in our work by Torabi Rad et al. [218]. However, the validity of these results is limited, mainly due to the assumption of periodic arrangements. Preliminary results have shown that a random arrangement strongly modifies the diffusion in the extragranular liquid and therefore the growth of the grain envelopes. This happens because a random arrangement introduces additional length and time scales and thus modifies the link between the undercooling and the rate of envelope growth and of phase change. This means that it is necessary to incorporate additional length scales into the macroscopic model to achieve a more general description of the solidification. This work is related to the forthcoming investigations on upscaling and is part of a more general project on diffusion-controlled phase transformations (which includes transformations at solid state). A PhD thesis on this topic is starting in autumn 2020 in collaboration with Benoît Appolaire (IJL), Alphonse Finel, and Yann Le Bouar (LEM, Onera, Paris).

Packing of equiaxed grains

The gradual pileup of equiaxed grains in the packing zone is a second important phenomenon. In the packing zone the spatial distribution of grains, and therefore their growth kinetics, vary considerably on a length scale of ~ 5 grains [99]. The phenomena involved in the concurrent growth, motion and packing are hard to investigate experimentally. Observations by in situ radiography can provide some information, but their quantitative value is limited due to the small thickness of the sample required for X ray transmission. The confinement by the thin sample is felt by the growth and by the motion of the grains [223]. 3D modeling appears to be the method of choice and can be done using the grain envelope method. Ideally, in situ imaging experiments (in collaboration with IM2NP, Marseille, for example) will provide complementary information.

Globular-dendritic morphology transition

The development of the grain morphology (dendritic or globular) in equiaxed growth is also governed by solutal interactions. This morphological transition is the central topic of a project that has been ready for a few years, is of increasing relevance, but still in search for funding. Mesoscopic solidification modeling in combination with in situ X ray imaging experiments (collaborations with IM2NP, Marseille and DLR, Köln) and phase-field modeling

(collaboration with Access, RWTH Aachen) would enable us to gain a better understanding of phenomena that lead to the morphology transition.

Columnar microstructure and convection

The collective interactions discussed above are under a significant influence of convection at the mesoscopic scale. The influence of natural convection is also important for the formation of the columnar microstructure, especially in hypergravity conditions (cf., Section 3.5). An extension of recent work on this topic [150] is planned in the near future and should tackle two aspects: (i) the analysis of larger spatial scales in order to avoid confinement effects on the flow structure and on the evolution of the primary arm arrangement patterns, and (ii) 3D analysis. These investigations will be done in collaboration with Access. Post mortem (IJL, Access) and in situ experimental observations (IM2NP, HZDR Dresden), can also give important information on these phenomena.

Mesosegregation

Chemical segregation at the mesoscopic scale (between \sim mm and \sim cm in the solidified structure) have become an industrial concern in the manufacture components of the primary circuit of nuclear reactors for power plants. It was shown that the presence of a heterogeneous structure at the mm scale leads to a decrease of impact toughness of the forged parts. This “mesostructure” of the forged parts originates from mesosegregations in the as cast material. A reduction of the intensity and density of these local heterogeneities in the ingots will lead to a reduced scatter of the impact toughness. A research project with this objective has been recently proposed in collaboration with Framatome and Industeel ArcelorMittal. It includes a PhD studentship. The objective of the project is to understand the formation of intergranular mesosegregations in the equiaxed zone and to propose realistic measures and modifications of the casting practice. The mesostructure and the mesosegregations in as cast ingots will be characterized in 3D. The industrial samples will be complemented by samples from lab scale experiments. Solute transport phenomena in a mushy zone at the cm scale will be analyzed by mesoscopic modeling. Different means of reducing interdendritic and intergranular segregation will be explored, for example via minor modification of the chemical composition of the steel.

Microstructure and texture in additive manufacturing

Currently, the key to progress in the understanding of the microstructure and the texture in additive manufacturing (Chapter 3) is the implementation of approaches that will allow us to reveal the 3D structure of the solidification microstructure. In numerical modeling of the microstructure,

even the mesoscopic model can present prohibitive computation cost in solidification conditions (high temperature gradient and cooling rate) that are encountered in additive manufacturing. We are aiming at developing a model with a coarser description of the microstructure, which must however keep a description of solutal interactions between neighboring grains, in order to be able to reproduce phenomena that lead to growth competition at grain boundaries. Experimentally, the challenge is to characterize the morphological, topological and crystallographic distribution of the solidification structure in 3D. The most suitable characterization technique available to us is nanotomography in a scanning electron microscope (SEM) equipped by a focused ion beam (FIB) device that is used for serial milling sample sections. With this device one can characterize the microstructure and texture (3D EBSD) with resolutions and for sample sizes relevant for the AM microstructure. This project is developed in collaboration with Julien Zollinger (IJL) and Nathalie Gey (LEM3, Metz)

5.2 Methodological developments of the grain envelope model

Several projects on the extension of the grain envelope model or on new methodological developments are in progress or planned. These developments are necessary in order to ensure simulations that faithfully reproduce the physics at the mesoscopic scale (Section 5.1) and to produce quantitative (sufficiently accurate) results for upscaling to macroscopic methods (Section 5.3).

Benchmarking of mesoscopic solidification models

In order to ensure quantitative simulation of microstructures on the mesoscopic scale by different models, a benchmarking project was recently started in collaboration with IMDEA Materials (Madrid) and Access. The objective of this benchmark is: (i) to rigorously determine the best choice of parameters, (ii) to delimit the relevant range of application of different mesoscopic models and (iii) to create a set of reference results for benchmarking solidification microstructure models. Two mesoscopic approaches (the grain envelope model (GEM) and the dendrite needle network model (DNN)) are compared to the reference calculations performed by phase field. Several prototype configurations for diffusive solidification, both equiaxed and columnar, are treated in 3D. The first results on equiaxed solidification are published [151]. The benchmark is being extended with work on columnar solidification. An extension of this work to cases with convection is planned in the future.

Modeling of grain motion

The recent major extension of the mesoscopic model with equiaxed grain motion (Section 3.6) requires careful and extensive validation before it can be used as a quantitative simulation tool. The objective is to describe the concurrent motion and growth of grains together with their interactions (solutal, hydrodynamic, and mechanical by contact). This will then allow us to simulate grain growth in the vicinity of the packing front. The primary motivation is the formulation of the new constitutive laws specific to this area for macroscopic volume-averaged models by upscaling.

Envelope destabilization and branching

Recent work on the organization of columnar microstructures, both in diffusive growth and with convection [138, 150] have shown that the mesoscopic model can represent the phenomena that trigger adjustments of primary spacing and grain competition at grain boundaries. These phenomena are the creation of new secondary and tertiary branches and the overgrowth of primary branches. They are, among others, a consequence of physical effects that are not directly represented by the envelope model: capillary effects, destabilization of the solid-liquid interface, diffusion at the dendrite tip scale. Nevertheless, branching phenomena are mimicked in mesoscopic simulations in a fairly realistic way by branching of the dendrite envelope [138], which is a virtual surface with a signification and with properties entirely different from those of the solid-liquid interface. A sound application of the envelope model for branching and spacing adjustment simulations would require a better understanding of the formation of envelope instabilities in the model. A stability analysis could clarify their physical significance and their dependence on model parameters and numerical parameters.

Modeling of the dendritic-globular transition

In many processes the equiaxed microstructure undergoes a dendritic-globular transition (cf. Section 5.1). The envelope method is based on the assumption that the tips of the branches behave as paraboloidal tips. A significant departure from this form, which occurs during the so-called “globular growth”, therefore cannot be described in a satisfactory way. This is the case for secondary tips in advanced growth stages (once the primary tips are essentially stopped because of the interactions between grains), but especially for the primary tips during early interaction stages which occur if the distance between the grains is small (high grain density). Advanced models for these regimes do not exist today [224] and could be developed with the help of quantitative phase field simulations (e.g. [225]). These works were considered in collaboration with Access and DLR (cf., project on morphology, section 5.1).

5.3 Upscaling

Meso \rightarrow macro upscaling

The objective of meso \rightarrow macroscopic upscaling is to develop new, more realistic constitutive laws for the description of the microstructure in macroscopic models. This will allow better prediction of microstructures in process modeling. The models used today are based on overly simplistic assumptions. In particular, they do not take into account collective interactions in an ensemble of grains [218]. We aim at developing a new framework for enriching macroscale models using extensive calculations at the mesoscale. This framework is intended to be general, such that it can be applied to any diffusion-controlled transformations (at the solid-state or solidification).

The first step will be to define and/or identify the best variables (descriptors) able to describe the spatial distribution of microstructures and to be incorporated into the macroscale models. Contrary to the currently used averaging procedures, we will pay particular attention to the correlations between the fluctuations of the fields (with respect to their averages), in order to go beyond the usual mean-field form of the current macroscale models.

The second step will consist of performing a significant number of mesoscopic calculations in order to quantify the correlation functions and their possible time evolution. Depending on the number of mesoscopic calculations that we will be able to run, the evolution of the fluctuations will be analyzed using state of the art algorithms of data science (e.g. neural networks). We are aiming at the development of a general approach that will give laws independent of the alloy (at least for the primary solidification of binary alloys), the density of the grains and the cooling rate. This project will be carried out in collaboration with the LEM laboratory (Onera, Paris).

In the long run, the upscaling methodology will be applied to physically more complex configurations. What I have in mind particularly, is the packing zone of equiaxed grains and the transition between the columnar and the equiaxed zone in the vicinity of the columnar front.

Micro \rightarrow meso upscaling

In parallel, efforts of micro \rightarrow mesoscopic upscaling will be carried out. The idea is to use phase field calculations as a starting point to refine the model parameters used in the mesoscopic model. This idea has been pursued for several years, but until now without success, because of the excessive cost of the necessary 3D phase field simulations. Modern phase field codes, based on GPU computation [151, 225], now make it possible to do these simulations. A first step towards micro \rightarrow mesoscopic upscaling is currently underway with a fairly pragmatic approach via the benchmarking of mesoscopic models (section 3) [151]. The parameters of the mesoscopic model

are first calibrated so that the growth of the envelopes is in good agreement with the dendrites simulated by the phase field. However, these calibration guidelines are not based on a formalism and are thus difficult to generalize. Furthermore, the extensions of the physical model that are underway or planned (convection, grain movement) introduce additional parameters and constitutive models. Such models are needed, for example, to describe the hydrodynamic permeability of the envelope and the distribution of drag force over the grain. The idea in the long run is to develop a more general and formal framework for micro \rightarrow mesoscopic upscaling. This framework could, at least partly, be based on the same foundations as the meso \rightarrow macroscopic upscaling, since the laws of conservation (of mass, momentum, etc.) are in both cases formulated by volume averaging.

Bibliography

- [1] C Y Wang and Christoph Beckermann. A unified solute diffusion model for columnar and equiaxed dendritic alloy solidification. *Materials Science and Engineering: A*, 171(1-2):199–211, nov 1993.
- [2] Philippe Thévoz, Jean-Luc Desbiolles, and Michel Rappaz. Modeling of equiaxed microstructure formation in casting. *Metallurgical Transactions A Transactions A*, 20(2):311–322, 1989.
- [3] Michel Rappaz. Modelling of microstructure formation in solidification processes. *International Materials Reviews*, 34(1):93–124, jan 1989.
- [4] Christoph Beckermann, Raymond Viskanta, and S. Ramadhyani. Natural convection in vertical enclosures containing simultaneously fluid and porous layers. *Journal of Fluid Mechanics*, 186(-1):257, jan 1988.
- [5] S. Ganesan and D. R. Poirier. Conservation of mass and momentum for the flow of interdendritic liquid during solidification. *Metallurgical Transactions B*, 21(1):173–181, 1990.
- [6] J Ni and C Beckermann. A Two-phase Model for Mass, Momentum, Heat, and Species Transport During Solidification. In M. Charmchi et al., editor, *Transport Phenomena in Materials Processing*, volume HTD-Vol. 132, pages 45–56. ASME, New York, 1990.
- [7] Jun Ni and Christoph Beckermann. A volume-averaged two-phase model for transport phenomena during solidification. *Metallurgical Transactions B*, 22B:349–361, 1991.
- [8] S. Ahuja, C. Beckermann, R. Zakhem, P.D. Weidman, and H.C. deGroh III. Drag Coefficient of an Equiaxed Dendrite Settling in an Infinite Medium. In C. Beckermann et al., editor, *Micro/Macro Scale Phenomena in Solidification*, volume HTD-Vol. 218, pages 85–9. ASME, New York, 1992.
- [9] Christoph Beckermann and Raymond Viskanta. Mathematical modeling of transport phenomena during alloy solidification. *Applied Mechanical Review*, 46:1–27, 1993.
- [10] C Y Wang and Christoph Beckermann. Equiaxed dendritic solidification with convection: Part I. Multiscale/multiphase modeling. *Metallurgical and Materials Transactions A*, 27(9):2754–2764, 1996.
- [11] Benoît Appolaire, Hervé Combeau, and Gérard Lesoult. Modeling of equiaxed growth in multicomponent alloys accounting for convection and for the globular/dendritic morphological transition. *Materials Science and Engineering: A*, 487(1-2):33–45, jul 2008.

- [12] Menghuai Wu and Andreas Ludwig. Modeling equiaxed solidification with melt convection and grain sedimentation-I. Model description. *Acta Materialia*, 57:5621–5631, 2009.
- [13] Menghuai Wu and Andreas Ludwig. Modeling equiaxed solidification with melt convection and grain sedimentation-II. Model verification. *Acta Materialia*, 57(19):5632–5644, 2009.
- [14] Menghuai Wu, A Fjeld, and Andreas Ludwig. Modelling mixed columnar-equiaxed solidification with melt convection and grain sedimentation - Part I: Model description. *Computational Materials Science*, 50:32–42, 2010.
- [15] Menghuai Wu, Andreas Ludwig, and A Fjeld. Modelling mixed columnar-equiaxed solidification with melt convection and grain sedimentation - Part II: Illustrative modelling results and parameter studies. *Computational Materials Science*, 50:32–42, 2010.
- [16] Nicolas Leriche. *Etude de la Transition Colonnaire-Equiaxe dans les lingots et en coulée continue d’acier et influence du mouvement des grains* Thèse. Phd thesis, Université de Lorraine, Nancy, France, 2015.
- [17] Nicolas Leriche, Hervé Combeau, Charles-André Gandin, and Miha Založnik. Modelling the Columnar-to-Equiaxed and Equiaxed-to-Columnar Transitions in Ingots Using a Multiphase Model. *IOP Conference Series: Materials Science and Engineering*, 84:012087, 2015.
- [18] Hervé Combeau, Miha Založnik, Stéphane Hans, and Pierre Emmanuel Richy. Prediction of Macroseggregation in Steel Ingots: Influence of the Motion and the Morphology of Equiaxed Grains. *Metallurgical and Materials Transactions B*, 40(3):289–304, 2009.
- [19] Jun Li, Menghuai Wu, Andreas Ludwig, and Abdellah Kharicha. Simulation of macroseggregation in a 2.45-ton steel ingot using a three-phase mixed columnar-equiaxed model. *International Journal of Heat and Mass Transfer*, 72:668–679, 2014.
- [20] Wensheng Li, Houfa Shen, Xiong Zhang, and Baicheng Liu. Modeling of species transport and macroseggregation in heavy steel ingots. *Metallurgical and Materials Transactions B: Process Metallurgy and Materials Processing Science*, 45(2):464–471, 2014. ISBN 1166301398624.
- [21] Wutao Tu, Houfa Shen, and Baicheng Liu. Two-Phase Modeling of Macroseggregation in a 231 t Steel Ingot. *ISIJ International*, 54(2):351–355, 2014.
- [22] Hervé Combeau, Miha Založnik, and Marie Bedel. Predictive Capabilities of Multiphysics and Multiscale Models in Modeling of Solidification of Steel Ingots and DC Casting of Aluminum. *JOM*, 68(8):2198–2206, aug 2016.
- [23] Thi-Thuy-My Nguyen, Charles-André Gandin, Hervé Combeau, Miha Založnik, and Michel Bellet. Finite Element Multi-scale Modeling of Chemical Segregation in Steel Solidification Taking into Account the Transport of Equiaxed Grains. *Metallurgical and Materials Transactions A*, 49(5):1725–1748, feb 2018.

- [24] Laurent Heyvaert, Marie Bedel, Miha Založnik, and Hervé Combeau. Modeling of the Coupling of Microstructure and Macroseggregation in a Direct Chill Cast Al-Cu Billet. *Metallurgical and Materials Transactions A*, 48(10):4713–4734, 2017.
- [25] Akash Pakanati, Knut Omdal Tveito, Mohammed M’Hamdi, Hervé Combeau, and Miha Založnik. Application of an Equiaxed Grain Growth and Transport Model to Study Macroseggregation in a DC Casting Experiment. *Metallurgical and Materials Transactions A*, 50(4):1773–1786, apr 2019.
- [26] Benjamin Gerin, Hervé Combeau, Miha Založnik, and Isabelle Poitroult. Prediction of solidification structures in a 9.8 ton steel ingot. *IOP Conference Series: Materials Science and Engineering*, in press, 2020.
- [27] Miha Založnik, Arvind Kumar, Hervé Combeau, Marie Bedel, Philippe Jarry, and Emmanuel Waz. Influence of Transport Mechanisms on Macroseggregation Formation in Direct Chill Cast Industrial Scale Aluminum Alloy Ingots. *Advanced Engineering Materials*, 13(7):570–580, jul 2011.
- [28] Marie Bedel, Knut Omdal Tveito, Miha Založnik, Hervé Combeau, and Mohammed M’Hamdi. A model study of the impact of the transport of inoculant particles on microstructure formation during solidification. *Computational Materials Science*, 102:95–109, 2015.
- [29] Jun Ni and Christoph Beckermann. Modeling of globulitic alloy solidification with convection. *Journal of Materials Processing & Manufacturing Science*, 2:217–231, 1993.
- [30] C Y Wang, S Ahuja, Christoph Beckermann, and H C De Groh III. Multiparticle interfacial drag in equiaxed solidification. *Metallurgical and Materials Transactions B*, 26(February):111–119, 1995.
- [31] A Ramani and Christoph Beckermann. Dendrite tip growth velocities of settling NH₄Cl equiaxed crystals, 1997.
- [32] H C De Groh III, P D Weidman, R Zakhem, S Ahuja, and Christoph Beckermann. Calculation of Dendrite Settling Velocities Using a Porous Envelope. *Metallurgical Transactions B*, 24(October):749–753, 1993.
- [33] Boubeker Rabia. *La formation des structures équiaxes : mouvement des grains, croissance-refusion, conséquences sur les macroségrégations*. Phd thesis, INPL, Nancy, 2004.
- [34] Hervé Combeau, Miha Založnik, Boubeker Rabia, Sylvain Charmond, Stéphane Hans, and Pierre Emmanuel Richy. Prediction of the macroseggregation in steel ingots: influence of the motion and the growth of the equiaxed grains. In Peter D Lee, A Mitchell, Jean-Pierre Bellot, and Alain Jardy, editors, *Proceedings of the 2007 International Symposium on Liquid Metal Processing and Casting*, pages 127–132. Nancy, France, 2007.
- [35] Christoph Beckermann and Chao Yang Wang. Incorporating interfacial phenomena in solidification models. *Jom*, 46(1):42–47, 1994.
- [36] Christoph Beckermann and C Y Wang. Equiaxed dendritic solidification with convection: Part III. Comparisons with NH₄Cl-H₂O experiments. *Metallurgical and Materials Transactions A*, 27(9):2784–2795, 1996.

- [37] C. Beckermann. Modeling segregation and grain structure development in equiaxed solidification with convection. *JOM*, 49(3):13–17, mar 1997.
- [38] J. P. Gu, C. Beckermann, and A. F. Giamei. Motion and remelting of dendrite fragments during directional solidification of a nickel-base superalloy. *Metallurgical and Materials Transactions A: Physical Metallurgy and Materials Science*, 28(7):1533–1542, 1997.
- [39] Benoît Appolaire and Hervé Combeau. Modelling of the Settling of Equiaxed Crystals During the Solidification of Large Steel Ingots. In Doru M Stefanescu, editor, *Modeling of Casting, Welding and Advanced Solidification Processes X*, pages 221–228. TMS, Warrendale (PA), USA, 2003.
- [40] I. Vannier, H. Combeau, and G. Lesoult. Numerical model for prediction of the final segregation pattern of bearing steel ingots. *Materials Science and Engineering A*, 173(1-2):317–321, 1993.
- [41] Thierry Mazet. *Etude des structures de solidification et des ségrégations dans les lingots d'acier*. Phd thesis, INPL, Nancy, 1995.
- [42] Gérard Lesoult, Virginie Albert, Benoît Appolaire, Hervé Combeau, Dominique Daloz, A Joly, Christian Stomp, Gerd-Ulrich Grün, and Philippe Jarry. Equi-axed Growth and Related Segregations in Cast Metallic Alloys. *Science and Technology of Advanced Materials*, 2:285–291, 2001.
- [43] Gérard Lesoult. Macrosegregation in steel strands and ingots: Characterisation, formation and consequences. *Materials Science and Engineering A*, 414:19–29, 2005.
- [44] Edward John Pickering. Macrosegregation in Steel Ingots: The Applicability of Modelling and Characterisation Techniques. *ISIJ International*, 53(6):935–949, 2013.
- [45] Benjamin Gerin, Hervé Combeau, Miha Založnik, Isabelle Poitault, and Maya Cherif. Prediction of solidification structures in a 9.8 t steel ingot. *IOP Conference Series: Materials Science and Engineering*, 529:012036, may 2019.
- [46] Miha Založnik and Hervé Combeau. The influence of the morphology evolution of free-floating equiaxed grains on the macrosegregation in a 3.3-ton steel ingot. In Steve L Cockroft and Daan M Maijer, editors, *Modeling of Casting, Welding and Advanced Solidification Processes XII*, pages 165–172. TMS, Warrendale (PA), USA, 2009.
- [47] J. D. Hunt. Steady state columnar and equiaxed growth of dendrites and eutectic. *Materials Science and Engineering*, 65(1):75–83, 1984. ISBN 0025-5416.
- [48] Miha Založnik, Arvind Kumar, Hervé Combeau, Marie Bedel, Philippe Jarry, and Emmanuel Waz. The Coupling of Macrosegregation With Grain Nucleation, Growth and Motion in DC Cast Aluminum Alloy Ingots. In John F Grandfield and Dmitry G Eskin, editors, *Essential Readings in Light Metals, Volume 3, Cast Shop for Aluminum Production*, pages 848–853. John Wiley & Sons, Hoboken (NJ), USA, 2013. ISBN 978-1-118-63571-1.

- [49] Christopher J. Vreeman, Matthew John Maximilian Krane, and Frank P. Incropera. The effect of free-floating dendrites and convection on macrosegregation in direct chill cast aluminum alloys Part I: Model development. *International Journal of Heat and Mass Transfer*, 43(5):677–686, 2000.
- [50] Christopher J Vreeman, J David Schloz, and Matthew John Maximilian Krane. Direct Chill Casting of Aluminum Alloys: Modeling and Experiments on Industrial Scale Ingots. *Journal of Heat Transfer*, 124(5):947, 2002.
- [51] Anand V Reddy and Christoph Beckermann. Simulation of the Effects of Thermosolutal Convection, Shrinkage Induced Flow and Solid Transport on Macrosegregation and Equiaxed Grain Size Distribution in a DC Continuous Cast Al-Cu Round Ingot. In Vaughan R Voller, Steve P Marsh, and Nagy El-Kaddah, editors, *Materials Processing in the Computer Age II*, pages 89–102. TMS, 1995.
- [52] Anand V Reddy and Christoph Beckermann. Modeling of Macrosegregation Due to Thermosolutal Convection and Contraction-Driven Flow in Direct Chill Continuous Casting of an Al-Cu Round Ingot. *Metallurgical and Materials Transactions B*, 28B:479–489, 1997.
- [53] Igor Vušanović and Matthew John Maximilian Krane. Macrosegregation in horizontal direct chill casting of ternary Al alloys: Investigation of solid motion. *IOP Conference Series: Materials Science and Engineering*, 27:012069, 2012.
- [54] Kyle Fezi, Alex Plotkowski, and Matthew John M. Krane. Macrosegregation modeling during direct-chill casting of aluminum alloy 7050. *Numerical Heat Transfer; Part A: Applications*, 70(9):939–963, 2016.
- [55] John Coleman and Matthew John Maximilian Krane. Influence of liquid metal feeding on the flow and macrosegregation in DC casting. *Materials Science and Technology (United Kingdom)*, 36(4):393–402, 2020.
- [56] Dag Mortensen, Øyvind Jensen, Gerd-Ulrich Grün, and Andreas Buchholz. Macrosegregation Modelling of Large Sheet Ingots Including Grain Motion, Solidification Shrinkage and Mushy Zone Deformation. In *Light Metals 2019*, pages 983–990. 2019.
- [57] A Joly, Gerd-Ulrich Grün, Dominique Daloz, Hervé Combeau, and Gérard Lesoult. Effect of Grain Refinement on Macrosegregation in Direct Chill Semi-Continuous Casting of Aluminium Sheet Ingot. *Materials Science Forum*, 329-330:111–120, 2000.
- [58] Dominique Daloz, Hervé Combeau, A Joly, Gérard Lesoult, Gerd-Ulrich Grün, Philippe Jarry, and Bruno Commet. Étude sur l’origine de la macroségrégation centrale dans la coulée semi-continue d’aluminium. In *Materiaux 2002: De la conception à la mise en œuvre*. Tours, France, 2002.
- [59] R Nadella, Dmitry G. Eskin, Qiang Du, and Laurens Katgerman. Macrosegregation in direct-chill casting of aluminium alloys. *Progress in Materials Science*, 53(3):421–480, mar 2008.
- [60] Samuel R Wagstaff and Antoine Allanore. Modification of macrosegregation patterns in rolling slab ingots by bulk grain migration. In Edward Williams, editor, *Light Metals 2016*, pages 715–719. TMS, Warrendale (PA), USA, 2016.

- [61] Marie Bedel, Laurent Heyvaert, Miha Založnik, Hervé Combeau, Dominique Daloz, and Gérard Lesoult. Process-scale modeling of microstructure in direct chill casting of aluminum alloys. *IOP Conference Series: Materials Science and Engineering*, 84:012100, 2015.
- [62] Akash Pakanati, Knut Omdal Tveito, Mohammed M’Hamdi, Hervé Combeau, and Miha Založnik. Impact of Inlet Flow on Macroseggregation Formation Accounting for Grain Motion and Morphology Evolution in DC Casting of Aluminium. In Olivier Martin, editor, *Light Metals 2018*, pages 1089–1096. TMS, Warrendale (PA), USA, 2018. ISBN 978-3-319-74065-2.
- [63] Akash Pakanati, Mohammed M’Hamdi, Miha Založnik, and Hervé Combeau. 3D modelling of the impact of inlet flow on macroseggregation formation in DC casting of aluminium alloys accounting for grain morphology and transport. In A Roósz, Zs Veres, M Svéda, and G Karacs, editors, *Solidification and Gravity 2018*, pages 161–166. Hungarian Academy of Sciences University of Miskolc, Miskolc, Hungary, 2018. ISBN 978-963-508-889-8.
- [64] Knut Omdal Tveito, Akash Pakanati, Mohammed M’Hamdi, Hervé Combeau, and Miha Založnik. A Simplified Three-Phase Model of Equiaxed Solidification for the Prediction of Microstructure and Macroseggregation in Castings. *Metallurgical and Materials Transactions A*, 49(7):2778–2794, jul 2018.
- [65] Akash Pakanati, Mohammed M’Hamdi, Hervé Combeau, and Miha Založnik. Investigation of Macroseggregation Formation in Aluminium DC Casting for Different Alloy Systems. *Metallurgical and Materials Transactions A*, 49(10):4710–4721, oct 2018.
- [66] Philippe Jarry and Michel Rappaz. Recent advances in the metallurgy of aluminium alloys. Part I: Solidification and casting. *Comptes Rendus Physique*, 1:1–16, 2018.
- [67] Akash Pakanati, Knut Omdal Tveito, Mohammed M’Hamdi, Hervé Combeau, and Miha Založnik. Analysis of the Interplay Between Thermo-solutal Convection and Equiaxed Grain Motion in Relation to Macroseggregation Formation in AA5182 Sheet Ingots. In Corleen Chesonis, editor, *Light Metals 2019*. TMS, San Antonio (TX), USA, 2019. ISBN 978-3-030-05863-0.
- [68] Akash Pakanati, Mohammed M’Hamdi, Hervé Combeau, and Miha Založnik. Modelling macroseggregation modification in DC casting of aluminium alloys in sheet ingots accounting for inlet melt flow, equiaxed grain morphology and transport. *IOP Conference Series: Materials Science and Engineering*, in press, 2020.
- [69] A Lindsay Greer, A M Bunn, Arnaud Tronche, P V Evans, and D J Bristow. Modelling of inoculation of metallic melts: application to grain refinement of aluminium by AlTiB. *Acta Materialia*, 48(11):2823–2835, jun 2000.
- [70] Tuomas Jalanti, M Swierkosz, Marco Gremaud, and Michel Rappaz. Modelling of macroseggregation in continuous casting of aluminium. In *DGM conference*. Frankfurt, Germany, 2000. ISBN 3527302832.

- [71] Miha Založnik and Božidar Šarler. Modeling of macrosegregation in direct-chill casting of aluminum alloys: Estimating the influence of casting parameters. *Materials Science and Engineering A*, 413-414:85–91, 2005.
- [72] L. Zhang, Dmitry G. Eskin, A. Miroux, T. Subroto, and L. Katgerman. Influence of Melt Feeding Scheme and Casting Parameters During Direct-Chill Casting on Microstructure of an AA7050 Billet. *Metallurgical and Materials Transactions B*, 43(6):1565–1573, dec 2012.
- [73] Qiang Du, Dmitry G Eskin, Alain Jacot, and Laurens Katgerman. Two-dimensional modelling and experimental study on microsegregation during solidification of an AlCu binary alloy. *Acta Materialia*, 55(5):1523–1532, mar 2007.
- [74] Arild Håkonsen, Dag Mortensen, Steinar Benum, and Hans Erik Vatne. A micro/macro model for the equiaxed grain size distribution in DC-cast aluminum ingots. In Edward C. Eckert, editor, *Light Metals 1999*, pages 821–827. TMS, Warrendale (PA), USA, 1999.
- [75] Arnaud Tronche. *Investigation and modelling of inoculation of aluminium by TiC*. Phd thesis, University of Cambridge, 2000.
- [76] R C Dorward and D J Beerntsen. Effects of casting practice on macrosegregation and microstructure of 2004 alloy billet. *Light Metals 1990*, pages 919–924, 1990.
- [77] Men G Chu and John E Jacoby. Macrosegregation characteristics of commercial size aluminum alloy ingot cast by the direct chill method. *Light Metals 1990*, pages 925–930, 1990.
- [78] Dmitry G. Eskin, Jan Zuidema Jr., V I Savran, and Laurens Katgerman. Structure Formation and Macrosegregation under Different Process Conditions during DC Casting. *Materials Science and Engineering A*, 384:232–244, 2004.
- [79] Ho Yu and D A Granger. Macrosegregation in Aluminum Alloy Ingot Cast by the Semicontinuous Direct Chill (DC) Method. In *Aluminum Alloys: Their Physical and Mechanical Properties*, pages 17–29. EMAS, Sheffield, UK, 1986.
- [80] T L Finn, Men G Chu, and W D Bennon. The Influence of Mushy Region Microstructure on Macrosegregation in Direct Chill Cast Aluminum-Copper Round Ingots. In Christoph Beckermann, L A Bertram, S J Pien, and R E Smelser, editors, *Micro/Macro Scale Phenomena in Solidification*, pages 17–24. ASME, New York, 1992.
- [81] Dmitry G. Eskin, R Nadella, and Laurens Katgerman. Effect of different grain structures on centerline macrosegregation during direct-chill casting. *Acta Materialia*, 56(6):1358–1365, 2008. ISBN 1359-6454.
- [82] Dmitry G. Eskin. *Physical Metallurgy of Direct Chill Casting of Aluminum Alloys*. Advances in Metallic Alloys. CRC Press, Boca Raton, FL, 2008. ISBN 978-1-4200-6281-6.
- [83] R Nadella, Dmitry G. Eskin, and Laurens Katgerman. Effect of grain refinement on structure evolution, "floating" grains, and centerline macrosegregation in direct-chill cast AA2024 alloy Billets. *Metallurgical and Materials Transactions A*, 39(2):450–461, 2008. ISBN 1073-5623.

- [84] Dmitry G. Eskin, A Jafari, and L Katgerman. Contribution of forced centre-line convection during direct chill casting of round billets to macrosegregation and structure of binary AlCu aluminium alloy. *Materials Science and Technology*, 27(5):890–896, 2011.
- [85] Miha Založnik, Arvind Kumar, Hervé Combeau, Marie Bedel, Philippe Jarry, and Emmanuel Waz. The Coupling of Macrosegregation With Grain Nucleation, Growth and Motion in DC Cast Aluminum Alloy Ingots. In S J Lindsay, editor, *Light metals 2011*, pages 699–704. TMS, Warrendale (PA), USA, 2011.
- [86] Marie Bedel, Miha Založnik, Arvind Kumar, Hervé Combeau, Philippe Jarry, and Emmanuel Waz. Influence of transport mechanisms on nucleation and grain structure formation in DC cast aluminium alloy ingots. *IOP Conference Series: Materials Science and Engineering*, 27:012070, jan 2012.
- [87] T. Wang, M. Wu, A. Ludwig, M. Abondano, B. Pustal, and A. Bührig-Polaczek. Modelling the thermosolutal convection, shrinkage flow and grain movement of globular equiaxed solidification using a three phase model. *International Journal of Cast Metals Research*, 18(4):221–228, 2005.
- [88] Ludovic Berthier and Laboratoire Charles Coulomb. Entre géométrie et physique statistique : structure d’un empilement désordonné. *Images de la physique 2011*, pages 28–34, 2011.
- [89] Jessica Baker and Arshad Kudrolli. Maximum and minimum stable random packings of Platonic solids. *Physical Review E - Statistical, Nonlinear, and Soft Matter Physics*, 82(6):1–5, 2010. ISBN 1550-2376 (Electronic)\r1539-3755 (Linking).
- [90] Alexander Jaoshvili, Andria Esakia, Massimo Porrati, and Paul M. Chaikin. Experiments on the Random Packing of Tetrahedral Dice. *Physical Review Letters*, 104(18):1–4, 2010.
- [91] Weining Man, Aleksandar Donev, Frank H. Stillinger, Matthew T. Sullivan, William B. Russel, David Heeger, Souheil Inati, Salvatore Torquato, and P. M. Chaikin. Experiments on random packings of ellipsoids. *Physical Review Letters*, 94(19):1–4, 2005.
- [92] I. Malinetskaya, V. V. Mourzenko, J. F. Thovert, and P. M. Adler. Random packings of spiky particles: Geometry and transport properties. *Physical Review E - Statistical, Nonlinear, and Soft Matter Physics*, 80(1):1–16, 2009.
- [93] Jonathan Barés, Yuchen Zhao, Mathieu Renouf, Karola Dierichs, and Robert Behringer. Structure of hexapod 3D packings: understanding the global stability from the local organization. *EPJ Web of Conferences*, 140:06021, jun 2017.
- [94] Carlos Avendaño and Fernando A. Escobedo. Packing, entropic patchiness, and self-assembly of non-convex colloidal particles: A simulation perspective. *Current Opinion in Colloid and Interface Science*, 30:62–69, 2017.
- [95] Chaoming Song, Ping Wang, and Hernán A Makse. A phase diagram for jammed matter. *Nature*, 453(7195):629–632, 2008. ISBN 0028-0836.
- [96] Antonio Olmedilla. GGDEM, 2017.

- [97] Antonio Olmedilla, Miha Založnik, and Hervé Combeau. DEM simulation of dendritic grain random packing: application to metal alloy solidification. *EPJ Web of Conferences*, 140:06002, jun 2017.
- [98] Antonio Olmedilla, Miha Založnik, Bernard Rouat, and Hervé Combeau. Packing of sedimenting equiaxed dendrites. *Physical Review E*, 97(1):012910, jan 2018.
- [99] Antonio Olmedilla, Miha Založnik, Thomas Messmer, Bernard Rouat, and Hervé Combeau. Packing dynamics of spherical and nonconvex grains sedimenting at low Stokes number. *Physical Review E*, 99(1):012907, jan 2019.
- [100] Miha Založnik and Hervé Combeau. An operator splitting scheme for coupling macroscopic transport and grain growth in a two-phase multiscale solidification model: Part I Model and solution scheme. *Computational Materials Science*, 48(1):1–10, jun 2010.
- [101] Miha Založnik, Arvind Kumar, and Hervé Combeau. An operator splitting scheme for coupling macroscopic transport and grain growth in a two-phase multiscale solidification model: Part II Application of the model. *Computational Materials Science*, 48(1):11–21, 2010.
- [102] Bruno Sportisse. An Analysis of Operator Splitting Techniques in the Stiff Case. *Journal of Computational Physics*, 161:140–168, 2000.
- [103] J. Guo and C. Beckermann. Three-dimensional simulation of freckle formation during binary alloy solidification: Effect of mesh spacing. *Numerical Heat Transfer; Part A: Applications*, 44(6):559–576, 2003.
- [104] Arvind Kumar, Joëlle Demurger, Jean Wendenbaum, Miha Založnik, and Hervé Combeau. Experimental and Numerical Studies on the Influence of Hot Top Conditions on the Macroseggregation in an Industrial Steel Ingot. In *International Conference on Ingot Casting, Rolling and Forging*, page 28. Aachen, Germany, 2012.
- [105] Hervé Combeau, Arvind Kumar, Miha Založnik, Isabelle Poitroult, Gilbert Lacagne, Andrew Gingell, Thierry Mazet, and Gérard Lesoult. Macroseggregation prediction in a 65 ton steel ingot. In *International Conference on Ingot Casting, Rolling and Forging*, page 27. Aachen, Germany, 2012.
- [106] Иванцов, Г. П. Температурное поле вокруг шарообразного, цилиндрического и иглообразного кристалла, растущего в переохлажденном расплаве. Доклады Академии Наук СССР, 58 (4):567–569, 1947.
- [107] G. Horvay and J. W. Cahn. Dendritic and spheroidal growth. *Acta Metallurgica*, 9(7):695–705, 1961.
- [108] W. J. Boettinger, James A. Warren, C. Beckermann, and A. Karma. Phase-field simulation of solidification. *Annual Review of Materials Science*, 32: 163–194, 2002.
- [109] Ingo Steinbach. Why Solidification? Why Phase-Field? *JOM*, 65(9):1096–1102, aug 2013. ISBN 1183701306.

- [110] Abhik Choudhury, Klemens Reuther, Eugenia Wesner, Anastasia August, Britta Nestler, and Markus Rettenmayr. Comparison of phase-field and cellular automaton models for dendritic solidification in Al-Cu alloy. *Computational Materials Science*, 55:263–268, 2012.
- [111] Vaughan R Voller. An enthalpy method for modeling dendritic growth in a binary alloy. *International Journal of Heat and Mass Transfer*, 51:823–834, 2008.
- [112] A. Kao and K. Pericleous. A numerical model coupling thermoelectricity, magnetohydrodynamics and dendritic growth. *Journal of Algorithms and Computational Technology*, 6(1):173–201, 2012.
- [113] K. Reuther and M. Rettenmayr. Perspectives for cellular automata for the simulation of dendritic solidification - A review. *Computational Materials Science*, 95:213–220, 2014.
- [114] Tomohiro Takaki, Takashi Shimokawabe, Munekazu Ohno, Akinori Yamanaoka, and Takayuki Aoki. Unexpected selection of growing dendrites by very-large-scale phase-field simulation. *Journal of Crystal Growth*, 382:21–25, 2013.
- [115] Z Guo and S M Xiong. Study of dendritic growth and coarsening using a 3-D phase field model: Implementation of the Para-AMR algorithm. *IOP Conference Series: Materials Science and Engineering*, 84:012067, 2015.
- [116] Charles-André Gandin, Jean-Luc Desbiolles, Michel Rappaz, and Philippe Thévoz. A three-dimensional cellular automation-finite element model for the prediction of solidification grain structures. ... *Materials Transactions A*, 30(December):3153–3165, 1999.
- [117] Charles-André Gandin, To Carozzani, H Dignonnet, S Chen, and Gildas Guillemot. Direct modeling of structures and segregations up to industrial casting scales. *JOM*, 65(9):1122–1130, 2013. ISBN 1183701306.
- [118] Ingo Steinbach, Christoph Beckermann, B Kauerauf, Q Li, and J Guo. Three-dimensional modeling of equiaxed dendritic growth on a mesoscopic scale. *Acta Materialia*, 47(3):971–982, feb 1999.
- [119] Youssef Souhar, Valerio Francesco De Felice, Christoph Beckermann, Hervé Combeau, and Miha Založnik. Three-dimensional mesoscopic modeling of equiaxed dendritic solidification of a binary alloy. *Computational Materials Science*, 112:304–317, feb 2016.
- [120] Shaun McFadden, David J Browne, and Charles-André Gandin. A Comparison of Columnar-to-Equiaxed Transition Prediction Methods Using Simulation of the Growing Columnar Front. *Metallurgical and Materials Transactions A*, 40(3):662–672, jan 2009.
- [121] Abdellah Kharicha, M Stefan-Kharicha, Andreas Ludwig, and Menghuai Wu. A scale adaptive dendritic envelope model of solidification at mesoscopic scales. *IOP Conference Series: Materials Science and Engineering*, 84:012032, 2015.
- [122] Y. Feng and A. B. Phillion. A 3D meso-scale solidification model for metallic alloy using a volume average approach. *Materialia*, 6(February), 2019.

- [123] Damien Tournet and Alain Karma. Multiscale dendritic needle network model of alloy solidification. *Acta Materialia*, 61(17):6474–6491, oct 2013.
- [124] Damien Tournet, You Song, Clarke Aj, Alain Karma, Amy J. Clarke, and Alain Karma. Phase-field Simulation Study of Dendritic Grain Growth Competition during Alloy Directional Solidification. In *Frontiers of Solidification Science, TMS Annual Meeting 2016*, pages 35–40, 2016.
- [125] D. Tournet, M. M. Francois, and A. J. Clarke. Multiscale dendritic needle network model of alloy solidification with fluid flow. *Computational Materials Science*, 162(January):206–227, 2019.
- [126] Stéphane Vernède, Philippe Jarry, and Michel Rappaz. A granular model of equiaxed mushy zones: Formation of a coherent solid and localization of feeding. *Acta Materialia*, 54(15):4023–4034, 2006.
- [127] M. Sistaninia, A. B. Phillion, J. M. Drezet, and M. Rappaz. Three-dimensional granular model of semi-solid metallic alloys undergoing solidification: Fluid flow and localization of feeding. *Acta Materialia*, 60(9):3902–3911, 2012.
- [128] W Wang, Peter D Lee, and M McLean. A model of solidification microstructures in nickel-based superalloys: Predicting primary dendrite spacing selection. *Acta Materialia*, 51:2971–2987, 2003. ISBN 1359-6454.
- [129] Lang Yuan and Peter D Lee. Dendritic solidification under natural and forced convection in binary alloys: 2D versus 3D simulation. *Modelling and Simulation in Materials Science and Engineering*, 18(5):055008, jul 2010.
- [130] Andrew Kao and Koulis Pericleous. TEMHD Effects On Solidification Under Microgravity Conditions. In *Materials Research in Microgravity*, pages 105–112. TMS, Warrendale (PA), USA, 2012.
- [131] Ingo Steinbach, Hermann-Josef Diepers, and Christoph Beckermann. Transient growth and interaction of equiaxed dendrites. *Journal of Crystal Growth*, 275(3-4):624–638, mar 2005.
- [132] Pierre Delaleau, Christoph Beckermann, Ragnvald H Mathiesen, and Lars Arnberg. Mesoscopic Simulation of Dendritic Growth Observed in X-ray Video Microscopy During Directional Solidification of AlCu Alloys. *ISIJ International*, 50(12):1886–1894, jan 2010.
- [133] Pierre Delaleau. *Mesoscale modeling of dendritic growth during directional solidification of aluminium alloys*. PhD thesis, NTNU, Trondheim, Norway, 2011.
- [134] Antonio Olmedilla, Miha Založnik, Martín Cisternas Fernández, Alexandre Viardin, and Hervé Combeau. Three-dimensional mesoscopic modeling of equiaxed dendritic solidification in a thin sample: effect of convection flow. *IOP Conference Series: Materials Science and Engineering*, 529:012040, may 2019.
- [135] G P Ivantsov. Thermal and diffusion processes in crystal growth. In A V Shubnikov and N N Sheftal', editors, *Growth of Crystals*, pages 76–85. Akademia Nauk SSSR, Moscow, USSR, 1961.

- [136] B Cantor and A Vogel. Dendritic solidification and fluid flow. *Journal of Crystal Growth*, 41(1):109–123, nov 1977.
- [137] Ying Sun and Christoph Beckermann. Sharp interface tracking using the phase-field equation. *Journal of Computational Physics*, 220(2):626–653, jan 2007.
- [138] Alexandre Viardin, Miha Založnik, Youssef Souhar, Markus Apel, and Hervé Combeau. Mesoscopic modeling of spacing and grain selection in columnar dendritic solidification: Envelope versus phase-field model. *Acta Materialia*, 122:386–399, jan 2017.
- [139] Ying Sun and Christoph Beckermann. A two-phase diffuse-interface model for HeleShaw flows with large property contrasts. *Physica D: Nonlinear Phenomena*, 237(23):3089–3098, dec 2008.
- [140] Jonathan A Dantzig and Michel Rappaz. *Solidification*. EPFL Press, Lausanne, 1st edition, 2009. ISBN 978-2-940222-17-9.
- [141] Yi Feng, Miha Založnik, B.G. Thomas, and A.B. Phillion. Meso-scale simulation of liquid feeding in an equiaxed dendritic mushy zone. *Materialia*, 9: 100612, mar 2020.
- [142] H. Meidani and A. Jacot. Phase-field simulation of micropores constrained by the dendritic network during solidification. *Acta Materialia*, 59(8):3032–3040, 2011.
- [143] M. Sistaninia, A. B. Phillion, J. M. Drezet, and M. Rappaz. Simulation of semi-solid material mechanical behavior using a combined discrete/finite element method. *Metallurgical and Materials Transactions A: Physical Metallurgy and Materials Science*, 42(1):239–248, 2011.
- [144] A.G. Murphy, Ragnvald H Mathiesen, Y. Houltz, J. Li, C. Lockowandt, K. Henriksson, Gerhard Zimmermann, N. Melville, and David J Browne. XRMON-SOL: Isothermal Equiaxed Solidification of a Grain Refined Al20wt%Cu Alloy. *Journal of Crystal Growth*, 440:38–46, 2016.
- [145] A. G. Murphy, R. H. Mathiesen, Y. Houltz, J. Li, C. Lockowandt, K. Henriksson, N. Melville, and David J Browne. Direct observation of spatially isothermal equiaxed solidification of an AlCu alloy in microgravity on board the MASER 13 sounding rocket. *Journal of Crystal Growth*, 454:96–104, 2016.
- [146] Antonio Olmedilla, Miha Založnik, and Hervé Combeau. Quantitative 3D mesoscopic modeling of grain interactions during equiaxed dendritic solidification in a thin sample. *Acta Materialia*, 173:249–261, jul 2019.
- [147] Andrew Murphy. *In Situ X-Ray Monitoring of Advanced Alloy Solidification Processes under Microgravity and Terrestrial Conditions*. Phd thesis, University College Dublin, 2013.
- [148] D. J. Browne. Personal Communication, 2 May 2018.
- [149] Adrian Bejan. *Convection Heat Transfer*. John Wiley and Sons, Hoboken, NJ, 3rd edition, 2004. ISBN 978-0471271505.

- [150] Alexandre Viardin, Youssef Souhar, Martín Cisternas Fernández, Markus Apel, and Miha Založnik. Mesoscopic modeling of columnar growth with convection. *Acta Materialia*, submitted, 2020.
- [151] Damien Tournet, Laszlo Sturz, Alexandre Viardin, and Miha Založnik. Comparing mesoscopic models for dendritic growth. *IOP Conference Series: Materials Science and Engineering*, in press, 2020.
- [152] Damien Tournet and Alain Karma. Growth competition of columnar dendritic grains: A phase-field study. *Acta Materialia*, 82:64–83, jan 2015.
- [153] Miha Založnik, Alexandre Viardin, Youssef Souhar, Hervé Combeau, and Markus Apel. Mesoscopic modeling of columnar solidification and comparisons with phase-field simulations. *IOP Conference Series: Materials Science and Engineering*, 84:012074, 2015.
- [154] Miha Založnik, Alexandre Viardin, Youssef Souhar, Hervé Combeau, and Markus Apel. Mesoscopic modelling of columnar solidification. *IOP Conference Series: Materials Science and Engineering*, 117:012013, 2016.
- [155] Silvère Akamatsu and Henri Nguyen-Thi. In situ observation of solidification patterns in diffusive conditions. *Acta Materialia*, 108:325–346, apr 2016.
- [156] Damien Tournet, Y Song, Amy J Clarke, and Alain Karma. Grain growth competition during thin-sample directional solidification of dendritic microstructures: A phase-field study Supplementary Material. *Acta Materialia*, 122:220–235, 2017.
- [157] A Pineau, Gildas Guillemot, Damien Tournet, Alain Karma, and Charles-André Gandin. Growth competition between columnar dendritic grains Cellular automaton versus phase field modeling. *Acta Materialia*, 155:286–301, 2018.
- [158] Y. Z. Zhou, A. Volek, and N. R. Green. Mechanism of competitive grain growth in directional solidification of a nickel-base superalloy. *Acta Materialia*, 56(11):2631–2637, 2008. ISBN 1359-6454.
- [159] J Li, Menghuai Wu, J Hao, A Kharicha, and Andreas Ludwig. Simulation of channel segregation using a two-phase columnar solidification model Part II: Mechanism and parameter study. *Computational Materials Science*, 55: 419–429, apr 2012.
- [160] Honglei Yu, Junjie Li, Xin Lin, Lilin Wang, and Weidong Huang. Anomalous overgrowth of converging dendrites during directional solidification. *Journal of Crystal Growth*, 402:210–214, 2014.
- [161] Yuze Li, Antonio Olmedilla, Miha Založnik, Julien Zollinger, Lucas Dembinski, and Alexandre Mathieu. Solidification microstructure during selective laser melting of Ni based superalloy: experiment and mesoscopic modelling. *IOP Conference Series: Materials Science and Engineering*, 529: 012004, 2019.
- [162] Ingo Steinbach. Pattern formation in constrained dendritic growth with solutal buoyancy. *Acta Materialia*, 57(9):2640–2645, 2009. ISBN 1359-6454.

- [163] A. Viardin, J. Zollinger, L. Sturz, M. Apel, J. Eiken, R. Berger, and U. Hecht. Columnar dendritic solidification of TiAl under diffusive and hypergravity conditions investigated by phase-field simulations. *Computational Materials Science*, 172:109358, feb 2020.
- [164] Julio Aguilar, Andre Schievenbusch, and Oliver Kättlitz. Investment casting technology for production of TiAl low pressure turbine blades - Process engineering and parameter analysis. *Intermetallics*, 19(6):757–761, 2011. ISBN 0966-9795.
- [165] Volker Güther, Melissa Allen, Joachim Klose, and Helmut Clemens. Metallurgical processing of titanium aluminides on industrial scale. *Intermetallics*, 103(August):12–22, 2018.
- [166] Ulrike Hecht, Can Huang, Julien Zollinger, Dominique Daloz, Miha Založnik, Martín Cisternas, Alexandre Viardin, Shaun McFadden, László Gránásy, Juraj Lapin, Nicolas Leriche, and Florian Kargl. The ESA-MAP project "GRADE CET" An overview of the joint research on solidification of TiAl-based alloys under hypergravity and microgravity conditions. In A Roósz, Zs Veres, M Svéda, and G Karacs, editors, *Solidification and Gravity 2018*, pages 27–36. Hungarian Academy of Sciences University of Miskolc, Miskolc, Hungary, 2018. ISBN 978-963-508-889-8.
- [167] Nicole Reilly. *Hétérogénéités de fabrication des aluminiures de titane : caractérisation et maîtrise de leurs formations en coulée centrifuge*. PhD thesis, Université de Lorraine, Nancy, France, 2016.
- [168] Corbett C. Battaile, R. N. Grugel, A. B. Hmelo, and T. G. Wang. The effect of enhanced gravity levels on microstructural development in Pb-50 wt pct Sn alloys during controlled directional solidification. *Metallurgical and Materials Transactions A*, 25(4):865–870, 1994.
- [169] M. Apel, H.-J. Diepers, and I. Steinbach. On the Effect of Interdendritic Flow on Primary Dendrite Spacing: A Phase Field Study and Analytical Scaling Relations. *Modeling of Casting, Welding and Advanced Solidification Processes*, pages 505–512, 2006. ISBN 0873396294.
- [170] Hermann-Josef Diepers and Ingo Steinbach. Interaction of Interdendritic Convection and Dendritic Primary Spacing: Phase-Field Simulation and Analytical Modeling. *Materials Science Forum*, 508:145–150, 2006.
- [171] Christoph Beckermann, Hermann-Josef Diepers, Ingo Steinbach, Alain Karma, and X Tong. Modeling Melt Convection in Phase-Field Simulations of Solidification. *Journal of Computational Physics*, 154(2):468–496, sep 1999.
- [172] Tomohiro Takaki, Shinji Sakane, Munekazu Ohno, and Yasushi Shibuta. Competitive growth during directional solidification of a binary alloy with natural convection: Two-dimensional phase-field study. *Modelling and Simulation in Materials Science and Engineering*, 27(5), 2019.
- [173] Shinji Sakane, Tomohiro Takaki, Roberto Rojas, Munekazu Ohno, Yasushi Shibuta, Takashi Shimokawabe, and Takayuki Aoki. Multi-GPUs parallel computation of dendrite growth in forced convection using the phase-field-lattice Boltzmann model. *Journal of Crystal Growth*, 474(November 2016): 154–159, 2017.

- [174] Tomohiro Takaki, Shinji Sakane, Munekazu Ohno, Yasushi Shibuta, and Takayuki Aoki. Largescale phasefield lattice Boltzmann study on the effects of natural convection on dendrite morphology formed during directional solidification of a binary alloy. *Computational Materials Science*, 171(September 2019):109209, 2020.
- [175] Benoît Appolaire, Virginie Albert, Hervé Combeau, and Gérard Lesoult. Free growth of equiaxed crystals settling in undercooled NH₄Cl-H₂O melts. *Acta materialia*, 46(16):5851–5862, 1998.
- [176] Benoît Appolaire, Virginie Albert, Hervé Combeau, and Gérard Lesoult. Experimental Study of Free Growth of Equiaxed NH₄Cl Crystals Settling in Undercooled NH₄Cl-H₂O Melts. *ISIJ International*, 39(3):263–270, 1999.
- [177] Charles-André Gandin, Gildas Guillemot, Benoît Appolaire, and N T Niane. Boundary layer correlation for dendrite tip growth with fluid flow. *Materials Science and Engineering A*, 342(1-2):44–50, feb 2003.
- [178] A. Badillo, D. Ceynar, and Christoph Beckermann. Growth of equiaxed dendritic crystals settling in an undercooled melt, Part 1: Tip kinetics. *Journal of Crystal Growth*, 309(2):197–215, dec 2007.
- [179] Antonio Olmedilla Gonzalez de Mendoza. *Grain motion and packing: application to metallic alloy solidification*. PhD thesis, Université de Lorraine, 2017.
- [180] Naomi Oreskes, Kristin Shrader-Frechette, and Kenneth Belitz. Verification, Validation, and Confirmation of Numerical Models in the Earth Sciences. *Science*, 263(5147):641–646, feb 1994.
- [181] Patrick J Roache. Quantification of Uncertainty in Computational Fluid Dynamics. *Annual Review of Fluid Mechanics*, 29(1):123–160, jan 1997.
- [182] Youssef Souhar, Valerio Francesco De Felice, Miha Založnik, Hervé Combeau, and Christoph Beckermann. The role of the stagnant-film thickness in mesoscopic modeling of equiaxed grain envelopes. *IOP Conference Series: Materials Science and Engineering*, 117:012014, mar 2016.
- [183] A J Melendez and Christoph Beckermann. Measurements of dendrite tip growth and sidebranching in succinonitrileacetone alloys. *Journal of Crystal Growth*, 340(1):175–189, feb 2012.
- [184] A. J. Clarke, Damien Tournet, Y. Song, S. D. Imhoff, P. J. Gibbs, J. W. Gibbs, K. Fezzaa, and A. Karma. Microstructure selection in thin-sample directional solidification of an Al-Cu alloy: In situ X-ray imaging and phase-field simulations. *Acta Materialia*, 129:203–216, 2017.
- [185] Damien Tournet and Alain Karma. Three-dimensional dendritic needle network model for alloy solidification. *Acta Materialia*, 120:240–254, 2016.
- [186] Minh Do-Quang and Gustav Amberg. Simulation of free dendritic crystal growth in a gravity environment. *Journal of Computational Physics*, 227(3):1772–1789, 2008.

- [187] T. Takaki, R. Rojas, M. Ohno, T. Shimokawabe, and T. Aoki. GPU phase-field lattice Boltzmann simulations of growth and motion of a binary alloy dendrite. *IOP Conference Series: Materials Science and Engineering*, 84(1), 2015.
- [188] László Rátkai, Tamás Pusztai, and László Gránásy. Phase-field lattice Boltzmann model for dendrites growing and moving in melt flow. *npj Computational Materials*, 5(1), 2019.
- [189] Shinji Sakane, Tomohiro Takaki, Munekazu Ohno, and Yasushi Shibuta. Simulation method based on phase-field lattice Boltzmann model for long-distance sedimentation of single equiaxed dendrite. *Computational Materials Science*, 164(January):39–45, 2019.
- [190] J R Williams and R. O’Connor. Discrete element simulation and the contact problem. *Archives of Computational Methods in Engineering*, 6(4):279–304, dec 1999.
- [191] V. R. Voller and F. Porté-Agel. Moore’s law and numerical modeling. *Journal of Computational Physics*, 179(2):698–703, 2002.
- [192] C Y Wang and Christoph Beckermann. Equiaxed dendritic solidification with convection: Part II. Numerical Simulations for an Al-4 Wt Pct Cu Alloy. *Metallurgical and Materials Transactions A*, 27(September):2765–2783, sep 1996.
- [193] Romain Fleurisson. *Modélisation multi-échelle parallélisée pour la prédiction de structures de grains dendritiques couplant les éléments finis, un automate cellulaire et un réseau de paraboles*. Phd thesis, Université Paris Sciences et Lettres, 2019.
- [194] V.R. Voller and C. Prakash. A fixed grid numerical modelling methodology for convection-diffusion mushy region phase-change problems. *International Journal of Heat and Mass Transfer*, 30(8):1709–1719, aug 1987.
- [195] S D Ridder, S Kou, and R Mehrabian. Effect of Fluid Flow on Macroseggregation in Axi-Symmetric Ingots. *Metallurgical Transactions B*, 12B:435–447, 1981.
- [196] W D Bennon and Frank P Incropera. The evolution of macrosegregation in statically cast binary ingots. *Metallurgical Transactions B*, 18(3):611–616, sep 1987.
- [197] Warren D. Bennon and Frank P. Incropera. Numerical analysis of a binary solid-liquid phase change using a continuum model. *Numerical Heat Transfer*, 13(3):277–296, 1988.
- [198] P. J. Prescott, Frank P. Incropera, and W. D. Bennon. Modeling of dendritic solidification systems: Reassessment of the continuum momentum equation. *International Journal of Heat and Mass Transfer*, 34(9):2351–2359, September 1991.
- [199] Matthew John Maximilian Krane and Frank P. Incropera. Solidification of ternary metal alloysII. Predictions of convective phenomena and solidification behavior in Pb-Sb-Sn alloys. *International Journal of Heat and Mass Transfer*, 40(16):3837–3847, oct 1997.

- [200] Matthew John Maximilian Krane. Macrosegregation development during solidification of a multicomponent alloy with free-floating solid particles. *Applied Mathematical Modelling*, 28(1):95–107, jan 2004.
- [201] Christopher J. Vreeman and Frank P. Incropera. The effect of free-floating dendrites and convection on macrosegregation in direct chill cast aluminum alloys: Part II: predictions for Al-Cu and Al-Mg alloys. *International Journal of Heat and Mass Transfer*, 43(5):687–704, mar 2000.
- [202] Jun Ni and Frank P Incropera. Extension of the continuum model for transport phenomena occurring during metal alloy solidification-II. Microscopic considerations. *International Journal of Heat and Mass Transfer*, 38(7):1285–1296, may 1995.
- [203] Kent D. Carlson, Zhiping Lin, and Christoph Beckermann. Modeling the effect of finite-rate hydrogen diffusion on porosity formation in aluminum alloys. *Metallurgical and Materials Transactions B*, 38(4):541–555, 2007. ISBN 1166300690132.
- [204] Arvind Kumar, Miha Založnik, and Hervé Combeau. Prediction of equiaxed grain structure and macrosegregation in an industrial steel ingot: comparison with experiment. *International Journal of Advances in Engineering Sciences and Applied Mathematics*, 2(4):140–148, sep 2011.
- [205] Marie Bedel. *Étude de la formation des structures de solidification et des macroségrégations en coulée semi-continue d'aluminium*. Phd thesis, Université de Lorraine, Nancy, France, 2014.
- [206] Donald A. Drew and Stephen L. Passman. *Theory of Multicomponent Fluids*, volume 135 of *Applied Mathematical Sciences*. Springer New York, New York, NY, 1999. ISBN 978-1-4684-9227-9. 287 pp.
- [207] Piotr Furmański. Modeling of transport phenomena during solidification of binary systems. *Computer Assisted Mechanics and Engineering Sciences*, Vol. 7, No. 3:391–402, 2000.
- [208] Tomasz A. Kowalewski and Dominique Gobin, editors. *Phase Change with Convection: Modelling and Validation*. Springer Vienna, Vienna, 2004. ISBN 978-3-211-20891-5.
- [209] A. I. Ciobanas and Y. Fautrelle. Ensemble averaged multiphase Eulerian model for columnar/equiaxed solidification of a binary alloy: I. the mathematical model. *Journal of Physics D: Applied Physics*, 40(12):3733–3762, 2007. ISBN 02555476 (ISSN); 0878499911 (ISBN); 9780878499915 (ISBN).
- [210] A. I. Ciobanas and Y. Fautrelle. Ensemble averaged multi-phase Eulerian model for columnar/equiaxed solidification of a binary alloy: II. Simulation of the columnar-to-equiaxed transition (CET). *Journal of Physics D: Applied Physics*, 40(14):4310–4336, 2007.
- [211] Patrick Bousquet-Melou, Adrian Neculae, Benoît Goyeau, and Michel Quintard. Averaged solute transport during solidification of a binary mixture: Active dispersion in dendritic structures. *Metallurgical and Materials Transactions B*, 33(3):365–376, jun 2002.

- [212] Patrick Bousquet-Melou, Benoît Goyeau, Michel Quintard, Florian Fichot, and Dominique Gobin. Average momentum equation for interdendritic flow in a solidifying columnar mushy zone. *International Journal of Heat and Mass Transfer*, 45(17):3651–3665, aug 2002.
- [213] A. Neculae, B. Goyeau, M. Quintard, and D. Gobin. Passive dispersion in dendritic structures. *Materials Science and Engineering A*, 323(1-2):367–376, 2002.
- [214] Stephen Whitaker. The Forchheimer equation: A theoretical development. *Transport in Porous Media*, 25:27–61, 1996.
- [215] Benoît Goyeau, Tahar Benihaddadene, Dominique Gobin, and Michel Quintard. Numerical calculation of the permeability in a dendritic mushy zone. *Metallurgical and Materials Transactions B*, 30(4):613–622, aug 1999.
- [216] Marcelo Aquino Martorano, Davi Teves Aguiar, and Juan Marcelo Rojas Arango. Multigrain and Multiphase Mathematical Model for Equiaxed Solidification. *Metallurgical and Materials Transactions A*, 46(January):377–395, 2015.
- [217] Gildas Guillemot and Charles André Gandin. An analytical model with interaction between species for growth and dissolution of precipitates. *Acta Materialia*, 134:375–393, 2017.
- [218] Mahdi Torabi Rad, Miha Založnik, Hervé Combeau, and Christoph Beckermann. Upscaling mesoscopic simulation results to develop constitutive relations for macroscopic modeling of equiaxed dendritic solidification. *Materialia*, 5:100231, mar 2019.
- [219] Michel Rappaz and Philippe Thévoz. Solute diffusion model for equiaxed dendritic growth: Analytical solution. *Acta Metallurgica*, 35(12):2929–2933, 1987.
- [220] Marcelo Aquino Martorano, Christoph Beckermann, and Charles-André Gandin. A solutal interaction mechanism for the columnar-to-equiaxed transition in alloy solidification. *Metallurgical and Materials Transactions A*, 34(8):1657–1674, aug 2003.
- [221] C Y Wang and Christoph Beckermann. Prediction of Columnar to Equiaxed Transition during Diffusion-Controlled Dendritic Alloy Solidification. *Metallurgical and Materials Transactions A*, 25(5):1081–1093, 1994. ISBN 1073-5623.
- [222] Christoph Beckermann and Marc C Schneider. Simulation of micro-/macrosegregation during the solidification of a low-alloy steel. *ISIJ international*, 35(6):665–672, 1995.
- [223] Georges Salloum-Abou-Jaoude, J Wang, Lara Abou-Khalil, Guillaume Reinhart, Z Ren, Nathalie Mangelinck-Noël, X Li, Yves Fautrelle, and Henri Nguyen-Thi. Motion of equiaxed grains during directional solidification under static magnetic field. *Journal of Crystal Growth*, 417:25–30, 2014.
- [224] Michel Rappaz. Modeling and characterization of grain structures and defects in solidification. *Current Opinion in Solid State and Materials Science*, 20(1):37–45, 2015.

- [225] Ahmed Kaci Boukellal, Jean-Marc Debierre, Guillaume Reinhart, and Henri Nguyen-Thi. Scaling laws governing the growth and interaction of equiaxed Al-Cu dendrites: A study combining experiments with phase-field simulations. *Materialia*, 1(March):62–69, 2018.

Appendix A

CV

Miha Založnik

Institut Jean Lamour
2 allée André Guinier, BP 50840
F-54011 Nancy CEDEX
France

Tél. : +33 3 7274 2672

email : miha.zaloznik@univ-lorraine.fr

Born 16 November 1976, Maribor, Slovenia

Areas of activity

Solidification • Heat & Mass Transfer • Multiscale Modeling • Numerical Methods

Multiscale modeling of solidification in metallic alloys in the presence of convection, from the crystal-grain to the product scale, seeking to understand, explain and predict the interactions of heat transfer, fluid flow, chemical segregations and the development of the microstructure.

Current position and main responsibilities

2009– Associate Scientist, *CNRS – Institut Jean Lamour*, Nancy, France
2018– Adjunct Associate Professor, *University of Nova Gorica*, Slovenia

Previous appointments

2012–2019 Workpackage co-leader (with S. Berbenni), *Multiscale modeling*, Laboratory of Excellence *Design of Alloy Metals for Low-Mass Structures – LabEx DAMAS*
2011–2019 Topic leader, *Multiscale modeling – Towards large scales*, Research network *Solidification of Metallic Alloys – GDR SAM* (24 groups from France and Switzerland)
2006–2009 Postdoctoral Fellow, *LSG2M*, *Institut National Polytechnique de Lorraine*, Nancy, France
2003, 2005 Visiting Researcher, *FAST*, *Université Pierre-et-Marie-Curie*, Orsay, France
2001–2006 Junior Researcher, *Laboratory of Multiphase Processes*, *University of Nova Gorica*, Ljubljana, Slovenia
2001–2006 Research Assistant, *Impol d.d.*, Slovenska Bistrica, Slovenia

Education

2006 PhD in Materials Characterization, *University of Nova Gorica*, Slovenia
Dissertation: “Modeling of Macrosegregation in Direct-Chill Casting” (advisor B. Šarler)
2001 MSc in Mechanical Engineering, *University of Ljubljana*, Slovenia

Awards & fellowships

- 2018 Habilitation for the grade of *Associate Professor*, University of Nova Gorica, Slovenia
- 2013 Scientific Excellence Award, CNRS
- 2012 Habilitation for the grade of *Docent* (Ass. Prof.), University of Nova Gorica, Slovenia
- 2009 Jožef Stefan Golden Emblem, national PhD award, *Institut Jožef Stefan*, Slovenia
- 2007 ECCOMAS PhD Award Finalist, European PhD award, *nominated by CEACM*, Central Europe

Professional activities

- 2008– Participation in European Projects, *FP6-Impress (2008–2009)*, *ESA ELIPS Gradecet (2011–2019)*
- 2007–2015 Participation in ANR-funded projects, *SMACS (2007–2011)*, *Principia (2011–2015)*
- 2006– Participation in industry-funded projects on *DC casting of aluminum alloys* and on *casting of large steel ingots*
- 2010– Co-supervision of 4 PhD theses, *Institut Jean Lamour*, Nancy, France
- 2010– Co-tutoring of 5 PhD students, *Institut Jean Lamour*, *Cemef – Mines ParisTech*, *NTNU* (Norway), *McMaster University* (Canada)
- 2011– Supervision of 6 postdoctoral researchers, *Institut Jean Lamour*, Nancy, France
- 2011– Supervision of 5 master internships, *Institut Jean Lamour*, Nancy, France
- 2018– Development of a computer software for simulation of casting processes, *OpenSolid*, Collaboration Institut Jean Lamour, O2M Solutions et Sciences & Computers Consultants, Nancy/St.-Étienne, France
- 2012– Development of a computer software for mesoscopic simulation of dendritic solidification, *CrystalFOAM*, Institut Jean Lamour, Nancy, France
- 2006– Development of a computer software for simulation of solidification, macrosegregation, and structure formation in static casting of ingots and direct-chill casting, *SOLID*, Logibox, no. IDDN : FR.001.360015.000.R.A.2007.000.30000, LSG2M, Nancy, France
- 2001–2006 Development of a computer software for simulation and optimization of direct-chill casting of aluminum alloys, *ImpolSim*, LMP-UNG & Impol d.d., Ljubljana, Slovenia
- 2019– Member of the council of *Institut Jean Lamour*, *UMR 7198 CNRS – Université de Lorraine*
- 2018– Member of the scientific council, HPC computing center *EXPLOR*
- 2011–2019 Member of the scientific council, Laboratory of Excellence *Design of Alloy Metals for Low-Mass Structures – LabEx DAMAS*
- 2019– Reviewer, *Agence Nationale de la Recherche*, France
- 2007– Reviewer, *Acta Mater.*, *Adv. Eng. Mater.*, *Comp. Mater. Sci.*, *Int. J. Heat Mass Tran.*, *Int. J. Therm. Sci.*, *J. Crystal Growth*, *Model. Simul. Mater. Sc.*, *Metall. Mater. Trans. A & B*, *Nature Comm.*, and many other

Teaching

- 2017 Multiscale Transport, *CNRS summer school on Solidification in Metal Alloys*, St.-Pierre d'Oléron, France
- 2017 Solidification/Macroseggregation, *Master Program in Metallurgy*, Université de Lorraine, Nancy, France
- 2014 Macroseggregation, *CNRS summer school on Solidification in Metal Alloys*, St.-Pierre d'Oléron, France
- 2012– Discretization Methods, *Doctoral Program in Physics*, University of Nova Gorica, Slovenia
- 2010– Interactions of materials and processes, *Master Program in Engineering*, ENSGSI, Nancy, France
- 2009– Numerical Metallurgy, *Master Program in Metallurgy*, Université de Lorraine, Nancy, France

2009 Natural Convection and Phase Change, *CNRS summer school on Solid-Liquid-Vapor Phase Change: Fundamentals and Applications*, Les Embiez, France
2008–2009 Fluid Dynamics, *Master Program in Engineering*, Ecole des Mines de Nancy, France
2007– Tutoring of student projects, *Master Program in Engineering*, Ecole des Mines de Nancy, France

Collaborations

Access e.V., RWTH Aachen, Germany
Sintef Industry, Oslo, Norway
University of Iowa, Iowa City, USA
Cemef, Mines ParisTech, Sophia Antipolis, France
IMDEA Materials, Madrid, Spain
McMaster University, Hamilton, Canada
IRT M2P, Metz, France
Institut Carnot Bourgogne, Le Creusot, France
SIMaP, Grenoble INP, Grenoble, France
Laboratory of Multiphase Processes, University of Nova Gorica, Slovenia
Institute of Metals and Technology, Ljubljana, Slovenia
Institut Jožef Stefan, Ljubljana, Slovenia
ArcelorMittal ARSA, Maizières-lès-Metz, France
ArcelorMittal Industeel, Creusot, France
Areva, Creusot, France
Ascometal CREAS, Hagondange, France
Aubert&Duval, Les Ancizes, France
Constellium C-TEC, Voreppe, France
EDF, Paris, France
Framatome, Paris, France
Safran Aircraft Engines, Gennevilliers, France
Sciences et Computers Consultants, Saint-Étienne, France *O2M Solutions*, Nancy, France

Appendix B

List of publications

Publications

Co-author of 2 book chapters, 40 articles in peer-reviewed journals, 57 articles in conference proceedings, 20 invited conference talks, 48 contributed conference talks, 19 invited seminars and 4 software packages.

Citations: 1172, *h*-index: 18 (source: Google Scholar, 1 Jun 2020)

BOOK CHAPTERS

- [B1] Miha Založnik, Arvind Kumar, Hervé Combeau, Marie Bedel, Philippe Jarry, and Emmanuel Waz. The Coupling of Macroseggregation With Grain Nucleation, Growth and Motion in DC Cast Aluminum Alloy Ingots. In John F Grandfield and Dmitry G Eskin, editors, *Essential Readings in Light Metals, Volume 3, Cast Shop for Aluminum Production*, pages 848–853. John Wiley & Sons, Hoboken (NJ), USA, 2013.
- [B2] Miha Založnik, Cédric Le Bot, and Eric Arquis. Convection naturelle et changement de phase. In Hervé Combeau and Lounès Tadrist, editors, *Les changements de phase solide-liquide-vapeur*. CNRS Editions, Paris, France, 2016.

ARTICLES IN PEER-REVIEWED JOURNALS

- [J1] Miha Založnik, Ivan Bajsić, and Božidar Šarler. A nondestructive experimental determination of the heat flux during cooling of direct-chill cast aluminum alloy billets. *Materiali in Tehnologije*, 36(3-4):121–125, 2002.
- [J2] Miha Založnik, Božidar Šarler, and Dominique Gobin. Simulation of macroseggregation in the DC casting of binary aluminum alloys. *Materials and Technologies*, 38(5):249–255, 2004.
- [J3] Miha Založnik and Božidar Šarler. Modeling of macroseggregation in direct-chill casting of aluminum alloys: Estimating the influence of casting parameters. *Materials Science and Engineering A*, 413-414:85–91, 2005.
- [J4] Robert Vertnik, Miha Založnik, and Božidar Šarler. Solution of transient direct-chill aluminium billet casting problem with simultaneous material and interphase moving boundaries by a meshless method. *Engineering Analysis with Boundary Elements*, 30(10):847–855, oct 2006.
- [J5] Miha Založnik, Shihe Xin, and Božidar Šarler. Verification of a numerical model of macroseggregation in direct chill casting. *International Journal of Numerical Methods for Heat & Fluid Flow*, 18(3/4):308–324, 2008.
- [J6] Michel Bellet, Hervé Combeau, Yves Fautrelle, Dominique Gobin, Mohamed A Rady, Eric Arquis, Olga Budenkova, Bernard Dussoubs, Yves Duterrail, Arvind Kumar, Charles-André Gandin, Benoît Goyeau, Miha Založnik, and Salem Mosbah. Call for contributions to a numerical benchmark problem for 2D columnar solidification of binary alloys. *International Journal of Thermal Sciences*, 48(11):2013–2016, 2009.
- [J7] Hervé Combeau, Arvind Kumar, and Miha Založnik. Modeling of Equiaxed Grain Evolution and Macroseggregations Development in Steel Ingots. *Transactions of the Indian Institute of Metals*, 62(4-5):285–290, jan 2009.
- [J8] Hervé Combeau, Miha Založnik, Stéphane Hans, and Pierre Emmanuel Richy. Prediction of Macroseggregation in Steel Ingots: Influence of the Motion and the Morphology of Equiaxed Grains. *Metallurgical and Materials Transactions B*, 40(3):289–304, 2009.

- [J9] Arvind Kumar, Bernard Dussoubs, Miha Založnik, and Hervé Combeau. Effect of discretization of permeability term and mesh size on macro- and meso-segregation predictions. *Journal of Physics D: Applied Physics*, 42(10):105503, 2009.
- [J10] Miha Založnik and Hervé Combeau. An operator splitting scheme for coupling macroscopic transport and grain growth in a two-phase multiscale solidification model: Part I – Model and solution scheme. *Computational Materials Science*, 48(1):1–10, jun 2010.
- [J11] Miha Založnik and Hervé Combeau. Thermosolutal flow in steel ingots and the formation of mesosegregates. *International Journal of Thermal Sciences*, 49(9):1500–1509, sep 2010.
- [J12] Miha Založnik, Arvind Kumar, and Hervé Combeau. An operator splitting scheme for coupling macroscopic transport and grain growth in a two-phase multiscale solidification model: Part II Application of the model. *Computational Materials Science*, 48(1):11–21, 2010.
- [J13] Dominique Daloz, Ulrike Hecht, Julien Zollinger, Hervé Combeau, Alain Hazotte, and Miha Založnik. Microsegregation, macrosegregation and related phase transformations in TiAl alloys. *Intermetallics*, 19(6):749–756, jun 2011.
- [J14] Gregor Kosec, Miha Založnik, Božidar Šarler, and Hervé Combeau. A meshless approach towards the solution of macrosegregation phenomena. *Computers, Materials & Continua*, 22(2):169–196, 2011.
- [J15] Arvind Kumar, Miha Založnik, and Hervé Combeau. Prediction of equiaxed grain structure and macrosegregation in an industrial steel ingot: comparison with experiment. *International Journal of Advances in Engineering Sciences and Applied Mathematics*, 2(4):140–148, sep 2011.
- [J16] Miha Založnik, Arvind Kumar, Hervé Combeau, Marie Bedel, Philippe Jarry, and Emmanuel Waz. Influence of Transport Mechanisms on Macrosegregation Formation in Direct Chill Cast Industrial Scale Aluminum Alloy Ingots. *Advanced Engineering Materials*, 13(7):570–580, jul 2011.
- [J17] Miha Založnik, Julien Zollinger, Hervé Combeau, Ulrike Hecht, and Dominique Daloz. Observations expérimentales et modélisation de la macroségrégation en coulée centrifuge d’alliages Ti-Al-Nb. *Revue de Métallurgie*, 107(10-11):449–455, jul 2011.
- [J18] Stephanie Fischer, Miha Založnik, Jean-Marie Seiler, Markus Rettenmayr, and Hervé Combeau. Experimental verification of a model on melting and resolidification in a temperature gradient. *Journal of Alloys and Compounds*, 540:85–88, nov 2012.
- [J19] Arvind Kumar, Miha Založnik, and Hervé Combeau. Study of the influence of mushy zone permeability laws on macro- and meso-segregations predictions. *International Journal of Thermal Sciences*, 54:33–47, apr 2012.
- [J20] Arvind Kumar, Miha Založnik, Hervé Combeau, Benoît Goyeau, and Dominique Gobin. A numerical simulation of columnar solidification: influence of inertia on channel segregation. *Modelling and Simulation in Materials Science and Engineering*, 21(4):045016, jun 2013.
- [J21] Georges Salloum-Abou-Jaoude, Guillaume Reinhart, Henri Nguyen-Thi, Hervé Combeau, Miha Založnik, Thomas Schenk, and Tamzin Lafford. In situ experimental observation of the time evolution of a dendritic mushy zone in a fixed temperature gradient. *Comptes Rendus Mécanique*, 341(4-5):421–428, feb 2013.

- [J22] Léa Deillon, Julien Zollinger, Dominique Daloz, Miha Založnik, and Hervé Combeau. In-situ observations of solutal melting using laser scanning confocal microscopy: The Cu/Ni model system. *Materials Characterization*, 97:125–131, nov 2014.
- [J23] Marie Bedel, Knut Omdal Tveito, Miha Založnik, Hervé Combeau, and Mohammed M’Hamdi. A model study of the impact of the transport of inoculant particles on microstructure formation during solidification. *Computational Materials Science*, 102:95–109, 2015.
- [J24] Georges Salloum-Abou-Jaoude, Guillaume Reinhart, Hervé Combeau, Miha Založnik, Tamzin Lafford, and Henri Nguyen-Thi. Quantitative analysis by in situ synchrotron X-ray radiography of the evolution of the mushy zone in a fixed temperature gradient. *Journal of Crystal Growth*, 411:88–95, feb 2015.
- [J25] Hervé Combeau, Miha Založnik, and Marie Bedel. Predictive Capabilities of Multiphysics and Multiscale Models in Modeling of Solidification of Steel Ingots and DC Casting of Aluminum. *JOM*, 68(8):2198–2206, aug 2016.
- [J26] Youssef Souhar, Valerio Francesco De Felice, Christoph Beckermann, Hervé Combeau, and Miha Založnik. Three-dimensional mesoscopic modeling of equiaxed dendritic solidification of a binary alloy. *Computational Materials Science*, 112:304–317, feb 2016.
- [J27] Laurent Heyvaert, Marie Bedel, Miha Založnik, and Hervé Combeau. Modeling of the Coupling of Microstructure and Macrosegregation in a Direct Chill Cast Al-Cu Billet. *Metallurgical and Materials Transactions A*, 48(10):4713–4734, 2017.
- [J28] André B. Phillion, Miha Založnik, Iris Spindler, Nicolas Pinter, Charles-Antoine Aledo, Georges Salloum-Abou-Jaoude, Henri Nguyen-Thi, Guillaume Reinhart, Guillaume Boussinot, Markus Apel, and Hervé Combeau. Evolution of a mushy zone in a static temperature gradient using a volume average approach. *Acta Materialia*, 141:206–216, dec 2017.
- [J29] Alexandre Viardin, Miha Založnik, Youssef Souhar, Markus Apel, and Hervé Combeau. Mesoscopic modeling of spacing and grain selection in columnar dendritic solidification: Envelope versus phase-field model. *Acta Materialia*, 122:386–399, jan 2017.
- [J30] Thi-Thuy-My Nguyen, Charles-André Gandin, Hervé Combeau, Miha Založnik, and Michel Bellet. Finite Element Multi-scale Modeling of Chemical Segregation in Steel Solidification Taking into Account the Transport of Equiaxed Grains. *Metallurgical and Materials Transactions A*, 49(5):1725–1748, feb 2018.
- [J31] Antonio Olmedilla, Miha Založnik, Bernard Rouat, and Hervé Combeau. Packing of sedimenting equiaxed dendrites. *Physical Review E*, 97(1):012910, jan 2018.
- [J32] Akash Pakanati, Mohammed M’Hamdi, Hervé Combeau, and Miha Založnik. Investigation of Macrosegregation Formation in Aluminium DC Casting for Different Alloy Systems. *Metallurgical and Materials Transactions A*, 49(10):4710–4721, oct 2018.
- [J33] Knut Omdal Tveito, Akash Pakanati, Mohammed M’Hamdi, Hervé Combeau, and Miha Založnik. A Simplified Three-Phase Model of Equiaxed Solidification for the Prediction of Microstructure and Macrosegregation in Castings. *Metallurgical and Materials Transactions A*, 49(7):2778–2794, jul 2018.
- [J34] Vanja Hatić, Martín Cisternas Fernández, Boštjan Mavrič, Miha Založnik, Hervé Combeau, and Božidar Šarler. Simulation of a macrosegregation benchmark in a cylindrical coordinate system with a meshless method. *International Journal of Thermal Sciences*, 142:121–133, aug 2019.

- [J35] Antonio Olmedilla, Miha Založnik, and Hervé Combeau. Quantitative 3D mesoscopic modeling of grain interactions during equiaxed dendritic solidification in a thin sample. *Acta Materialia*, 173:249–261, jul 2019.
- [J36] Antonio Olmedilla, Miha Založnik, Thomas Messmer, Bernard Rouat, and Hervé Combeau. Packing dynamics of spherical and nonconvex grains sedimenting at low Stokes number. *Physical Review E*, 99(1):012907, jan 2019.
- [J37] Akash Pakanati, Knut Omdal Tveito, Mohammed M’Hamdi, Hervé Combeau, and Miha Založnik. Application of an Equiaxed Grain Growth and Transport Model to Study Macroseggregation in a DC Casting Experiment. *Metallurgical and Materials Transactions A*, 50(4):1773–1786, apr 2019.
- [J38] Mahdi Torabi Rad, Miha Založnik, Hervé Combeau, and Christoph Beckermann. Upscaling mesoscopic simulation results to develop constitutive relations for macroscopic modeling of equiaxed dendritic solidification. *Materialia*, 5:100231, mar 2019.
- [J39] Martín Cisternas Fernández, Miha Založnik, Hervé Combeau, and Ulrike Hecht. Thermosolutal convection and macroseggregation during directional solidification of TiAl alloys in centrifugal casting. *International Journal of Heat and Mass Transfer*, 154:119698, jun 2020.
- [J40] Yi Feng, Miha Založnik, B.G. Thomas, and A.B. Phillion. Meso-scale simulation of liquid feeding in an equiaxed dendritic mushy zone. *Materialia*, 9:100612, mar 2020.

ARTICLES IN PEER-REVIEWED CONFERENCE PROCEEDINGS

- [P1] Miha Založnik, Božidar Šarler, and Ivan Bajsić. DRBEM computational modelling and non-destructive experiments for surface heat flux determination in direct chill casting of aluminium alloy billets. In Bengt Sundén and Carlos A Brebbia, editors, *Heat Transfer VII: Advanced Computational Methods in Heat Transfer*, pages 143–154, Boston, Southampton, 2002. WIT Press.
- [P2] Miha Založnik, Božidar Šarler, and Ivan Bajsić. A nondestructive experimental approach for heat flux determination on direct-chill cast aluminium alloy billet surface. *Proceedings in Applied Mathematics and Mechanics*, 2(1):300–301, mar 2003.
- [P3] Božidar Šarler, Janez Perko, Robert Vertnik, and Miha Založnik. Diffuse approximate method for casting simulations. In A Tadeu and Satya N Atluri, editors, *Advances in Computational & Experimental Engineering & Sciences (ICCES’04)*, pages 1357–1363. Tech Science Press, 2004.
- [P4] Božidar Šarler, Miha Založnik, Robert Vertnik, Janez Perko, Rajko Šafhalter, Marina Jelen, Viljem Strnad, and Franci Tomazini. A simulation system for direct chill casting of aluminium alloys. In Nadežda Talijan, editor, *Proceedings, 2nd International Symposium of Light Metals and Composite Materials, 19-20 May 2004, Belgrade*, pages 31–34, Belgrade, Serbia and Montenegro, 2004. Association of Metallurgical Engineers SCG.
- [P5] Janez Perko, C S Chen, Božidar Šarler, and Miha Založnik. Numerical diffusion in meshless diffuse approximate method. In S M Sivakumar, editor, *Advances in Computational & Experimental Engineering & Sciences (ICCES’05)*, pages 180–185. Tech Science Press, 2005.
- [P6] Miha Založnik and Božidar Šarler. New insights into flow structure in the DC casting of aluminum alloys. In Halvor Kvande, editor, *Light metals 2005*, pages 1031–1036, Warrendale (PA), USA, 2005. TMS.

- [P7] Miha Založnik and Božidar Šarler. Melt flow and macrosegregation in DC casting of binary aluminum alloys. *Materials Science Forum*, 508:515–522, 2006.
- [P8] Miha Založnik and Božidar Šarler. Thermosolutal flow in metals and implications for DC casting. In Charles-André Gandin and Michel Bellet, editors, *Modeling of Casting, Welding and Advanced Solidification Processes XI*, pages 243–250, Warrendale (PA), USA, 2006. TMS.
- [P9] Hervé Combeau, Miha Založnik, Boubeker Rabia, Sylvain Charmond, Stéphane Hans, and Pierre Emmanuel Richy. Prediction of the macrosegregation in steel ingots: influence of the motion and the growth of the equiaxed grains. In Peter D Lee, A Mitchell, Jean-Pierre Bellot, and Alain Jardy, editors, *Proceedings of the 2007 International Symposium on Liquid Metal Processing and Casting*, pages 127–132, Nancy, France, 2007.
- [P10] Hervé Combeau, Miha Založnik, Stéphane Hans, and Pierre Emmanuel Richy. Prédiction des macroségrégations dans les lingots d’acier : influence du mouvement et de la croissance des grains équiaxes. In *Congrès de la Société Française de Thermique 2008*, pages 9–14, Toulouse, France, 2008.
- [P11] Hervé Combeau, Arvind Kumar, and Miha Založnik. Modeling of Equiaxed Grain Evolution and Macrosegregations Development in Steel Ingots. *Transactions of the Indian Institute of Metals*, 62(4-5):285–290, jan 2009.
- [P12] Arvind Kumar, Bernard Dussoubs, Miha Založnik, and Hervé Combeau. Effect of Discretization of Permeability Term and Mesh Size on Macro- and Meso-segregation Predictions. In *19ème Congrès Français de Mécanique*, 2009.
- [P13] Miha Založnik and Hervé Combeau. Effects of solidification kinetics and liquid density in modeling of macrosegregation in castings. In Steve L Cockroft and Daan M Maijer, editors, *Modeling of Casting, Welding and Advanced Solidification Processes XII*, pages 253–260, Warrendale (PA), USA, 2009. TMS.
- [P14] Miha Založnik and Hervé Combeau. The influence of the morphology evolution of free-floating equiaxed grains on the macrosegregation in a 3.3-ton steel ingot. In Steve L Cockroft and Daan M Maijer, editors, *Modeling of Casting, Welding and Advanced Solidification Processes XII*, pages 165–172, Warrendale (PA), USA, 2009. TMS.
- [P15] Hervé Combeau, Michel Bellet, Yves Fautrelle, Dominique Gobin, Eric Arquis, Olga Budenkova, Bernard Dussoubs, Yves Duterrail, Arvind Kumar, Salem Mosbah, Mohamed A Rady, Charles-André Gandin, Benoît Goyeau, and Miha Založnik. Formation de macroségrégations pendant la solidification d’un alliage Sn-Pb : Synthèse des premiers résultats d’un benchmark. In *Matériaux 2010*, pages 1–9, 2010.
- [P16] Hervé Combeau, Michel Bellet, Yves Fautrelle, Dominique Gobin, Mohamed A Rady, Eric Arquis, Olga Budenkova, Bernard Dussoubs, Yves du Terrail, Arvind Kumar, Charles-André Gandin, Benoît Goyeau, Salem Mosbah, and Miha Založnik. Benchmark sur la simulation des macroségrégations lors de la solidification d’un alliage : première synthèse. In *Congrès de la Société Française de Thermique 2010*, 2010.
- [P17] Miha Založnik, Arvind Kumar, Hervé Combeau, Marie Bedel, Philippe Jarry, and Emmanuel Waz. Influence of transport mechanisms on macrosegregation formation in direct chill cast industrial scale aluminum alloy ingots. In *Matériaux 2010*, Nantes, France, 2010.
- [P18] Miha Založnik, Julien Zollinger, Hervé Combeau, Ulrike Hecht, and Dominique Daloz. Etablissement et modélisation de la macroségrégation en coulée centrifuge d’alliages Ti-Al-Nb. In *Matériaux 2010*, 2010.

- [P19] Hervé Combeau, Michel Bellet, Yves Fautrelle, Dominique Gobin, Eric Arquis, Olga Budenkova, Bernard Dussoubs, Yves Duterrail, Arvind Kumar, Benoît Goyeau, Salem Mosbah, Thibault Quatravaux, Mohamed A Rady, Charles-André Gandin, and Miha Založnik. A Numerical Benchmark on the Prediction of Macrosegregation in Binary Alloys. In *Frontiers in Solidification Science*, pages 755–760, Warrendale (PA), USA, 2011. TMS.
- [P20] Gregor Kosec and Miha Založnik. Solution of solidification of a binary alloy by a local meshless technique. In Nikos E Mastorakis, editor, *Proceedings of the 2nd International Conference on Fluid Mechanics and Heat and Mass Transfer 2011 (FLUIDSHEAT '11)*, pages 201–206, Corfu, Greece, 2011. WSEAS.
- [P21] Mathieu Revil-Baudard, Alain Jardy, Miha Založnik, Hervé Combeau, Faustine Leclerc, and Veronique Rebeyrolle. Detailed modeling of the solidification of vacuum arc remelted zirconium ingots. In *Proceedings of the 2011 International Symposium on Liquid Metal Processing and Casting*, volume 4, Nancy, France, 2011.
- [P22] Miha Založnik, Arvind Kumar, Hervé Combeau, Marie Bedel, Philippe Jarry, and Emmanuel Waz. The Coupling of Macrosegregation With Grain Nucleation, Growth and Motion in DC Cast Aluminum Alloy Ingots. In S J Lindsay, editor, *Light metals 2011*, pages 699–704, Warrendale (PA), USA, 2011. TMS.
- [P23] Marie Bedel, Miha Založnik, Arvind Kumar, Hervé Combeau, Philippe Jarry, and Emmanuel Waz. Influence of transport mechanisms on nucleation and grain structure formation in DC cast aluminium alloy ingots. *IOP Conference Series: Materials Science and Engineering*, 27:012070, jan 2012.
- [P24] Hervé Combeau, Michel Bellet, Yves Fautrelle, Dominique Gobin, Eric Arquis, Olga Budenkova, Bernard Dussoubs, Yves du Terrail, Arvind Kumar, Charles-André Gandin, Benoît Goyeau, Salem Mosbah, Thibault Quatravaux, Mohamed A Rady, and Miha Založnik. Analysis of a numerical benchmark for columnar solidification of binary alloys. *IOP Conference Series: Materials Science and Engineering*, 33:012086, jul 2012.
- [P25] Hervé Combeau, Arvind Kumar, Miha Založnik, Isabelle Poitroult, Gilbert Lacagne, Andrew Gingell, Thierry Mazet, and Gérard Lesoult. Macrosegregation prediction in a 65 ton steel ingot. In *International Conference on Ingot Casting, Rolling and Forging*, page 27, Aachen, Germany, 2012.
- [P26] Valerio Francesco De Felice, Knut Omdal Tveito, Miha Založnik, Hervé Combeau, and Mohammed M'Hamdi. Three-dimensional study of macro- and mesosegregation formation in a rectangular cavity cooled from one vertical side. *IOP Conference Series: Materials Science and Engineering*, 33:012088, jul 2012.
- [P27] Arvind Kumar, Joëlle Demurger, Jean Wendenbaum, Miha Založnik, and Hervé Combeau. Experimental and Numerical Studies on the Influence of Hot Top Conditions on the Macrosegregation in an Industrial Steel Ingot. In *International Conference on Ingot Casting, Rolling and Forging*, page 28, Aachen, Germany, 2012.
- [P28] Arvind Kumar, Bernard Dussoubs, Miha Založnik, and Hervé Combeau. Influence of Discretization of Permeability Term and Mesh Size on the Prediction of Channel Segregations. *IOP Conference Series: Materials Science and Engineering*, 27:012039, jan 2012.
- [P29] Arvind Kumar, Miha Založnik, Hervé Combeau, Benoît Goyeau, and Dominique Gobin. Channel segregation during columnar solidification: influence of inertia. In Kambiz Vafai, editor, *Porous Media and its Applications in Science, Engineering and Industry*, pages 43–48. American Institute of Physics, 2012.

- [P30] Mathieu Revil-Baudard, Alain Jardy, Faustine Leclerc, Miha Založnik, Veronique Reberolle, and Hervé Combeau. A Multiscale Model for the Simulation of V.A.R. Ingot Solidification. In Laurentiu Nastac, Lifeng Zhang, Brian G Thomas, Adrian Sabau, Nagy El-Kaddah, Adam C Powell, and Hervé Combeau, editors, *CFD Modeling and Simulation in Materials Processing, TMS Annual Meeting 2012*, pages 107–114, Warrendale (PA), USA, 2012. TMS.
- [P31] Knut Omdal Tveito, Marie Bedel, Miha Založnik, Hervé Combeau, and Mohammed M’Hamdi. The effect of finite microscopic liquid solute diffusion on macrosegregation formation. *IOP Conference Series: Materials Science and Engineering*, 27:012040, jan 2012.
- [P32] Knut Omdal Tveito, Marie Bedel, Miha Založnik, Hervé Combeau, Mohammed M’Hamdi, Arvind Kumar, and Pradip Dutta. Numerical study of the impact of inoculant and grain transport on macrosegregation and microstructure formation during solidification of an Al-22%Cu alloy. *IOP Conference Series: Materials Science and Engineering*, 33:012089, jul 2012.
- [P33] Knut Omdal Tveito, Mohammed M’Hamdi, Hervé Combeau, Miha Založnik, Kader Zaïdat, Xiaodong Wang, Bachir Saadi, and Yves Fautrelle. Numerical analysis of the influence of melting and application of electromagnetic stirring prior to solidification on macrosegregation formation during casting of a binary alloy. In Laurentiu Nastac, Lifeng Zhang, Brian G Thomas, Adrian Sabau, Nagy El-Kaddah, Adam C Powell, and Hervé Combeau, editors, *CFD Modeling and Simulation in Materials Processing, TMS Annual Meeting 2012*, pages 253–260, Warrendale (PA), USA, 2012. TMS.
- [P34] Marie Bedel, Laurent Heyvaert, Miha Založnik, Hervé Combeau, Dominique Daloz, and Gérard Lesoult. Process-scale modeling of microstructure in direct chill casting of aluminum alloys. *IOP Conference Series: Materials Science and Engineering*, 84:012100, 2015.
- [P35] Nicolas Leriche, Hervé Combeau, Charles-André Gandin, and Miha Založnik. Modelling the Columnar-to-Equiaxed and Equiaxed-to-Columnar Transitions in Ingots Using a Multiphase Model. *IOP Conference Series: Materials Science and Engineering*, 84:012087, 2015.
- [P36] Thi-Thuy-My Nguyen, Hervé Combeau, Miha Založnik, Michel Bellet, and Charles-André Gandin. Multi-scale finite element modelling of solidification structures by a splitting method taking into account the transport of equiaxed grains. *IOP Conference Series: Materials Science and Engineering*, 84:012007, 2015.
- [P37] Isabelle Poitroult, David Cardinaux, Miha Založnik, Hervé Combeau, and Chantal David. Characterization and prediction of solidification structures and macrosegregations in heavy steel ingots. In *Steelsim 2015*, Bardolino, Italy, 2015.
- [P38] Miha Založnik, Alexandre Viardin, Youssef Souhar, Hervé Combeau, and Markus Apel. Mesoscopic modeling of columnar solidification and comparisons with phase-field simulations. *IOP Conference Series: Materials Science and Engineering*, 84:012074, 2015.
- [P39] Hervé Combeau and Miha Založnik. Multiphysics and multiscale modeling and simulation of solidification processes. In *Frontiers of Solidification Science, TMS Annual Meeting 2016*, pages 171–174, 2016.
- [P40] Youssef Souhar, Valerio Francesco De Felice, Miha Založnik, Hervé Combeau, and Christoph Beckermann. The role of the stagnant-film thickness in mesoscopic modeling of equiaxed grain envelopes. *IOP Conference Series: Materials Science and Engineering*, 117:012014, mar 2016.

- [P41] Miha Založnik, Youssef Souhar, Christoph Beckermann, and Hervé Combeau. Upscaling from Mesoscopic to Macroscopic Solidification Models by Volume Averaging. In *Frontiers of Solidification Science, TMS Annual Meeting 2016*, pages 59–63. TMS, 2016.
- [P42] Miha Založnik, Alexandre Viardin, Youssef Souhar, Hervé Combeau, and Markus Apel. Mesoscopic modelling of columnar solidification. *IOP Conference Series: Materials Science and Engineering*, 117:012013, 2016.
- [P43] Katarina Mramor, Miha Založnik, Alain Jardy, and Hervé Combeau. Assessment of the effect of solutal boundary layer thickness on macrosegregation formation during VAR process in Zirconium ingots. In Z Fan, editor, *Solidification Processing 2017: Proceedings of the 6th Decennial International Conference on Solidification Processing*, pages 508–511, London, UK, 2017. Brunel University.
- [P44] Antonio Olmedilla, Miha Založnik, and Hervé Combeau. DEM simulation of dendritic grain random packing: application to metal alloy solidification. *EPJ Web of Conferences*, 140:06002, jun 2017.
- [P45] Mahdi Torabi Rad, Miha Založnik, Hervé Combeau, and Christoph Beckermann. Constitutive relations for macroscopic modelling of equiaxed solidification. In Z Fan, editor, *Solidification Processing 2017: Proceedings of the 6th Decennial International Conference on Solidification Processing*, pages 326–329, London, UK, 2017. Brunel University.
- [P46] Ulrike Hecht, Can Huang, Julien Zollinger, Dominique Daloz, Miha Založnik, Martín Cisternas, Alexandre Viardin, Shaun McFadden, László Gránásky, Juraj Lapin, Nicolas Leriche, and Florian Kargl. The ESA-MAP project "GRADE CET" – An overview of the joint research on solidification of TiAl-based alloys under hypergravity and microgravity conditions. In A Roósz, Zs Veres, M Svéda, and G Karacs, editors, *Solidification and Gravity 2018*, pages 27–36, Miskolc, Hungary, 2018. Hungarian Academy of Sciences – University of Miskolc.
- [P47] Akash Pakanati, Knut Omdal Tveito, Mohammed M'Hamdi, Hervé Combeau, and Miha Založnik. Impact of Inlet Flow on Macrosegregation Formation Accounting for Grain Motion and Morphology Evolution in DC Casting of Aluminium. In Olivier Martin, editor, *Light Metals 2018*, pages 1089–1096. TMS, Warrendale (PA), USA, 2018.
- [P48] M. Cisternas Fernández, Miha Založnik, Hervé Combeau, C. Huang, J. Zollinger, and Ulrike Hecht. Effect of the Coriolis force on the macrosegregation of aluminum in the centrifugal casting of Ti-Al alloys. *IOP Conference Series: Materials Science and Engineering*, 529:012033, may 2019.
- [P49] Yi Feng, Miha Založnik, Brian Thomas, and André Phillion. A 3D discrete-element model for simulating liquid feeding during dendritic solidification of steel. *IOP Conference Series: Materials Science and Engineering*, 529:012031, 2019.
- [P50] Benjamin Gerin, Hervé Combeau, Miha Založnik, Isabelle Poittrault, and Maya Cherif. Prediction of solidification structures in a 9.8 t steel ingot. *IOP Conference Series: Materials Science and Engineering*, 529:012036, may 2019.
- [P51] Yuze Li, Antonio Olmedilla, Miha Založnik, Julien Zollinger, Lucas Dembinski, and Alexandre Mathieu. Solidification microstructure during selective laser melting of Ni based superalloy: experiment and mesoscopic modelling. *IOP Conference Series: Materials Science and Engineering*, 529:012004, 2019.
- [P52] Antonio Olmedilla, Miha Založnik, M. Cisternas Fernández, Alexandre Viardin, and Hervé Combeau. Three-dimensional mesoscopic modeling of equiaxed dendritic solidification

in a thin sample: effect of convection flow. *IOP Conference Series: Materials Science and Engineering*, 529:012040, may 2019.

- [P53] Akash Pakanati, Knut Omdal Tveito, Mohammed M’Hamdi, Hervé Combeau, and Miha Založnik. Analysis of the Interplay Between Thermo-solutal Convection and Equiaxed Grain Motion in Relation to Macroseggregation Formation in AA5182 Sheet Ingots. In Corleen Chesonis, editor, *Light Metals 2019*, San Antonio (TX), USA, 2019. TMS.
- [P54] Savya Sachi, Miha Založnik, Hervé Combeau, Charles-André Gandin, Marvin Gennesson, Joëlle Demurger, Michaël Stoltz, and Isabelle Poitraul. Analysis of columnar-to-equiaxed transition experiment in lab scale steel casting by a multiphase model. *IOP Conference Series: Materials Science and Engineering*, 529:012039, 2019.
- [P55] Benjamin Gerin, Hervé Combeau, Miha Založnik, and Isabelle Poitraul. Prediction of solidification structures in a 9.8 ton steel ingot. *IOP Conference Series: Materials Science and Engineering*, in press, 2020.
- [P56] Akash Pakanati, Mohammed M’Hamdi, Hervé Combeau, and Miha Založnik. modelling macroseggregation modification in DC casting of aluminium alloys in sheet ingots accounting for inlet melt flow, equiaxed grain morphology and transport. *IOP Conference Series: Materials Science and Engineering*, in press, 2020.
- [P57] Damien Turret, Laszlo Sturz, Alexandre Viardin, and Miha Založnik. Comparing mesoscopic models for dendritic growth. *IOP Conference Series: Materials Science and Engineering*, in press, 2020.

INVITED CONFERENCE TALKS

- [I1] Miha Založnik, Božidar Šarler, and Ivan Bajsić. DRBEM computational modelling and non-destructive experiments for surface heat flux determination in direct chill casting of aluminium alloy billets. In Bengt Sundén and Carlos A Brebbia, editors, *Heat Transfer VII: Advanced Computational Methods in Heat Transfer*, pages 143–154, Boston, Southampton, 2002. WIT Press.
- [I2] Božidar Šarler, Miha Založnik, Robert Vertnik, Janez Perko, Rajko Šafhalter, Marina Jelen, Viljem Strnad, and Franci Tomazini. A simulation system for direct chill casting of aluminium alloys. In Nadežda Talijan, editor, *Proceedings, 2nd International Symposium of Light Metals and Composite Materials, 19-20 May 2004, Belgrade*, pages 31–34, Belgrade, Serbia and Montenegro, 2004. Association of Metallurgical Engineers SCG.
- [I3] Janez Perko, C S Chen, Božidar Šarler, and Miha Založnik. Numerical diffusion in meshless diffuse approximate method. In S M Sivakumar, editor, *Advances in Computational & Experimental Engineering & Sciences (ICCES’05)*, pages 180–185. Tech Science Press, 2005.
- [I4] Hervé Combeau, Arvind Kumar, and Miha Založnik. Modeling of equiaxed grain evolution and macroseggregations development in steel ingots. In *4th International Conference on Solidification Science and Processing*, Chennai, India, 2009.
- [I5] Hervé Combeau, Michel Bellet, Yves Fautrelle, Dominique Gobin, Eric Arquis, Olga Budenkova, Bernard Dussoubs, Yves Duterrail, Arvind Kumar, Salem Mosbah, Mohamed A Rady, Charles-André Gandin, Benoît Goyeau, and Miha Založnik. Formation de macrosegregations pendant la solidification d’un alliage Sn-Pb : Synthèse des premiers résultats d’un benchmark. In *Matériaux 2010*, pages 1–9, 2010.

- [I6] Miha Založnik, Arvind Kumar, Hervé Combeau, Marie Bedel, Philippe Jarry, and Emmanuel Waz. Influence of transport mechanisms on macrosegregation formation in direct chill cast industrial scale aluminum alloy ingots. In *Matériaux 2010*, Nantes, France, 2010.
- [I7] Hervé Combeau, Michel Bellet, Yves Fautrelle, Dominique Gobin, Eric Arquis, Olga Budenkova, Bernard Dussoubs, Yves du Terrail, Arvind Kumar, Charles-André Gandin, Benoît Goyeau, Salem Mosbah, Thibault Quatrayaux, Mohamed A Rady, and Miha Založnik. Analysis of a numerical benchmark for columnar solidification of binary alloys. *IOP Conference Series: Materials Science and Engineering*, 33:012086, jul 2012.
- [I8] Hervé Combeau and Miha Založnik. Multiscale and multiphysics models in CFD modeling and simulation of solidification process. In *CFD Modeling and Simulation in Materials Processing Symposium, TMS Annual Meeting 2012*, Orlando (FL), USA, 2012.
- [I9] Miha Založnik, Hervé Combeau, Arvind Kumar, and Valerio Francesco De Felice. Volume-Averaged Modeling of Channel Mesosegregation. In *5th International Conference on Solidification Science and Processing*, Bhubaneswar, India, 2012.
- [I10] Hervé Combeau and Miha Založnik. Multiphysics and multiscale models in modeling and simulation of solidification processes. In N Massarotti, P Nithiarasu, and Božidar Šarler, editors, *Thermacomp 2014*, Bled, Slovenia, 2014.
- [I11] Miha Založnik and Hervé Combeau. Multiphysics and multiscale modeling of solidification processes. In *Coupled Problems 2015*, Venice, Italy, 2015.
- [I12] Miha Založnik, Hervé Combeau, Youssef Souhar, Alexandre Viardin, and Markus Apel. Mesoscopic Modeling of Solidification in Alloys. In *6th International Conference on Solidification Science and Processing*, Hyderabad, India, 2015.
- [I13] Hervé Combeau and Miha Založnik. Multiphysics and multiscale modeling and simulation of solidification processes. In *Frontiers of Solidification Science, TMS Annual Meeting 2016*, pages 171–174, 2016.
- [I14] Laurent Heyvaert, Hervé Combeau, Miha Založnik, Philippe Jarry, and Emmanuel Waz. Microporosity Prediction in Aluminium DC Casting. In *CFD Modeling and Simulation in Materials Processing, TMS Annual Meeting 2016*, Nashville (TN), USA, 2016.
- [I15] Miha Založnik and Hervé Combeau. Multiphysics and multiscale modeling of solidification in casting processes. In *Thermec 2016*, Graz, Austria, 2016.
- [I16] Ulrike Hecht, Can Huang, Julien Zollinger, Dominique Daloz, Miha Založnik, Martín Cisternas, Alexandre Viardin, and Guillaume Martin. The columnar-to-equiaxed transition in TiAl-alloys under hypergravity and microgravity conditions. In *33rd Annual Meeting American Society for Gravitational and Space Research*, Seattle (WA), USA, 2017. American Society for Gravitational and Space Research.
- [I17] Miha Založnik and Hervé Combeau. Multiphysics and Multiscale Modeling of Solidification in Casting Processes. In *6th Decennial International Conference on Solidification Processing*, Old Windsor, UK, 2017.
- [I18] Ulrike Hecht, Can Huang, Julien Zollinger, Dominique Daloz, Miha Založnik, Martín Cisternas, Alexandre Viardin, Shaun McFadden, László Gránágy, Juraj Lapin, Nicolas Leriche, and Florian Kargl. The ESA-MAP project "GRADE CET" – An overview of the joint research on solidification of TiAl-based alloys under hypergravity and microgravity conditions. In A Roósz, Zs Veres, M Svéda, and G Karacs, editors, *Solidification and Gravity 2018*, pages 27–36, Miskolc, Hungary, 2018. Hungarian Academy of Sciences – University of Miskolc.

- [I19] Yi Feng, Miha Založnik, Brian Thomas, and André Phillion. A 3D discrete-element model for simulating liquid feeding during dendritic solidification of steel. In Charles-André Gandin and Menghuai Wu, editors, *5th International Conference on Advances in Solidification Processes (ICASP-5) and 5th International Symposium on Cutting Edge of Computer Simulation of Solidification, Casting and Refining (CSSCR-5)*, Salzburg, Austria, 2019.
- [I20] Damien Tournet, Laszlo Sturz, Alexandre Viardin, and Miha Založnik. Comparing mesoscopic models for dendritic growth. 2020.

CONTRIBUTED CONFERENCE TALKS

- [C1] Hervé Combeau, Arvind Kumar, and Miha Založnik. Modeling of equiaxed grain evolution and macrosegregations development in steel ingots. In *4th International Conference on Solidification Science and Processing*, Chennai, India, 2009.
- [C2] Hervé Combeau and Miha Založnik. Multiscale and multiphysics models in CFD modeling and simulation of solidification process. In *CFD Modeling and Simulation in Materials Processing Symposium, TMS Annual Meeting 2012*, Orlando (FL), USA, 2012.
- [C3] Valerio Francesco De Felice, Hervé Combeau, Miha Založnik, and Thibault Quatravaux. Three-dimensional study of channel mesosegregation formation during solidification of a metal alloy. In *7th OpenFOAM Workshop*, Darmstadt, Germany, 2012. Technische Universität Darmstadt.
- [C4] Valerio Francesco De Felice, Miha Založnik, and Hervé Combeau. Mesoscopic simulation of dendritic crystal growth in binary metal alloys. In *7th OpenFOAM Workshop*, Darmstadt, Germany, 2012. Technische Universität Darmstadt.
- [C5] Knut Omdal Tveito, Marie Bedel, Miha Založnik, Hervé Combeau, and Mohammed M’Hamdi. Numerical simulation of macrosegregation formation during solidification accounting for inoculant and equiaxed grain transport. In *CFD Modeling and Simulation in Materials Processing Symposium, TMS Annual Meeting 2012*, Orlando (FL), USA, 2012.
- [C6] Miha Založnik, Hervé Combeau, Arvind Kumar, and Valerio Francesco De Felice. Volume-Averaged Modeling of Channel Mesosegregation. In *5th International Conference on Solidification Science and Processing*, Bhubaneswar, India, 2012.
- [C7] Miha Založnik, Cédric Le Bot, Stéphane Glockner, Olga Budenkova, Yves du Terrail, Marius-Vasile Bejinariu, Dominique Gobin, Gregor Kosec, and Hervé Combeau. A Numerical Benchmark Exercise on Thermal and Thermosolutal Natural Convection in Liquid Alloys. In *CFD Modeling and Simulation in Materials Processing Symposium, TMS Annual Meeting 2012*, Orlando (FL), USA, 2012.
- [C8] Valerio Francesco De Felice, Miha Založnik, Hervé Combeau, and Christoph Beckermann. Mesoscopic Modeling of Equiaxed Dendrites – A Closer Look. In *Frontiers of Solidification Science, TMS Annual Meeting 2013*, San Antonio (TX), USA, 2013.
- [C9] Laurent Heyvaert, Hervé Combeau, and Miha Založnik. Two-phase Flow in Direct Chill Cast Aluminum Alloy Sheet Ingots. In *Euromat 2013*, Sevilla, Spain, 2013.
- [C10] Nicolas Leriche, Hervé Combeau, Miha Založnik, Arvind Kumar, Joëlle Demurger, Jean Wendenbaum, and Charles-André Gandin. Numerical and experimental studies of the grain morphological transitions and macrosegregation in the sedimentation cone of an industrial steel ingot. In *Frontiers of Solidification Science, TMS Annual Meeting 2013*, San Antonio (TX), USA, 2013.

- [C11] Marie Bedel, Laurent Heyvaert, Miha Založnik, Hervé Combeau, Dominique Daloz, and Gérard Lesoult. Process-scale modeling of microstructure in direct chill casting of aluminum alloys. In *International Conference on Advances in Solidification Processes 4*, Old Windsor, UK, 2014.
- [C12] Hervé Combeau and Miha Založnik. Multiphysics and multiscale models in modeling and simulation of solidification processes. In N Massarotti, P Nithiarasu, and Božidar Šarler, editors, *Thermacomp 2014*, Bled, Slovenia, 2014.
- [C13] Léa Deillon, Julien Zollinger, Dominique Daloz, Miha Založnik, and Hervé Combeau. In-situ Investigation of Solutal Melting using Laser Scanning Confocal Microscopy. In *International Conference on Advances in Solidification Processes 4*, Old Windsor, UK, 2014.
- [C14] Laurent Heyvaert, Marie Bedel, Miha Založnik, and Hervé Combeau. Macrosegregation in direct chill casting of an Al-Cu billet: the link between microstructure and hydrodynamics. In *International Conference on Advances in Solidification Processes 4*, Old Windsor, UK, 2014.
- [C15] Nicolas Leriche, Hervé Combeau, Charles-André Gandin, and Miha Založnik. Modelling the Columnar-to-Equiaxed and Equiaxed-to-Columnar Transitions in Ingots Using a Multiphase Model. In *International Conference on Advances in Solidification Processes 4*, Old Windsor, UK, 2014.
- [C16] Julien Zollinger, Léa Deillon, Benoît Appolaire, Dominique Daloz, Miha Založnik, and Hervé Combeau. Fusion solutale dans le système Cu-Ni : observations in-situ et modélisation. In *Matériaux 2014*, Montpellier, France, 2014.
- [C17] Miha Založnik and Hervé Combeau. Multiphysics and multiscale modeling of solidification processes. In *Coupled Problems 2015*, Venice, Italy, 2015.
- [C18] Miha Založnik, Hervé Combeau, Youssef Souhar, Alexandre Viardin, and Markus Apel. Mesoscopic Modeling of Solidification in Alloys. In *6th International Conference on Solidification Science and Processing*, Hyderabad, India, 2015.
- [C19] Hervé Combeau and Miha Založnik. Multiphysics and multiscale models in modeling and simulation of solidification processes. In *Colloque "La Métallurgie, quel avenir !"*, Saint-Étienne, France, 2016.
- [C20] Laurent Heyvaert, Hervé Combeau, Miha Založnik, Philippe Jarry, and Emmanuel Waz. Microporosity Prediction in Aluminium DC Casting. In *CFD Modeling and Simulation in Materials Processing, TMS Annual Meeting 2016*, Nashville (TN), USA, 2016.
- [C21] Alexandre Viardin, Miha Založnik, Markus Apel, and Hervé Combeau. Mesoscopic and phase field simulations of columnar and equiaxed dendritic growth. In *Multiscale Materials Modeling 2016*, Dijon, France, 2016.
- [C22] Miha Založnik and Hervé Combeau. Multiphysics and multiscale modeling of solidification in casting processes. In *Thermec 2016*, Graz, Austria, 2016.
- [C23] Miha Založnik, Youssef Souhar, Christoph Beckermann, and Hervé Combeau. Upscaling from Mesoscopic to Macroscopic Solidification Models by Volume Averaging. In *Multiscale Materials Modeling 2016*, Dijon, France, 2016.
- [C24] Ulrike Hecht, Can Huang, Julien Zollinger, Dominique Daloz, Miha Založnik, Martín Cisternas, Alexandre Viardin, and Guillaume Martin. The columnar-to-equiaxed transition in TiAl-alloys under hypergravity and microgravity conditions. In *33rd Annual Meeting American Society for Gravitational and Space Research*, Seattle (WA), USA, 2017. American Society for Gravitational and Space Research.

- [C25] Miha Založnik and Hervé Combeau. Multiphysics and Multiscale Modeling of Solidification in Casting Processes. In *6th Decennial International Conference on Solidification Processing*, Old Windsor, UK, 2017.
- [C26] Julien Zollinger, Ulrike Hecht, Miha Založnik, Nicole Reilly, Dominique Daloz, Hervé Combeau, and Alexandre Viardin. The columnar-to-equiaxed transition in peritectic TiAl-based alloys under hypergravity and microgravity conditions. In *25th European Low Gravity Research Association Biennial Symposium and General Assembly (ELGRA-25)*, Juan-les-Pins, France, 2017.
- [C27] Martín Cisternas Fernández, Miha Založnik, Ulrike Hecht, and Hervé Combeau. Macroscopic modeling of solidification of TiAl alloys in hypergravity. In *Solidification and Gravity 2018*, Miskolc, Hungary, 2018.
- [C28] Ulrike Hecht, Julien Zollinger, Can Huang, Miha Založnik, Martín Cisternas, Nicole Reilly, Dominique Daloz, Hervé Combeau, and Alexandre Viardin. GRAvity DEpendent Columnar-to-Equiaxed Transition in TiAl alloys: Part. I. Solidification of Ti-46Al-8Nb in hyper gravity and multi-physics modelling. In *ESA LDC Hypergravity Workshop*, Noordwijk, Netherlands, 2018.
- [C29] Ulrike Hecht, Julien Zollinger, Can Huang, Miha Založnik, Martín Cisternas, Nicole Reilly, Dominique Daloz, Hervé Combeau, and Alexandre Viardin. GRAvity DEpendent Columnar-to-Equiaxed Transition in TiAl alloys: Part. II. Solidification of Ti-48Al-2Cr-2Nb in hyper gravity and multi-physics modelling. In *ESA LDC Hypergravity Workshop*, Noordwijk, Netherlands, 2018.
- [C30] Antonio Olmedilla, Miha Založnik, Bernard Rouat, and Hervé Combeau. Packing dynamics of spherical and nonconvex equiaxed dendritic grains sedimenting at low Stokes number. In *ECCM 6 – 6th European Conference on Computational Mechanics*, Glasgow, UK, 2018.
- [C31] Akash Pakanati, Mohammed M’Hamdi, Hervé Combeau, and Miha Založnik. Numerical Investigation of Macroseggregation Mechanisms in DC Casting for Different Alloy Systems. In *Frontiers of Solidification Science, TMS Annual Meeting 2018*, Phoenix (AZ), USA, 2018. TMS.
- [C32] Akash Pakanati, Mohammed M’Hamdi, Miha Založnik, and Hervé Combeau. 3D modelling of the impact of inlet flow on macroseggregation formation in DC casting of aluminium alloys accounting for grain morphology and transport. In A Roósz, Zs Veres, M Svéda, and G Karacs, editors, *Solidification and Gravity 2018*, pages 161–166, Miskolc, Hungary, 2018. Hungarian Academy of Sciences – University of Miskolc.
- [C33] Alexandre Viardin, Miha Založnik, Youssef Souhar, Markus Apel, and Hervé Combeau. Mesoscopic envelope model for equiaxed and columnar dendritic growth coupled with flow. In *Frontiers of Solidification Science, TMS Annual Meeting 2018*, Phoenix (AZ), USA, 2018. TMS.
- [C34] Sabine Ziri, Laszlo Sturz, Alexandre Viardin, Miha Založnik, and Damien Tournet. A quantitative benchmark of multiscale models for dendritic growth. In *Solidification and Gravity 2018*, Miskolc, Hungary, 2018.
- [C35] Martín Cisternas F., Miha Založnik, Hervé Combeau, and Ulrike Hecht. Effect of the Coriolis force on the macroseggregation of aluminum in the centrifugal casting of TiAl alloys. In *Colloque "La Métallurgie, quel avenir !"*, Nancy, France, 2019.

- [C36] Hanadi Ettroudi, Gildas Guillemot, Hervé Combeau, Miha Založnik, and Charles-André Gandin. Finite element modeling of solidification grain structures. In *Euromat 2019*, 2019.
- [C37] Benjamin Gerin, Hervé Combeau, Miha Založnik, Isabelle Poitault, and Maya Cherif. Prediction of solidification structures in a 9.8 t steel ingot. In *Colloque "La Métallurgie, quel avenir !"*, Nancy, France, 2019.
- [C38] Can Huang, Alexandre Viardin, Ulrike Hecht, Martín Cisternas, Miha Založnik, and Julien Zollinger. Solidification of Ti-46Al-8Nb in hyper-gravity and multi-physics modelling. In Charles-André Gandin and Menghuai Wu, editors, *5th International Conference on Advances in Solidification Processes (ICASP-5) and 5th International Symposium on Cutting Edge of Computer Simulation of Solidification, Casting and Refining (CSSCR-5)*, page 2018, Salzburg, Austria, 2019.
- [C39] Antonio Olmedilla, Miha Založnik, and Hervé Combeau. Modélisation des interactions solutales en croissance dendritique équiaxe dans des échantillons minces. In *Colloque "La Métallurgie, quel avenir !"*, Nancy, France, 2019.
- [C40] Akash Pakanati, Mohammed M'Hamdi, Hervé Combeau, and Miha Založnik. Analysis of the impact of inlet induced forced convection on macrosegregation formation in DC casting of aluminium sheet ingots. In Charles-André Gandin and Menghuai Wu, editors, *5th International Conference on Advances in Solidification Processes (ICASP-5) and 5th International Symposium on Cutting Edge of Computer Simulation of Solidification, Casting and Refining (CSSCR-5)*, Salzburg, Austria, 2019.
- [C41] Savya Sachi, Miha Založnik, Hervé Combeau, Charles-André Gandin, Marvin Gennesson, Joëlle Demurger, Michaël Stoltz, and Isabelle Poitault. Etude expérimentale et modélisation de l'ajout d'inoculant en coulée de lingots d'acier. In *Colloque "La Métallurgie, quel avenir !"*, Nancy, France, 2019.
- [C42] Damien Turret, Y Song, Alain Karma, A Pineau, Gildas Guillemot, Charles-André Gandin, Alexandre Viardin, Laszlo Sturz, Miha Založnik, Sabrine Ziri, A Ma, and Javier Llorca. Phase-field as a benchmark for other models of solidification and microstructure evolution. In *PF 19 – The 4th International Symposium on Phase-Field Modelling in Materials Science*, Bochum, Germany, 2019.
- [C43] Alexandre Viardin, Miha Založnik, Laszlo Sturz, and Gerhard Zimmermann. Mesoscale envelope modelling of columnar growth and conditions for CET in NPG-DC alloy. In Charles-André Gandin and Menghuai Wu, editors, *5th International Conference on Advances in Solidification Processes (ICASP-5) and 5th International Symposium on Cutting Edge of Computer Simulation of Solidification, Casting and Refining (CSSCR-5)*, Salzburg, Austria, 2019.
- [C44] Alexandre Viardin, Julien Zollinger, Miha Založnik, Guillaume Boussinot, Janin Eiken, Markus Apel, Laszlo Sturz, Ralf Berger, and Ulrike Hecht. Mécanique des fluides et solidification à l'échelle microscopique. In *Colloque "La Métallurgie, quel avenir !"*, Nancy, France, 2019.
- [C45] Martín Cisternas Fernández, Miha Založnik, and Hervé Combeau. Modeling of equiaxed grain motion during solidification of TiAl alloys under centrifugal conditions. In *Modeling of Casting, Welding and Advanced Solidification Processes XV*, Djurönäset, Sweden, 2020.
- [C46] Yuze Li, Antonio Olmedilla, Julien Zollinger, Alexandre Viardin, and Miha Založnik. Mesoscopic modeling of primary spacing and grain selection during columnar solidification in conditions of selective laser melting. In *Modeling of Casting, Welding and Advanced Solidification Processes XV*, Djurönäset, Sweden, 2020.

- [C47] Antonio Olmedilla and Miha Založnik. 3D mesoscopic modeling of settling and packing of equiaxed dendrites. In *Modeling of Casting, Welding and Advanced Solidification Processes XV*, Djurönäset, Sweden, 2020.
- [C48] Savya Sachi, Antonio Olmedilla, Miha Založnik, Hervé Combeau, and Charles-André Gandin. Coupling a multiphase solidification model with a neural-network based model for thermodynamic equilibria in multicomponent alloys. In *Modeling of Casting, Welding and Advanced Solidification Processes XV*, Djurönäset, Sweden, 2020.

INVITED SEMINARS AND WORKSHOP LECTURES

- [S1] Miha Založnik. Modeling of Thermosolutal Flow and Macroseggregation in DC Casting. In *Alcan CRV*, Voreppe, France, 2005.
- [S2] Miha Založnik. Formation of macroseggregation: modeling and simulation. In *Ecole des Mines de Nancy – LSG2M*, Nancy, France, 2007.
- [S3] Miha Založnik. Modeling of Macroseggregation Including Grain Motion. In *Sintef Materials & Chemistry*, Oslo, Norway, 2008.
- [S4] Miha Založnik. Modeliranje in simulacija livarskih procesov (Modeling and simulation of casting processes). In *Institut Jožef Stefan*, Ljubljana, Slovenia, 2008.
- [S5] Miha Založnik, Cédric Le Bot, and Eric Arquis. Convection naturelle et changement de phase. In *École thématique Les changements de phases solide-liquide-vapeur – fondements et applications*, Les Embiez, France, 2009.
- [S6] Hervé Combeau, Bernard Dussoubs, Arvind Kumar, and Miha Založnik. Etude de la mise en place des structures de solidification et des macroségrégations. In *Journée M2P3, Institut Jean Lamour*, Nancy, France, 2010.
- [S7] Miha Založnik, Valerio Francesco De Felice, and Hervé Combeau. Le modèle mésoscopique du champ d'enveloppe – les premiers pas. In *Journées GDR SAM Expériences In-situ et Simulations*, Marseille, France, 2012.
- [S8] Miha Založnik. Modélisation multi-échelles de la solidification. In *Institut de Chimie et des Matériaux Paris-Est (ICMPE)*, Thiais, France, 2013.
- [S9] Miha Založnik. Solidification des alliages métalliques : Modélisation de la zone pâteuse. In *Séminaire ANR Principia sur les milieux poreux*, Paris, France, 2013.
- [S10] Miha Založnik. Macroségrégation. In *École thématique Solidification d'Alliages Métalliques*, St. Pierre d'Oléron, France, 2014.
- [S11] Miha Založnik. Combining in situ experiments and numerical modeling of solidification of metallic alloys. In *International workshop Metallurgy with synchrotrons*, Nancy, France, 2016.
- [S12] Miha Založnik, Youssef Souhar, Valerio Francesco De Felice, and Hervé Combeau. Modeling of crystal growth during solidification. In *1ère Journée Française des Utilisateurs OpenFOAM*, Rouen, France, 2016.
- [S13] Miha Založnik, Alexandre Viardin, Youssef Souhar, Markus Apel, and Hervé Combeau. Simulation mésoscopique de la croissance dendritique et comparaisons avec le champ de phase. In *Journées annuelles du GDR SAM (Solidification des Alliages Métalliques)*, Grenoble, France, 2016.

- [S14] Miha Založnik. Multiscale Modeling of Solidification. In *Univerza v Novi Gorici, Ajdovščina, Slovenia*, 2017.
- [S15] Miha Založnik. Transferts multi-échelles : II. Transferts dans la zone pâteuse. In *École thématique Solidification d'Alliages Métalliques et Modèles*, St. Pierre d'Oléron, France, 2017.
- [S16] Antonio Olmedilla, Miha Založnik, and Hervé Combeau. Modélisation des interactions solutales en croissance dendritique équiaxe dans des échantillons minces. In *Journées annuelles du GDR SAM (Solidification des Alliages Métalliques)*, pages TECH News FONDERIE, no. 10, 2019, p. 28, Lille, France, 2018.
- [S17] Miha Založnik. Modélisation multi-échelles de la solidification: de la microstructure au procédé de coulée. In *IM2NP, Université Aix-Marseille*, Marseille, France, 2018.
- [S18] Miha Založnik. Multiscale modeling of solidification: from microstructures to castings. In *CNRS – McMaster University Joint Workshop*, Hamilton, Canada, 2018.
- [S19] André B Phillion, Miha Založnik, Pardis Mohammadpour, Yuze Li, and Julien Zollinger. Prediction of solidification microstructures during laser powder bed fusion via analytical and numerical approaches. In *CNRS – McMaster University Joint Workshop*, Grenoble, France, 2019.

COMPUTER SOFTWARE

- [W1] Jure Mencinger, Miha Založnik, Robert Vertnik, and Božidar Šarler. ImpolSim, 2002.
- [W2] Hervé Combeau and Miha Založnik. SOLID – module Côte2D, 2009.
- [W3] Martín Cisternas, Miha Založnik, and Hervé Combeau. MacroS3D, 2018.
- [W4] Miha Založnik, Antonio Olmedilla, Youssef Souhar, Valerio Francesco De Felice, Alexandre Viardin, and Hervé Combeau. CrystalFOAM, versions 1–9 (2012–2019), 2019.